TECHNISCHE UNIVERSITÄT WIEN

Diploma Thesis

EVALUATING CATALYTIC METHODS FOR STARCH OXIDATION

for the purpose of obtaining the degree of Master of Science (MSc),

submitted at TU Wien, Faculty of Technical Chemistry, by

Verena Scheibelreiter

Mat.Nr.: 01611403

[redacted]

under the supervision of

Univ. Prof. Dipl.-Ing. Dr.techn. Marko Mihovilovic

Associate Prof. Dipl.-Ing. Dr.techn. Rudroff Florian

Dipl.-Ing. Dr.techn. Christian Stanetty

Dipl.-Ing. Hubert Kalaus

Institute of Applied Synthetic Chemistry, E163

Vienna, 12.06.2023

Acknowledgements

This past year has been challenging, and I am grateful for the many people who have supported me during this time.

First, I want to thank Christian Stanetty. You have brought me into the world of sugars for my bachelor thesis and since have given me many opportunities to prove myself in various fields. Thank you for your encouragement during this thesis, for your valuable scientific advice, and for trusting me with some freedom to make my own decisions during this project.

I also want to thank Marko Mihovilovic for his supervision during this thesis and his scientific input during meetings and seminars, and for igniting my first interest in organic chemistry during my first ochem lectures in my bachelor studies.

Further, I would like to thank Florian Rudroff and Michael Schnürch for their input during the seminars. In particular Florian, your suggestions during the “Biocafes” have often led me to refine my experimental approach and improve the quality of my data.

Thank you, Hubert Kalaus, for your support. I knew I could always rely on you and ask for your help anytime, with no question being too stupid. Thank you for your advice inside and outside chemistry, it was greatly appreciated.

I was lucky to be able to conduct this thesis among a very special group of people. Thank you to my wonderful G20 labmates, Christoph Suster, Lara Maltrovsky, Sebastian Hecko and Emmanuel Reichsöllner for providing such a nice atmosphere and enduring my sometimes questionable music choices. Very special thanks go to my Boulder Buddies Stefan Giparakis and Max Wutscher. You are two of the most genuine people I have ever met, and I am grateful for your friendship. Thank you also to the people of the “sugar-team”, Nina, Viktor, Simon and Christoph, starting my weeks early on mondays was easier with you. I also want to thank everyone else in the BSC research group, Astrid, Björn, Chrise, Dominik, Eleni, Freddy, Farooq, Julia, Johanna, Kathi, Lydia, Michi, Nanditha, Rahele, Richie, and Tom. I have learned so much from you, you have helped me so often when I encountered a broken machine or another chemistry-related problem, and I have made many amazing memories with you, inside and outside of the lab. For this I am very grateful.

I would also like to thank my other friends at university, who have started this journey along with me and now have ended up in different groups, in particular Andreas, for still listening to me whine and rant.

I want to thank my family for supporting me in many ways during my education, especially my parents. Without you I would not have come this far.

Last but not least, I need to thank my partner, Stefan Zeman. You have been on my side ever since we met in our first semester, and your unending patience and support has been invaluable during this time. You are the very best.

Table of contents

Abstract

Dialdehyde starch (DAS) is a material derived from renewable sources with promising characteristics for crosslinking biodegradable films or resins. Currently, its production consists of stoichiometric oxidation with $NaIO_4$, which makes it a cost intensive and non-ecofriendly process.

Within this thesis, a new approach for the production of DAS is explored. The new process envisioned would include the selective oxidation of starch to 3-keto starch with a Pd based catalyst, followed by cleavage towards DAS. This thesis focuses on the first step, the selective oxidation, and on the establishment of a new, convenient high throughput method for the determination of oxidation degree of DAS. For the exploration of these subjects, starch-mimicking model compounds based on glucose and maltose were synthesized.

For the determination of the DAS oxidation degree, an UV-absorption-based assay utilizing the reaction between 2-aminobenzamidoxime (ABAO) and the aldehydes of DAS was demonstrated. The reaction was tested with an oxidized model compound and followed *via* ^{1}H-NMR. Applying the assay to starches oxidized with varying amounts of $NaIO_4$ showed a correlation of the absorption of the DAS-ABAO adducts to the amount of $NaIO_4$ used.

The Pd based dimeric catalyst tested within this thesis has been reported for the selective oxidation of carbohydrates in the literature. To examine its applicability on starch, glucose- and maltose-based model compounds were synthesized and NMR experiments testing various conditions were conducted. The reaction conditions were tuned to perform in D_2O and O_2 was used as the terminal oxidant, with phenol as additive to mitigate catalyst degradation. Further experiments with oligosaccharides such as cyclodextrins and maltodextrins confirmed the reactivity of the catalyst with compounds structurally similar to starch. Finally, starch was oxidized with the Pd catalyst in D_2O with O_2 as the terminal oxidant, oxidizing about 20% of the glucose units according to ^{1}H-NMR.

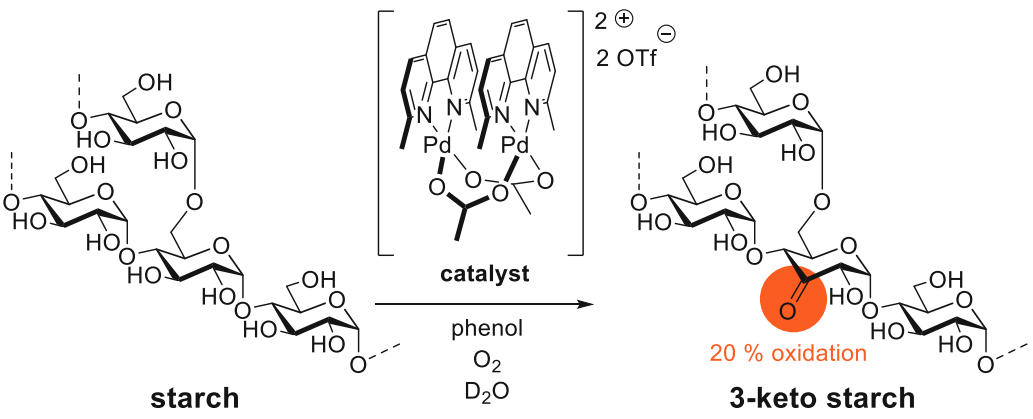

Deutsche Kurzfassung

Dialdehyd-Stärke (DAS) ist ein aus erneuerbaren Ressourcen erzeugtes Material mit vielversprechenden Eigenschaften für die Vernetzung von Biofilmen oder Harzen. Ihre Herstellung erfolgt aktuell mittels stöchiometrischer Oxidation mit $NaIO_4$ und ist deshalb sehr unwirtschaftlich und umweltschädlich.

In dieser Arbeit wurde eine neue Methode zur DAS-Herstellung untersucht. Diese neue Methode würde mit der selektiven Oxidation von Stärke zu 3-Keto-Stärke beginnen, gefolgt von seiner Spaltung zu DAS. Diese Arbeit konzentriert sich auf den ersten Schritt, die selektive Oxidation, und auf die Entwicklung einer neuen, praktischen high throughput Methode zur Carbonylgehalt-Bestimmung von DAS. Zur Untersuchung dieser Themen wurden stärkeähnliche, glukose- und maltosebasierte Modellverbindungen synthetisiert.

Für die Bestimmung des DAS Oxidationsgrades wurde ein Assay entwickelt, der auf der UV-absorption des Produkts zwischen 2-Aminobenzamidoxim (ABAO) und den DAS-Aldehyden basiert. Diese Reaktion wurde mit einer oxidierten Modellverbindung untersucht und mittels ^{1}H-NMR verfolgt. Der Test des Assays mit DAS-Proben, die mit unterschiedlichen Mengen $NaIO_4$ hergestellt wurden, zeigte eine Korrelation zwischen der Absorption der DAS-ABAO Addukte und der $NaIO_4$-Menge.

Der dimere Pd-Katalysator, der in dieser Arbeit untersucht wurde, ist literaturbekannt für seine selektive Oxidation von Kohlenhydraten. Um seine Anwendbarkeit für Stärke zu eruieren, wurden die Reaktionen der Modellverbindungen mit dem Katalysator in verschiedenen Reaktionsbedingungen *via* ^{1}H-NMR verfolgt. Die Reaktionsbedingungen wurden für D_2O abgestimmt und O_2 wurde als Oxidans verwendet. Phenol wurde als Additiv eingesetzt, um den Abbau des Katalysators zu verhindern. Weitere Experimente mit Oligosacchariden wie Cyclodextrinen und Maltodextrinen bestätigten die Reaktivität des Katalysators mit stärkeähnlichen Substraten. Schlussendlich wurde Stärke mit dem Katalysator in D_2O mit O_2 oxidiert, wobei etwa 20% der Glukoseeinheiten (bestimmt mittels ^{1}H-NMR) oxidiert wurden.

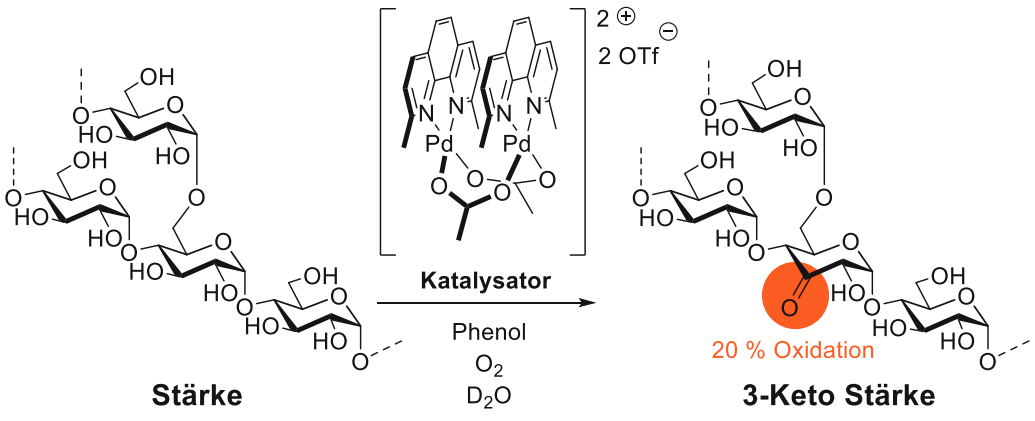

General schemes

Synthesis of model compounds and catalyst

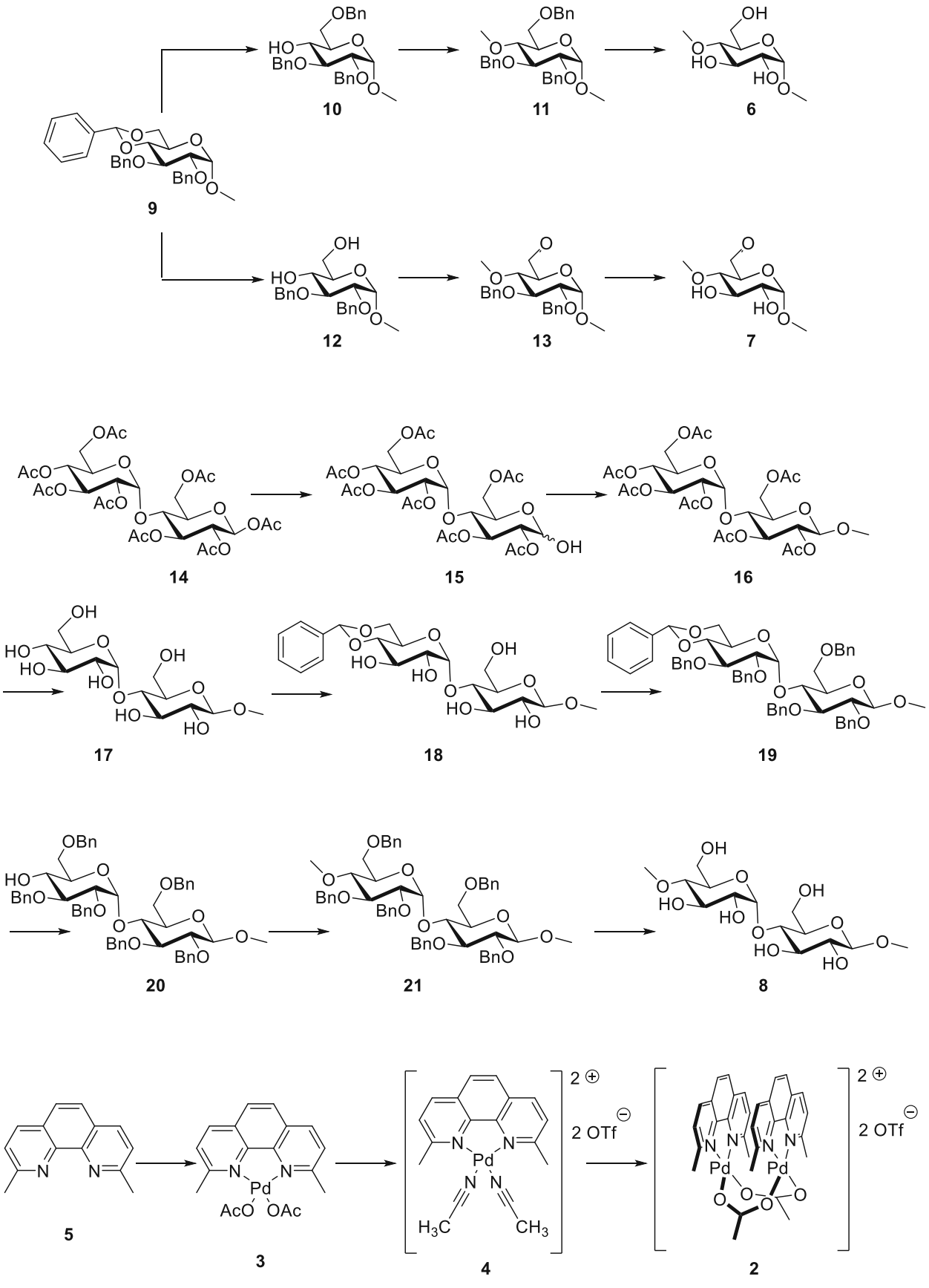

Oxidations of model compounds

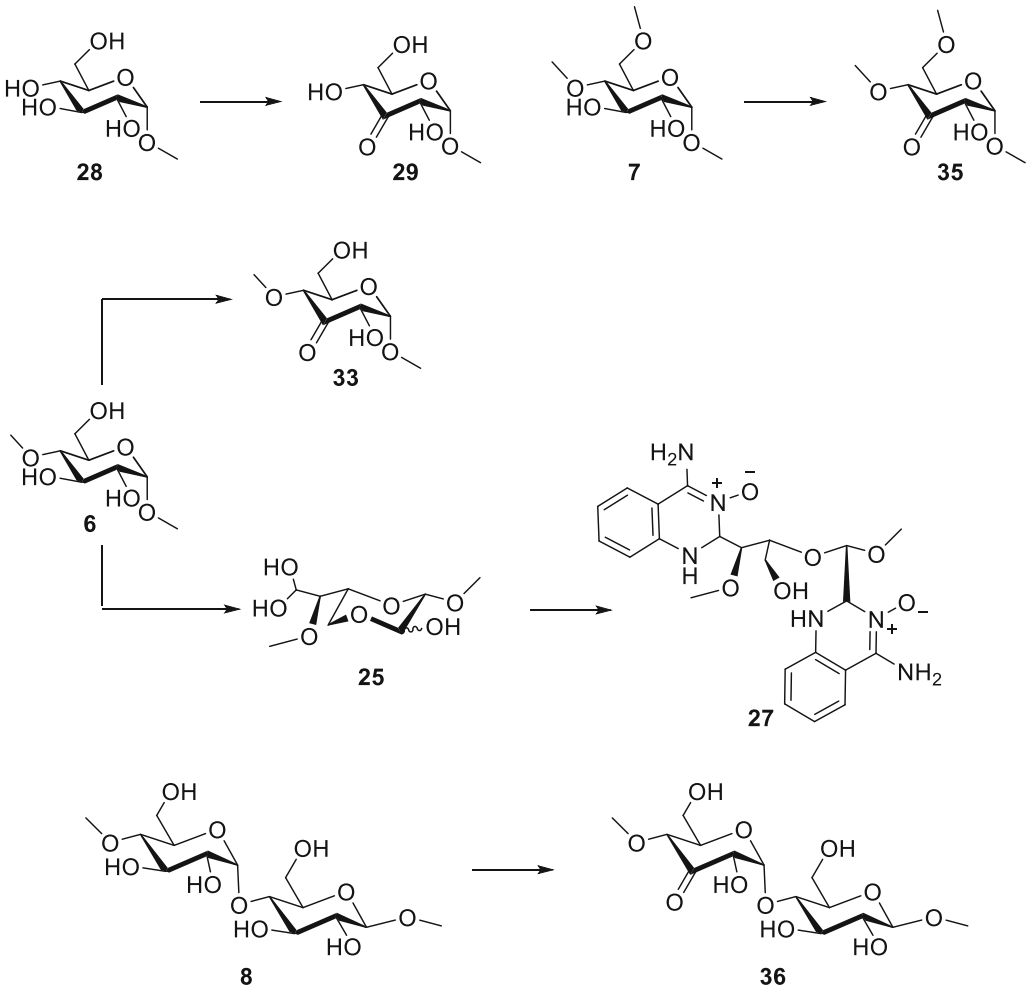

Abbreviations

ABAO	2-aminobenzamidoxime
AGU	anhydrate glucose unit
BQ	benzoquinone
COSY	correlation spectroscopy
c	concentration
d	doublet
DAS	dialdehyde starch
DCM	dichloromethane
DMAPA	dimethylaminopropylamine
DMSO	dimethylsulfoxide
equiv	equivalent
HPTLC	high-performance thin-layer chromatography
HSQC	heteronuclear single quantum coherence
J	coupling constant
LP	light petroleum
lit	literature
m	multiplet
M	molecular weight
m.p.	melting point
NMR	nuclear magnetic resonance
q	quartet
R_f	retention factor
rt	room temperature
s	singlet
t	triplet
TLC	thin-layer chromatography
THF	tetrahydrofuran

UV	ultra-violet
δ	chemical shift

1 Introduction

1.1 Modified starches

1.1.1 Starch as a versatile renewable resource

In recent years, a general push toward a more widespread use of renewable materials was made. One of the most interesting materials in this regard is starch. As it is used by many plants to store energy, it is one of the most abundant biobased resources. Globally, the most important sources for starch production are maize, cassava, wheat and potatoes.[1]

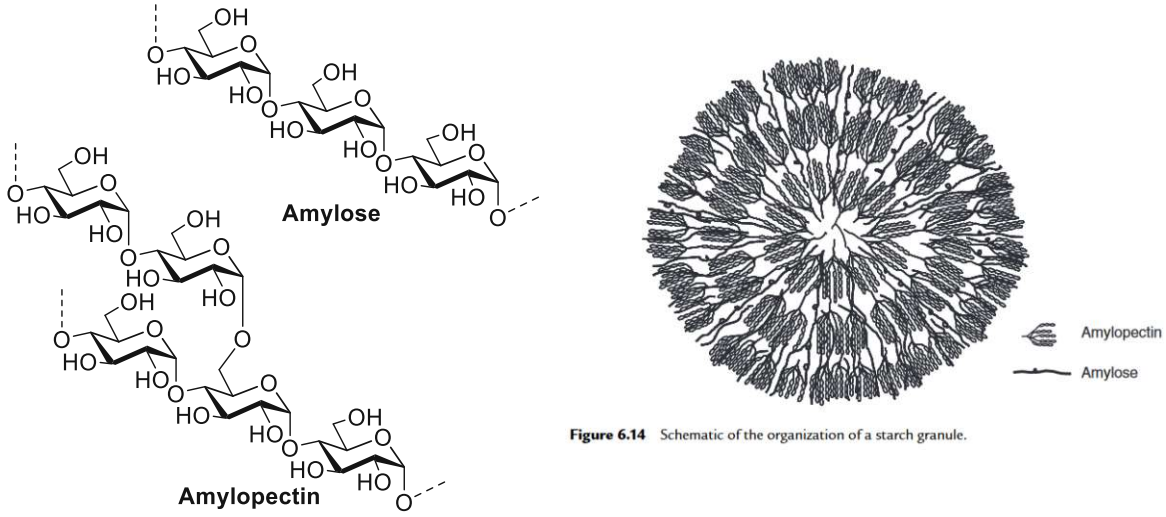

Figure 1 Structures of amylose and amylopectin and diagram of the starch granule as proposed by Jane[2]

Starch mainly consists of amylose and amylopectin, both are polymers of α-1,4 linked D-glucose and are organized in granules as depicted in Figure 1.[2] The ratio of the two and the composition of starch is dependent on its source. However, amylopectin is the major component of most starches. In it around 5% of the glucose units are additionally linked with α-1,6 glycosidic bonds, making it a highly branched polymer with a much higher molecular weight than amylose. Amylose contains a negligible amount of α-1,6 branches, making it a primarily linear polymer that tends to form insoluble semi-crystalline aggregates.[3] Native starch is industrially used in various sectors, *e.g.* the food and cosmetics industry, as flocculant for purification, the pharmaceutical industry or the paper industry.[4]

However, some properties of starch limit its usefulness in industrial applications. Its solubility is limited, and the viscosity of starch dispersions tends to be high. To mitigate these constraints and further expand the versatility of starch materials, it can be modified physically or chemically.[5]

The many free hydroxy groups available in starch allow a wide range of modifications *via* esterification, etherification or phosphorylation. A prominent example of this concept is acetylated starch. The acetyl groups increase its hydrophobicity and prevent the formation of hydrogen bonds between starch branches. This can prevent the formation of cloudiness in starch dispersions.[6] Another valuable property of acetylated starch is its reduced retrogradation tendency and a lower gelatinization temperature.[5] Other important examples of modified starches synthesized by attaching small molecules to their hydroxy groups include carboxymethylated starch, hydroxypropylated starch and starch phosphate.[6]

Another important concept of starch modification is its degradation. Breakage of glycosidic bonds, lowering the molecular weight of starch, and weakening its granules results in a lowered viscosity of starch pastes and increased solubility. This can classically be achieved by treatment with HCl or H_2SO_4.[5] Another popular form of degradation is starch oxidation, which additionally introduces new carbonyl and carboxyl groups which further alter the properties and can serve of new handles of chemistry or crosslinking.[7]

The most common oxidation reagent for starch is sodium hypochlorite, which produces mainly carboxylic acids and a minor amount of carbonyl groups.[8] The proposed location of the oxidation varies between publications. While experiments by Whistler *et al.*[9] and Floor *et al.*[10] suggest only the glycol at C2 and C3 is oxidatively cleaved, Boruch[11] described solely oxidations at C1 and C6. The resulting oxidized starch is widely used for surface sizing, most prominently within the paper industry.[12] Carboxylic acids increase the hydrophilicity of the starch,[13] stabilize the viscosity of starch pastes and reduce retrogradation.[12] Retrogradation is the recrystallization or reaggregation of amylopectin and amylose after starch has been gelatinized and for example a major factor in bread becoming stale, thus undesirable in some food applications.[14]

Another, less widely used oxidation reagent is H_2O_2, which mainly leads to carbonyl formation with minor amounts of carboxyls.[8]

A more chemically specific but less industrially used variant of oxidized starch is dialdehyde starch.

1.1.2 Dialdehyde starch

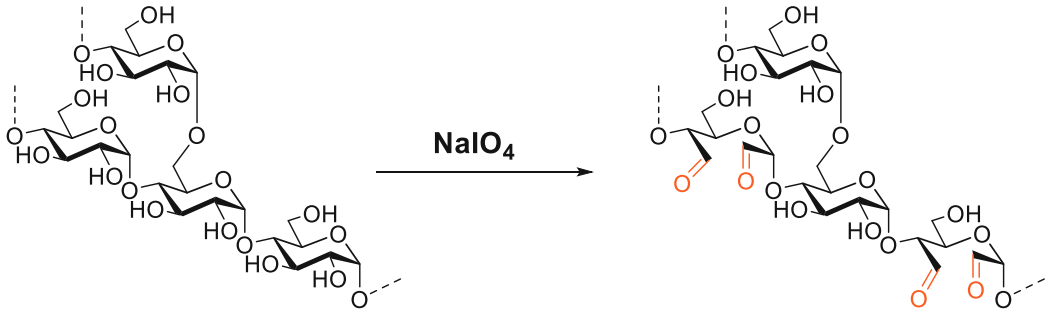

Scheme 1 Production of DAS

Dialdehyde starch (DAS) is produced by oxidative cleavage of the 2,3-diol with sodium periodate, as shown in Scheme 1. Figure 2 shows the correlation between the amount of $NaIO_4$ used for the oxidation and the percentage of glucose units oxidized as determined by Zhang *et al.*[15] There is an increase of oxidation degree up until 1 equivalent of periodate relative to glucose units. The slight decrease for amounts with stoichiometric excess could have been caused by potential overoxidation to carboxylic acids, or degradation to smaller, soluble fragments which are removed during work up as speculated by the authors of this publication. The loss of soluble compartments is also the cause of the decreasing yield. Higher oxidation degrees lead to lower viscosities of dispersed starches.[15] During oxidation, the molecular weight of the starch as well as the radius of the starch molecules, decreases.[16] With increasing amount of oxidized glucose units, the crystallinity of the starch granules is destroyed, as measured by X-ray diffraction. A total loss of crystallinity is observed already above 15% oxidized units.[16]

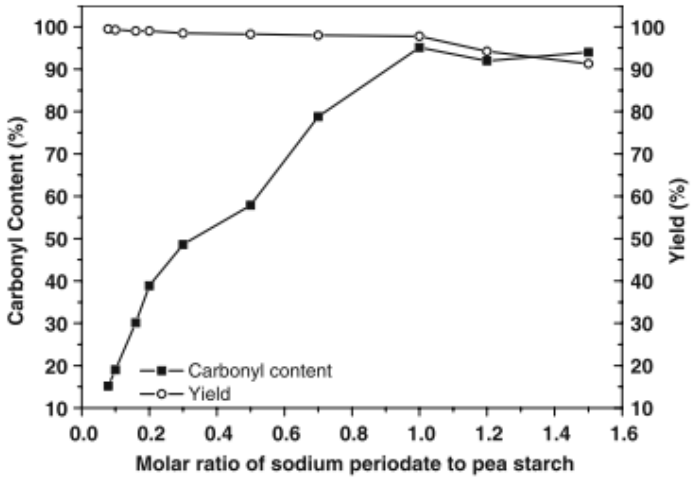

Figure 2 Relation of molar ratio of $NaIO_4$ and oxidation degree of DAS, as determined by Zhang *et al.*[15]

Amylose segments are more crystalline and thus more resistant to oxidation compared to amylopectine.[15] Examinations of starches with different oxidation degrees with scanning electron microscopy reveal that amorphous regions located at the center of the starch granule are oxidized first, leaving the crystalline regions closer to the surface relatively untouched. This leads to the formation of rings.[17]

Compared to native starch at around 300°C,[18] the decomposition temperature of DAS is lower at around 250-265 °C[15] due to the thermal instability of the aldehyde group. The higher the amount of carbonyl units in the starch, the lower the decomposition temperature. Stabilization can occur when glycol is added, as the formed acetals are more stable than the aldehydes, leading to an increase of the decomposition temperature to 285-315 °C.[15]

One area where this acetal formation has a beneficial effect is thermoplastic starch. Starch is turned into thermoplastic starch by the addition of plasticizers, most commonly glycerol, and heating. However, a significant drawback of thermoplastic starch is its tendency to recrystallize during storage, which causes the material to become brittle.[19] Thermoplastic DAS however mitigates such recrystallization, as Yu *et al*. found in a publication with DAS plasticized by glycerol.[17] The films produced within this study had increased tensile strength and decreased elongation at break compared to native plasticized starch, an effect which is amplified with the increase of oxidation degree. The underlying cause is the formation of acetals and hemiacetals by the aldehydes within the DAS, forming a crosslinked polymer. Interestingly, while DAS is more water absorbent than native starch, thermoplastic DAS absorbs less water, which is caused by the crosslinking taking place during the plasticizing process.[17] In a study by Zhang *et al*. it was shown that DAS that was treated with glycol before plasticizing with glycerol also had good water resistance and good tensile strength. When the oxidation degree of DAS was 95%, these glycol-DAS mixtures could even form films without additional plasticizers.[15]

The many aldehyde groups available in DAS can be used in a myriad of ways as a handle for further chemical modifications. Jelkmann *et al.* reported the synthesis of aminated starch, achieved by reductive amination with ammonia. The resulting cationic starch was reported to have potential for application in drug delivery.[20] Another group reported the synthesis of dihydrazone starch, by reacting DAS with hydrazine sulfate. In a study published by Para *et al*., its complex formation with various metal ions was reported, aiming for usage as a metal ion trap in sewage treatment.[21] Similar studies for the same purpose have been published with aminothiazoles,[22] semicarbazones,[23] and oximes.[24]

Various attempts have been made to utilize DAS as a crosslinking agent in biodegradable polymers and films. A study published by Martucci *et al*. reported the production of films with gelatin, DAS and glycerol, however with insufficient mechanical properties.[25] Tang *et al.* reported a successful production of films with chitosan and DAS; crosslinked by the formation

of Schiff Bases between the DAS-aldehydes and the chitosan-amines. This improved the tensile strength of the chitosan with 5 w% DAS while retaining its antimicrobial effects.[26]

An economically important field in which aldehydes are used for crosslinking is wood adhesives. For this purpose, formaldehyde based resins are widely used today.[27] However, this comes with harmful formaldehyde emissions, which makes the partial or complete substitution of formaldehyde in these resins of great interest.[28] Resins with a mixture of resorcinol and formaldehyde with DAS had similar properties to neat resorcinol and formaldehyde resins, with some properties, like the bonding strength, thermal stability and decomposition temperature even slightly improved.[29] The toughness of melamine-urea-formaldehyde resin improved when DAS was added.[28]

In an effort to produce a resin based on renewable materials without any formaldehyde, Chen *et al.* tested resins made with glyoxalated lignin, DAS and urea. Particleboards made from this mixture showed acceptable mechanical properties.[27]

As shown above, DAS is a promising material derived from an abundant renewable resource. However, its potential is currently limited by its production cost. The oxidant, sodium periodate, is needed stoichiometrically in relation to the desired oxidized glucose units, and very expensive.[12] Although efforts of electrochemical regeneration of the oxidant have been made,[30] the industrial use of DAS is still limited. Thus, finding an economical, green alternative for DAS production is of great importance.

1.1.3 Carbonyl content determination of oxidized starch

As described above, the carbonyl content (also described as degree of oxidation) of DAS is an important factor to consider, as it drastically affects its properties. However, the analysis of the carbonyl content is a complex endeavor.

Currently, the most common determination method (used in some of the literature mentioned above[13, 15, 17]) is based on a procedure as described by Smith in 1967.[31] The DAS sample is dissolved in water, gelatinized, the pH adjusted to 3.2 and reacted with hydroxylamine in a water bath for several hours. The excess hydroxylamine is then titrated back to pH 3.2 with HCl. Not only is this method time consuming and labor-intensive, but additionally, findings by Veelaert *et al*. suggest that only a fraction of the aldehyde groups actually react with hydroxylamine. In their study, the carbonyl contents of DAS were determined *via* HPLC. The carbonyl groups in DAS were reduced with $NaBH_4$ and then hydrolyzed with H_2SO_4. This means previously oxidized glucose units were present as erythritol and unoxidized units as glucose. The ratio of these compounds was determined *via* HPLC analysis. When the same DAS samples were treated with hydroxylamine at pH 5, 52-66% of the aldehydes determined by HPLC reacted and the remaining unreactive ones were presumed to have formed

hemiacetals and acetals.[32] Later studies suggest that heating DAS at pH 5 and higher prior to the hydroxylamine reaction increases the ratio of unavailable aldehyde groups even further.[33]

Another method utilizing $NaBH_4$ was published by Rankin and Mehltretter.[34] It determines the carbonyl content of DAS by quantifying the amount of H_2 formed during reduction. This produced similar results to another method presented within the same publication, which consists of fully oxidizing the DAS sample with periodate and then determining the amount of oxidant consumed.[34]

For DAS with lower carbonyl contents, a method based on absorption measurements is described. Starch is gelatinized in water and reacted with *p*-nitrophenylhydrazine under heating. The precipitating hydrazone is then filtrated and dissolved in ethanol. The resulting solution's absorbance is measured to determine the carbonyl content.[31]

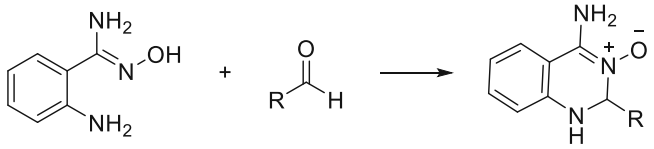

1 **1a**

UV active

Scheme 2 Reaction of ABAO 1 with aldehydes

Finding a more convenient method to determine aldehyde contents would be useful, as none of the methods mentioned above are suitable for high-throughput screenings. One reagent that has been used before for the detection and quantification of aldehydes within our group is 2-aminobenzamidoxime (ABAO) **1**.[35-37] The selective reaction of ABAO with aldehydes is shown in Scheme 2. The adduct **1a** formed in this reaction is UV-active and has a significant shift of absorption maximum compared to the starting material **1**, an essential property for aldehyde labeling and detection purposes. Its usefulness was first reported by Kitov *et al.*, describing the rapid formation of the stable adducts and successfully utilizing it to label aldehyde terminated peptides.[38] Since, ABAO-derivatives have been used for the quantification of aldehydes [35, 36] and even ketones[39] in biotransformations and for the determination of open chain contents of aldoses.[37]

Utilizing this reaction for the determination of carbonyl content in DAS would simplify its analysis.

1.2 Catalytic oxidation of diols

1.2.1 Literature reported diol cleavages yielding dialdehydes

While several methods are reported within the literature for the oxidation of vicinal diols, aiming for starch as the target substrate comes with limiting factors. Both hydroxy groups of the targeted diol are equatorial and thus oriented *trans* regarding each other. Additionally, the glycosidic bonds involving *O*4, *O*1, and (less frequent) *O*6 induce a significant steric hindrance. Selective oxidation of *O*2 and *O*3 is desired with little overoxidation and no involvement of *O*6. Ecologic and economic factors also must be considered when aiming for an industrially feasible process, making water the preferred solvent and oxygen or air the preferred terminal oxidant.

Several methods for the oxidative catalytic cleavage of vicinal diols to aldehydes are reported in the literature. For example, Amadio *et al.* published the oxidative C-C Bond cleavage of an impressive library of diols utilizing vanadium amino triphenolates. This rapid reaction was reported with very low catalyst loadings and with air or O_2 as final oxidants. However, quite high reaction temperatures (80 - 100 °C) were necessary and only reactions in organic solvents were reported.[40] In addition to the high toxicity of vanadium[41], this makes this method rather unfit for big scale starch oxidation.

Another catalytic method for the catalytic oxidative cleavage of diols was reported by Garcia *et al.* The cleavage of a broad range of diols was performed with $MoO_2Cl_2(dmso)_2$ as the catalyst and DMSO acting as solvent and terminal oxidant. Selectivity issues were reported in the absence of molecular sieves, hinting at possible complications when water is present.[42]

Other catalytic approaches in the literature involving Ru[43] and Mn[44] catalysts similar encounter problems with overoxidation, non-compatibility with water, and reduced reactivity with sterically hindered substrates.

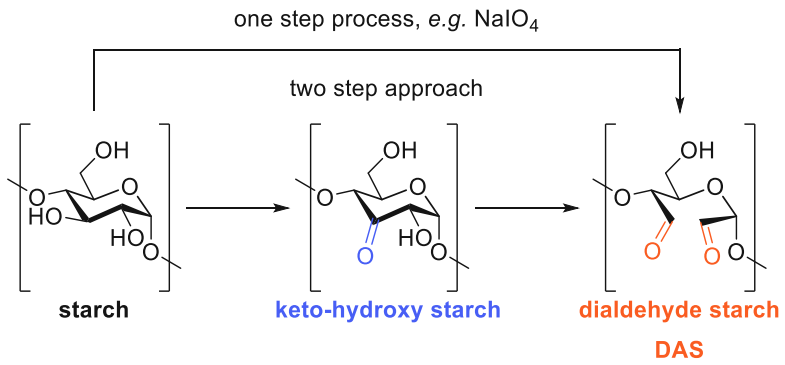

Scheme 3 Two possible approaches for the catalytic oxidation of starch

As depicted in Scheme 3, direct oxidation from starch to DAS is not the only feasible option. Another possible approach is a two-step method, involving oxidation towards a keto-hydroxy

starch and followed by cleavage to DAS. Selective cleavage could be achieved *via* a retro-benzoin reaction catalyzed by N-heterocyclic carbenes[45, 46] or cyanides.[47] This approach could be less prone to overoxidation and gives rise to a new keto-starch derivative which could have interesting properties as well. This thesis was focused on the first step of this approach utilizing a cationic Pd catalyst which is described in detail below.

1.2.2 Alcohol oxidation with [(neocuproine)Pd(OAc)]$_2$(OTf)$_2$ (2)

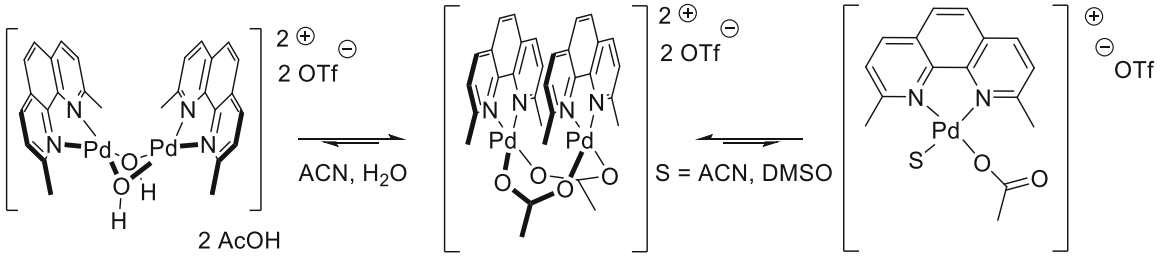

Scheme 4 Pd catalyst 2 and its equilibrium forms in solvent

The most appealing option for a selective 3-keto oxidation of carbohydrates found in literature is [(neocuproine)Pd(OAc)]$_2$(OTf)$_2$ **(2)**, as described by the groups of Minnaard[48-54] and Waymouth.[55-61] Catalyst **2**, as depicted in Scheme 4, was first reported by Conley *et al.* in 2007.[57] It is a dimeric catalyst specifically designed for fast aerobic oxidation of alcohols. Its effectiveness stems from the combination of the advantages of its anionic ligands: Acetate is coordinated to Pd^{2+} and acts as an intermolecular base during catalysis, while the triflate anion is not coordinated and thus leaves an open coordination site. When compared to (neocuproine)Pd(OAc)$_2$ **3** and (neocuproine)Pd(OTf)$_2$ **4**, catalyst **2** is far more effective for the catalysis of 2-heptanol oxidation, having a more than 200 times faster initial reaction rate. In solvent, an equilibrium with monomer **2a** is formed. When water is added, an equilibrium with μ-OH derivative **2b** is formed, which is a slightly less effective catalyst compared to the original dimer **2** due to its slower dissociation.[57]

A possible pathway for the alcohol oxidation with catalyst **2** is depicted in Scheme 5. After disassociation into the active monomer **2a**, a Pd-alkoxide complex **2c** is formed. The following β-H-elimination yields the oxidized substrate and Pd-hydride species **2d**. The reoxidation mechanism of Pd-hydride **2d** is can occur through several pathways: through the PeroxoPd(II) species **2e** as depicted in Scheme 5, but also though Pd-peroxide species, and through trinuclear (neocuproine-Pd)$_3$(μ^3-O)$_2$ species.[59] The resulting aforementioned μ-hydroxo dimer **2b** can either react directly with the alcohol to form alkoxide **2c** or regenerate species **2a** first.[57, 58]

Scheme 5 also depicts two known degradation products. Pd black is formed in aerobic oxidations with higher temperatures.[61] Carboxylate species **2g** is formed after H-atom abstraction from the neocuproine ligand of the Pd-catalyst, leading to the formation of radical

2f. It is currently unknown which Pd species in the pathway undergoes this initial H-atom abstraction and which reactive oxygen species is causing this.[58] The resulting carboxylate **2g** however, was isolated after aerobic oxidations and proven to be stable and inactive.[57]

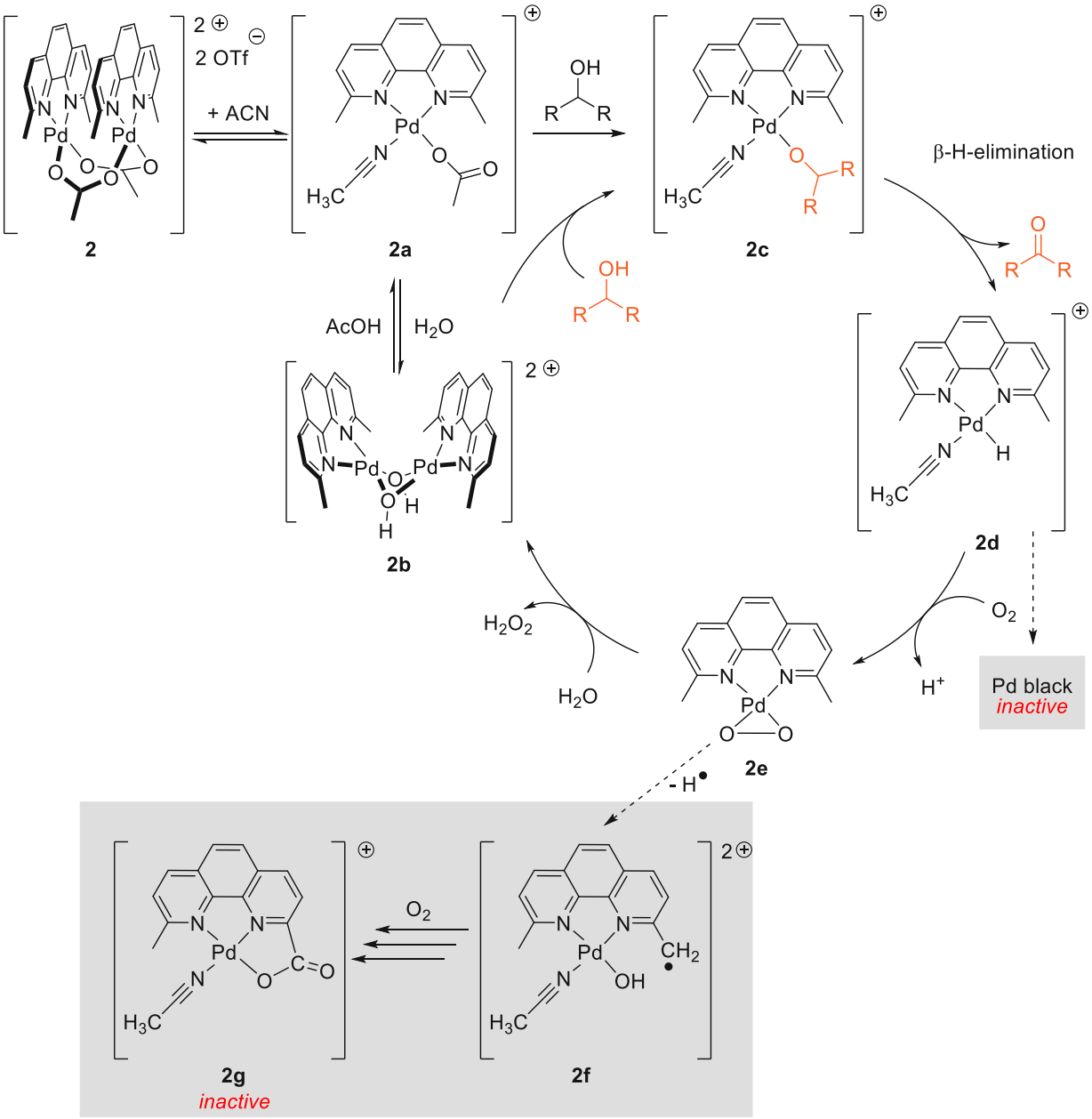

Scheme 5 Proposed mechanism of alcohol oxidation and deactivation (grey boxes) of catalyst 2 by Ho *et al.*[58]

Within the literature, various attempts have been made to prolong catalyst lifetime during aerobic oxidation. As one of the main deactivation pathways is initiated by H-atom abstraction at the methyl group of the neocuproine ligand **5**, modifications of the ligand, as shown in Figure 3, are a feasible approach. When the methyl group is omitted as in ligand **5a**, the catalyst is not active for alcohol oxidation, presumably because the dimeric complex is too stable and does not disintegrate into the active monomer analog to **2a**.[48] Substituting the methyl group with an ethyl group (ligand **5b**) also results in an inactive catalyst.[58] A successful modification

of the catalyst is the exchange of the CH_3 group with CD_3 resulting in deuterated ligand **5**-d_6, as the breakage of the C-D bond requires more energy compared to the C-H bond. While the initial turnover frequency of catalysts derived from **5** and **5**-d_6 was the same, the overall turnover number of the deuterated catalyst was reported 1.6 times higher in two separate publications.[48, 58] A similar improvement was achieved by attaching electron withdrawing NO_2 to the neocuproine ligand (ligand **5c**), which also impedes H-atom obstruction.[58] Another strategy employed in the literature is the exchange of CH_3 with CF_3 resulting in ligand **5d**, which has no benzylic protons near the Pd center. This leads to a 1.8 time increase of the turnover number.[60]

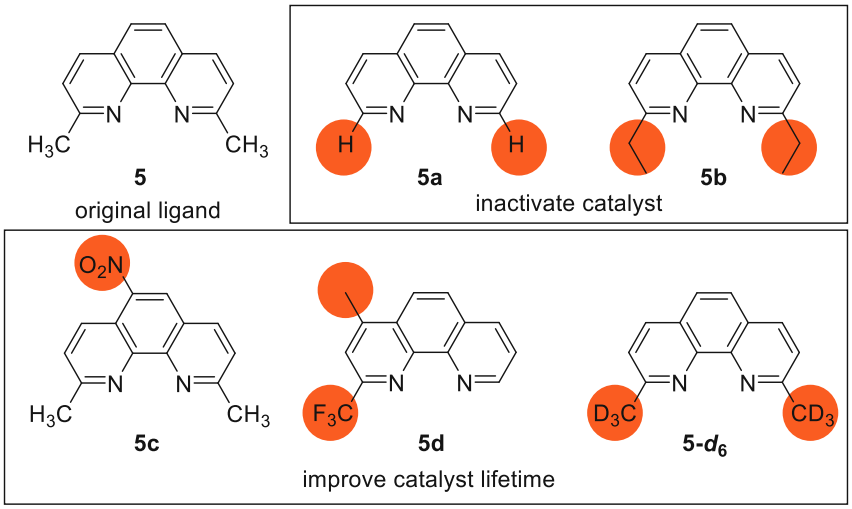

Figure 3 Modified ligands of catalyst 2 found in the literature

Another approach for lifetime elongation is the addition of additives. Effective additives which function as H-atom donors, thus regenerating **2a**, include phenols and 1-phenylethyl hydroperoxide.[58] Styrene was reported to be another beneficial additive by providing another pathway of catalyst regeneration and producing 1-phenylethyl hydroperoxide.[58]

Oxidations with benzoquinone instead of O_2 as terminal oxidant drastically improved catalyst lifetime.[61]

1.2.3 Selective oxidation of carbohydrates with [(neocuproine)Pd(OAc)]$_2$(OTf)$_2$ (2)

Experiments by Chung *et al.* revealed increased reactivity of catalyst **2** with diols in relation to mono-alcohols. Interestingly, while the catalyst typically favors primary alcohols, within diols the secondary alcohol oxidation is favored, meaning α-keto-hydroxy products are formed before α-aldehyde-hydroxy products. Chung *et al.* argue that the reason for this selectivity is a change in mechanism compared to mono-alcohols. This causes the rate determining step to become the β-hydride elimination, which is faster with secondary alkoxides.[55]

The selective oxidation of glucoside derivatives to their 3-keto equivalents was first reported by Jäger *et al.* in 2013[51] and later expanded to an impressive compilation of carbohydrates by the groups of Minnaard and Waymouth.[49-51, 53, 56]

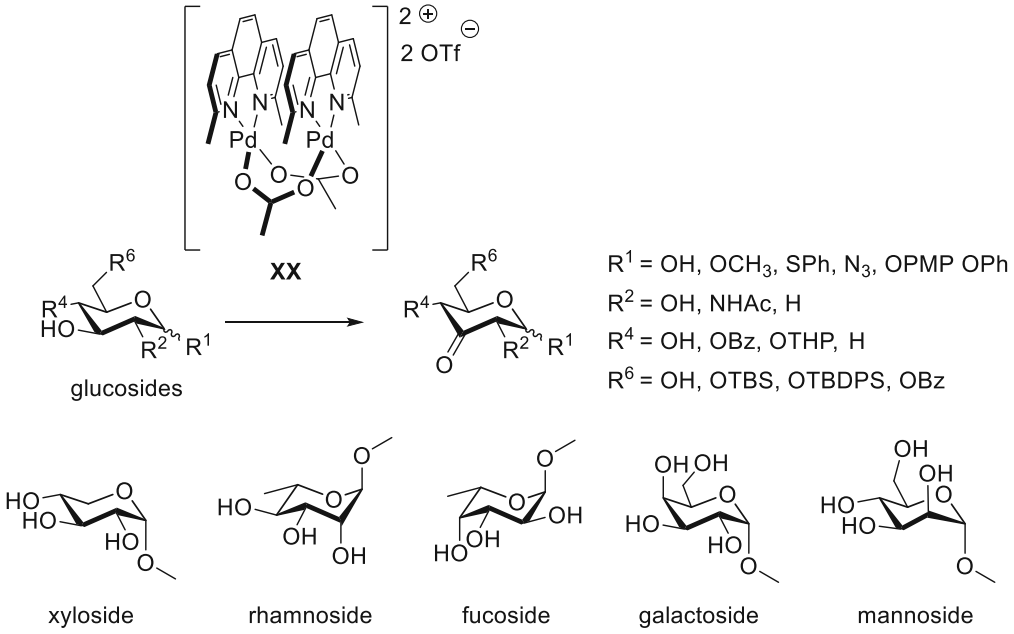

Scheme 6 Selection of literature reported carbohydrate substrates for selective oxidation with catalyst 2[49-51, 53, 56]

The selectivity for the oxidation of position 3 in the pyranose rings is mainly caused by the relation to the ring oxygen. Position 3 has the lowest activation barrier for the β-hydride elimination, as positions 2 and 4 are neighbors of the positively polarized carbons bound to the ring oxygen and would thus be disfavored during this step. This was determined *via* DFT calculations.[54]

The scope of substrates is shown in Scheme 6 and includes several protected and unprotected monosaccharides with equatorial alcohols as well as fucoside, galactoside, and mannoside, which contain axial hydroxy groups. A broad scope of glucosides was oxidized with catalyst **2**, including glucosides without hydroxy groups in positions 2, 4 or 6 and with the anomeric center in α- and β-configuration. Protecting groups in positions *O*4 and *O*6 were tolerated by the catalyst, [50, 51, 56] bulky protecting groups such as benzoyl and THP in position 4 decreased the reactivity but did not fully inhibit the reaction.[50] This decreased reactivity was further demonstrated in the selective oxidation of oligomaltosyl azides, glucans with up to seven 1,4-α-linked glucoses. The non-reducing ends of the chains were oxidized selectively with only minor amounts of byproducts reported, as shown in Scheme 7.[49]

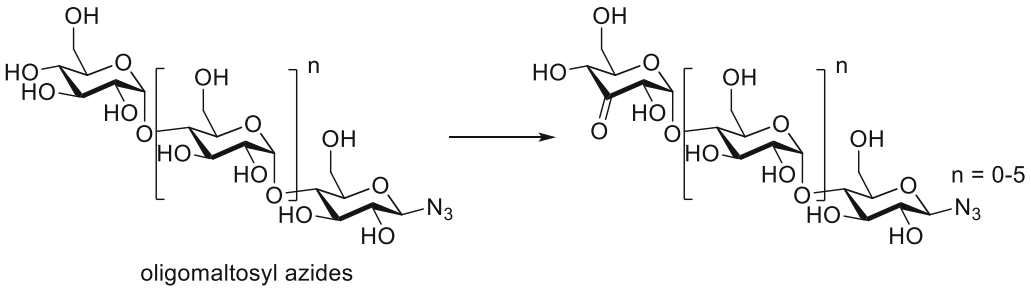

Scheme 7 Selective oxidation of oligomaltosyl azides with catalyst 2[49]

While most published reactions were accomplished with methyl pyranosides or glycosyl azides, Jumde *et al*. reported the oxidation of free α- and β-glucoses.[53] The reactions were carried out in DMSO, where no mutarotation is possible and the anomers are stable. The oxidation of α-glucose and N-Acetyl-α-glucosamine was selective, while the oxidation of β-glucose produced a side product as shown in Figure 4. This product is a result of overoxidation where the anomeric position is oxidized additionally to position 3, followed by tautomerization, another oxidation and rearrangement to form the bislactone shown in Figure 4.[53] A similar overoxidation was reported by the same group for the oxidation of methyl 4-deoxy-α-glucopyranoside, β-xylopyranoside, α-mannopyranoside, and β-galactopyranoside.[50] This overoxidation was mitigated by reducing the amount of benzoquinone, the final oxidant, from three to one equivalent.

Another selectivity deviation was reported by Chung *et al*. concerning the additional formation of 4-keto pyranosides with higher temperatures. This was most prominent with α-glucoside, 6-deoxy-α-glucoside, α-xyloside, rhamnoside, fucoside and arabinoside.[56]

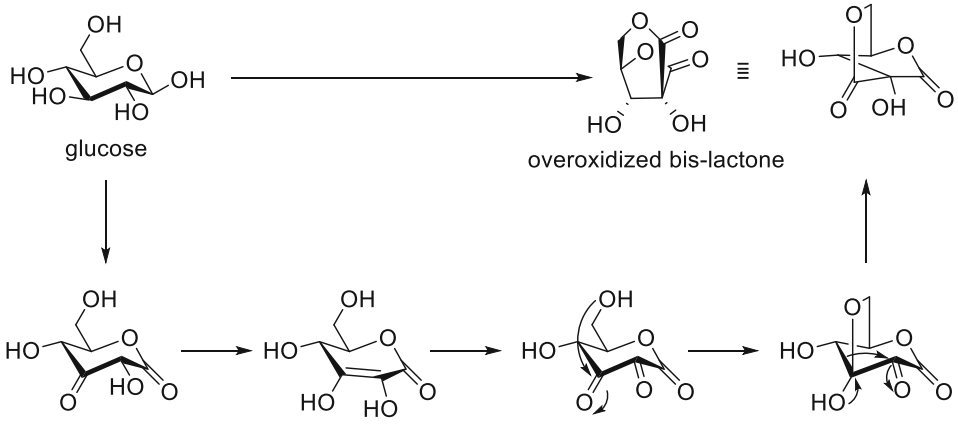

Figure 4 Side product formed by overoxidation of β-glucose

1.3 Aim of this thesis

DAS is a promising material, but its use is very limited by its expensive and environmentally harmful production. Finding an economical and greener alternative for its synthesis would allow this renewable material to be used for a wide range of applications.

The main goal of this thesis is the exploration of a new catalytic method towards DAS production. For this purpose, a pathway towards 3-keto starch with catalyst **2** was chosen as a midway target, as shown in Scheme 8. Further, 3-keto starch is an interesting intermediate for other routes of derivatization by itself.

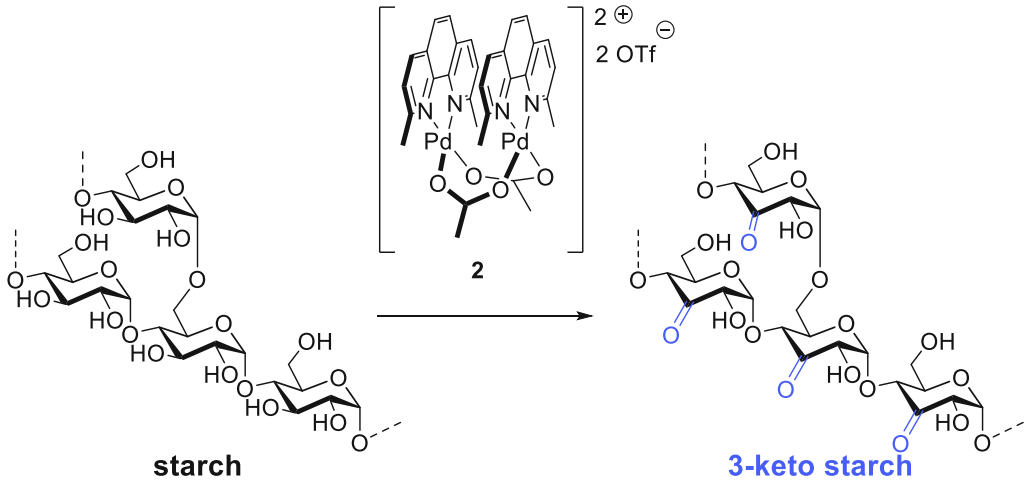

Scheme 8 Oxidation of starch with catalyst 2

Because starch is a complex substrate, model compounds based on glucose and maltose, mimicking the bonds and steric hindrances of the glucose units in starch, were chosen for the exploration of this reaction. The three model compounds depicted in Figure 5 are not commercially available and needed to be synthesized.

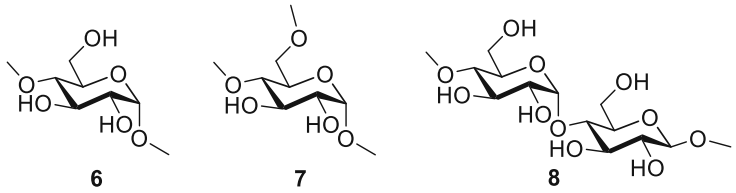

Figure 5 Model compounds synthesized within this thesis

With these model compounds in hand, the reaction with catalyst **2** should be tested under conditions suitable for starch industry, meaning water as the solvent and ideally O_2 as the final oxidant. Moving from simple model compounds **6**, **7** and **8** to more complex substrates, oligosaccharides such as maltodextrins and cyclodextrins should be explored. The ultimate goal was to test the catalyst **2** with starch materials on the base of the gathered experience gained with the model compounds.

Another critical aspect for the experimentation on DAS is finding a more efficient method for carbonyl content determination, as currently used methods are labor-intensive and unsuited for high-throughput screenings. Utilizing the reaction between ABAO **1** and aldehydes was envisioned, which would allow the measurement of aldehyde concentrations *via* absorption measurements. Towards a valid assay for DAS, also this reaction will be studied with the oxidized model compound to understand whether the influence of putatively formed acetals is of importance. Experiments with periodate oxidized starch should then demonstrate the applicability of this approach for DAS.

2 Results and discussion

2.1 Synthesis of model compounds

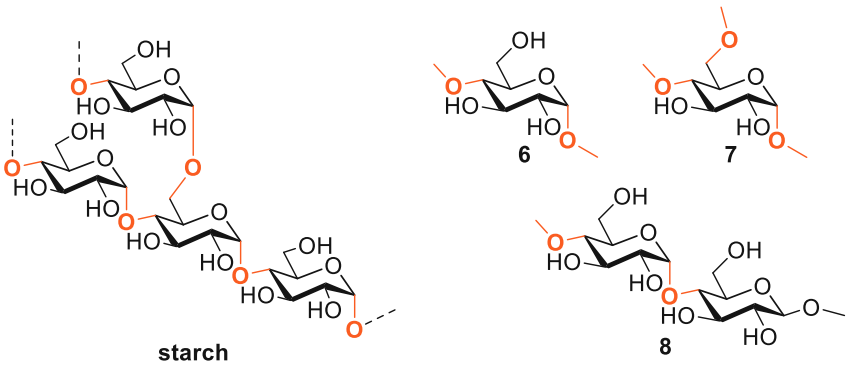

Figure 6 Comparison of starch to the three chosen model compounds.

Starch is a very complex substrate. In order to gain insights into the reactions within this thesis, small model compounds were chosen to enable simpler analysis. The model compounds chosen are shown in Figure 6. Like starch, they are based on glucose and were designed to mimic its 1,4-α glycosidic bonds. Compounds **6** and **7** are methyl-α-glucopyranoside derivatives with the alcohol in position 4 capped off with a methyl group. Compound **7** is additionally protected *via* a methoxy group in position 6, leaving only the alcohols the positions of interest – 2 and 3 – unprotected. This model compound was chosen to mimic elements with additional 1,6-α glycosidic bonds also found in starch and to rule out interferences of the primary alcohol, for example through internal acetal formation. Methyl 4'-*O*-methyl-β-maltopyranoside (**8**) was selected for the same reasons, with an 1,4-α bond connecting the two glucose units. This derivative was synthesized instead of the even more fitting initially targeted alternative methyl 4'-*O*-methyl-α-maltopyranoside (**8α**) because of its more accessible synthesis as discussed in chapter 2.1.2.

2.1.1 Synthesis of glucopyranoside model compounds 6 and 7

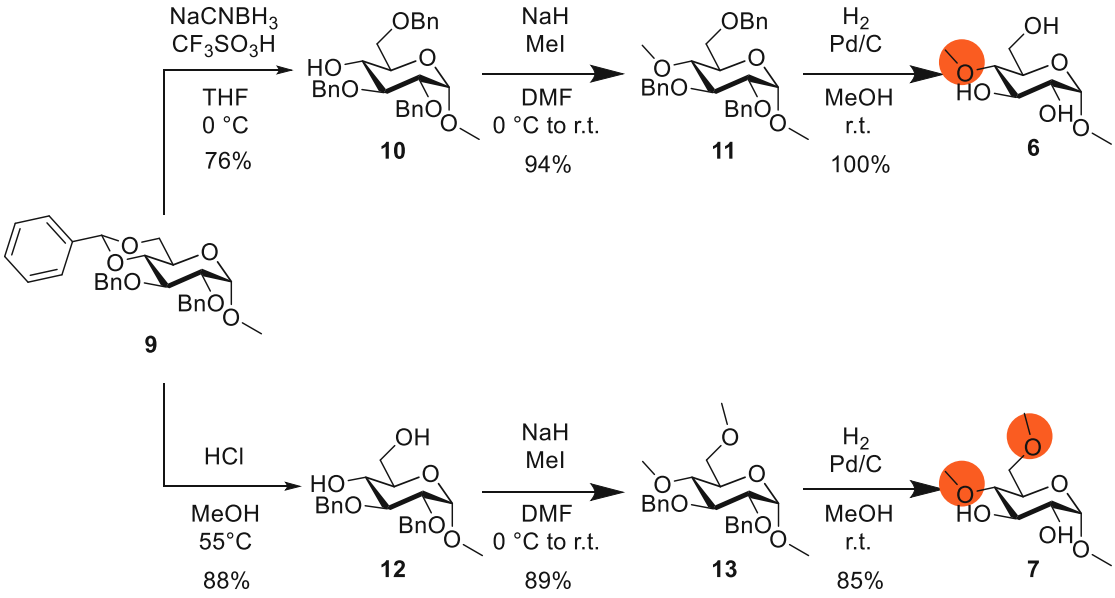

Scheme 9 Synthesis of methylated glucopyranoside model compounds 6 and 7

Synthesis of the methylated glucopyranoside model compounds **6** and **7** was accomplished by following literature procedures as shown in Scheme 9.[62, 63] The acetal protected compound **9** (synthesized within the group) was the starting material for both glucoside model compounds. Selective reductive opening of the acetal was achieved by treatment with $NaCNBH_3$ and CF_3SO_3H to give compound **10**, deprotected at the *O*4 position. Subsequent methylation with NaH and MeI yielded the protected compound **11**, which was deprotected with standard hydrogenolysis conditions to yield the target substance **6**.

Towards target substance **7**, the acetal of starting material **9** was cleaved completely with harsher, acidic conditions, freeing both alcohols at positions *O*4 and *O*6. After methylation and deprotection under the same conditions as used for compound **11**, target substance **6** was acquired.

All steps involved in the synthesis of glucoside model compounds **6** and **7** resulted in good to excellent yields; comparable to the yields reported within the literature,[62, 63] with no complications worth of further remarks.

2.1.2 Synthesis of methyl 4'-*O*-methyl-β-maltopyranoside (8)

Compared to glucose, the availability of maltose derivatives is much more limited. For this reason, the synthesis of maltose-based model compound **8** involved several additional steps, as shown in Scheme 10, Scheme 12, and Scheme 13.

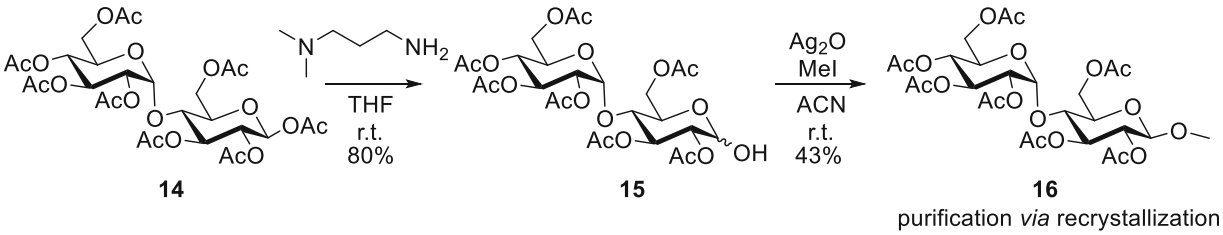

Scheme 10 Route to acetylated intermediate 16 in β configuration

Initially, the anomeric derivative 4'-*O*-methyl-α-maltopyranoside (**8α**) was targeted as the desired maltose model compound, with both anomeric centers in α-configuration and thereby more closely resembling the structure of starch. Thus, literature procedures of a paper titled "A convenient large-scale synthesis of methyl α-maltoside: a simple model for amylose"[64] were followed as shown in Scheme 10 and Scheme 12.

Peracetylated maltoside (**14**) was selectively deacetylated at the anomeric position using DMAPA.[65] Using DMAPA as the nucleophile allowed for a simple workup *via* acidic aqueous extraction, and compound **15** was obtained in an anomeric mixture without further purification and with good yield. The anomeric center was methylated as described in the aforementioned paper with Ag_2O and MeI,[64] and purified *via* recrystallization in EtOH. However, ^{1}H-NMR revealed the formed anomer to be the β-anomer **8** instead of the claimed acetylated methyl α-maltoside **8α**. The yield achieved (43%) was significantly lower compared to the reported literature yield (83%). Upon closer inspection, the reported target product in the paper was wrongly assigned. Instead of methyl α-maltoside (**8α**), methyl β-maltoside (**8**) was synthesized in the literature procedure, the two isomers being clearly distinguishable by ^{1}H-NMR. The coupling constant reported in the NMR code of the paper for the peak at 4.29 ppm (assigned to H1') was 8 Hz, which clearly points to the β-anomer in sugars with glucose stereochemistry.

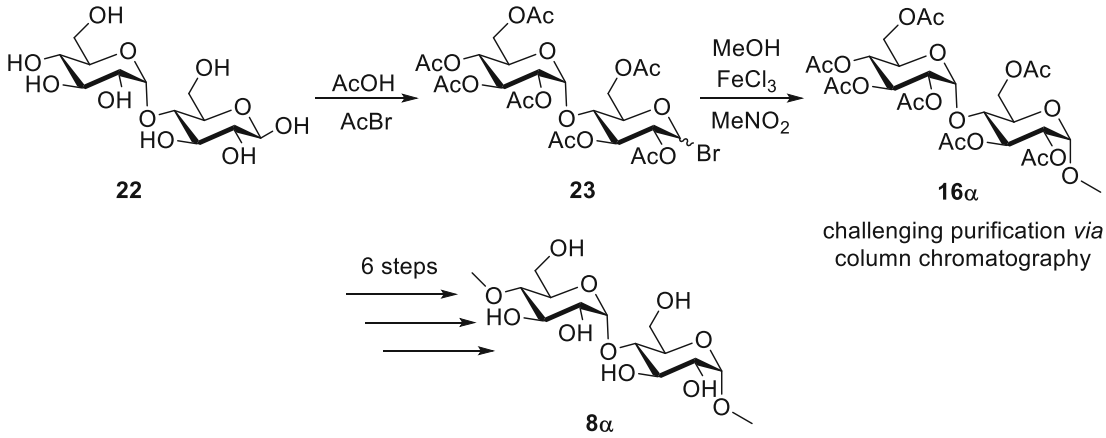

Scheme 11 Attempted route to obtain α-maltoside intermediate 16α[66]

To obtain the correct α-anomer, another literature procedure[66] was attempted, as depicted in Scheme 11. This procedure started with simultaneous acetylation and anomeric bromination of maltose (**22**) with acetyl bromide in acetic acid to yield compound **23**. This peracetylated

bromide maltoside **23** was pure according to ^{1}H-NMR and was further reacted without additional purification, as described in the literature. Methylation at the anomeric position commenced via reaction with $FeCl_3$ and MeOH in $MeNO_2$ and yielded the desired peracetylated methyl α-maltoside **16α**, in mixture with the β-maltoside **16** and other unidentifiable impurities according to ^{1}H-NMR. The anomeric ratio was not determinable due to these other impurities. Recrystallization of the crude was not successful, and while column chromatography with LP:EtOAc led to ^{1}H-NMR spectra with less impurities, an unsatisfactory amount still remained. From here, target compound **8α** would have required 6 additional reaction steps. Column chromatography at this early stage was highly undesirable, especially compared to the easily scalable purification *via* recrystallisation of the β-anomer **16** as described above. For this reason, the route to α-maltoside **8α** was abandoned and the route was continued with β-anomer **8** as shown in Scheme 12.

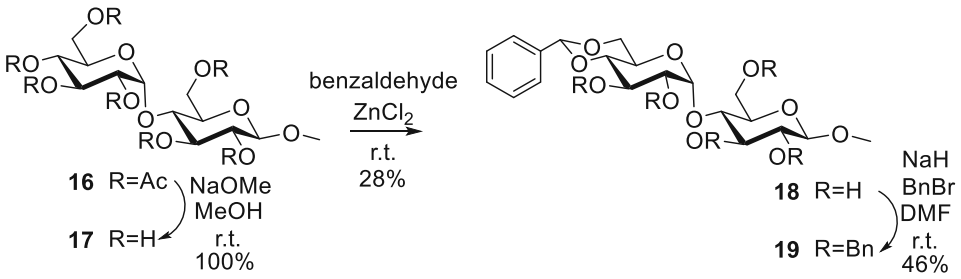

Scheme 12 Route to intermediate 19

Compound **16** was deacetylated *via* standard Zemplén conditions, obtaining intermediate **17** without any complications. After the installment of the benzylidene group at position 4' and 6' to obtain compound **18**, purification was achieved upon acetylation, column chromatography, and subsequent deacetylation with standard Zemplén conditions as described within the literature.[67] This led to an overall yield of 28%. Benzylation of compound **18** afforded the protected maltopyranoside **19**, the compound analogous to the similarly protected glucoside **9**.

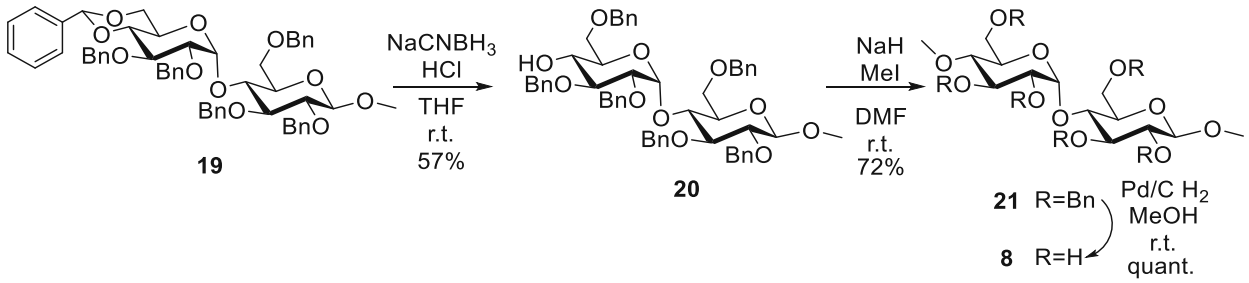

Scheme 13 Final steps of synthesis of methyl 4'-O-methyl-β-maltopyranoside (8)

The last four steps as shown in Scheme 13 were analogous to the synthesis of glucoside model compound **6** above. For the selective opening of the benzylidene group, first, the same conditions as used for the glucoside were attempted, using CF_3COOH as acid and reacting the reagents at 0°C.[63] There was no conversion visible *via* TLC, so the temperature was raised

to room temperature, which achieved full conversion after 1h. However, NMR analysis revealed the formed product to be the maltoside-diol with the acetal fully cleaved instead selectively opening it to compound **20**. A literature procedure using the same compound **19** as starting material described using HCl in dry ether as the acid, while reacting at room temperature.[68] Employing this method proved to be successful and compound **20** was obtained in 57% yield. For the methylation and deprotection the same methods were employed as were used for the glucoside model compounds **6** and **7** to yield the final compound **8**, both steps resulting in excellent yields. The overall yield of the maltoside model compound **8** synthesis was 2% over eight steps.

2.2 Establishing an ABAO based aldehyde quantification for DAS

As described in 1.1.3, carbonyl contents are important factors regarding the properties of DAS. Their methods of quantification, however, are currently very labor intensive and time consuming. A more convenient approach could be based on the application of ABAO (2-amionbenzamidoxime) (**1**).

ABAO (**1**) reacts selectively with aldehydes, forming an adduct which is UV-active and quantifiable *via* absorption measurements. This reaction has been used in the past for the quantification of aldehydes utilizing a convenient, high through put assay.[36] Within the group an assay had been developed for the aldehyde quantification of C6 oxidized starches. As mentioned in 1.1.3, the carbonyl groups of DAS are capable of forming hemiacetals, which are slightly more protected and less reactive than open aldehydes. ABAO (**1**) has been used before to measure the equilibrium between aldehydes and hemiacetals to determine the open chain content of aldoses.[37] To investigate the influence of such hemiacetals on the ABAO (**1**) application on DAS, first experiments were conducted with model compound **6**.

2.2.1 Reaction of ABAO (1) with oxidized model compound 24

To obtain a smaller model dialdehyde compound similar to DAS, model compound **6** was oxidized with $NaIO_4$.

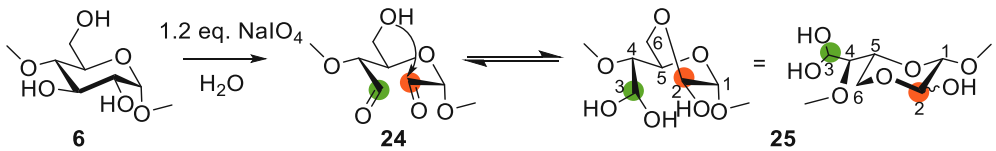

Scheme 14 Reaction of glucoside 6 with $NaIO_4$ and subsequent hemiacetal formation

Scheme 14 shown in Scheme 14, after the oxidation of model compound **6** the hemiacetal **25** involving the primary alcohol in position 6 and the aldehyde in position 2 was formed, as reported in the literature.[69] The ^{1}H-NMR was interpreted and compared to the literature, and the *cis*:*trans* ratio (regarding the center at position 2) of compound **25** was determined to be

1:0.6. Noteworthy, when starch is oxidized to DAS, the same internal acetal formation can occur.[32]

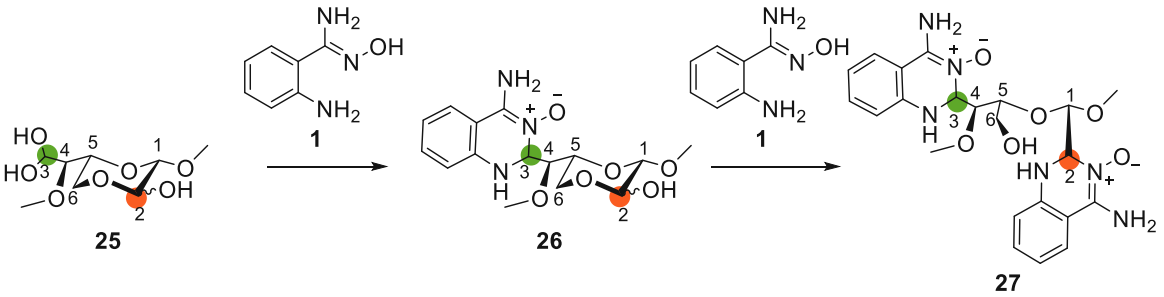

Scheme 15 Proposed sequential addition of ABAO (1) to compound 25. The sequential addition to the two groups with different reactivities was confirmed by ^{1}H-NMR

For the ABAO assay to be applicable, ABAO (**1**) must react with both the aldehyde/dihydrate and the aforementioned hemiacetals. In order to confirm this, compound **25** was reacted with ABAO (**1**). We expected ABAO to react with the more reactive dihydrate group in position 3 (green) first, followed by the subsequent, slower reaction with the less reactive hemiacetal in position 2 (red), as depicted in Scheme 15. In order to test this hypothesis, compound **25** was reacted with varying equivalents of ABAO (**1**) (0.5, 2.5 and 10 eq.) in deuterated aqueous buffer. The resulting ^{1}H-NMR spectra are shown in Figure 7. Depicted are peaks between 4.25 and 5.55 ppm, which include the protons on positions 1, 2 and 3 of the compounds **25**, **26** and **27** due to their similar oxidation states. These peaks were assigned based on their shifts and coupling constants in ^{1}H-NMR and their signals in HSQC spectra. As compound **25** has two diastereomers (declared as *trans t* and *cis c* in relation to the neighboring OH group) due to the hemiacetal in position 2, we expected compound **26** to exhibit 4 diastereomers in ^{1}H-NMR due to the newly formed chiral center in position 3, and compound **27** to yield 4 diastereomers as well. Surprisingly, for both compound **26** and compound **27** only two diastereomers were formed. Compound **26** (blue in Figure 7) emerged as a *trans/cis* diastereomer, varying in position 2, as is clearly shown by the coupling constants of positions 1 and 2. This suggests that the ABAO (**1**) in position 3 (the former hydrate) was added stereoselectively. The signals of the compound with two added ABAO groups **27** (green in Figure 7) suggest the formation of two distinct diastereomers, meaning that after the stereoselective addition of ABAO (**1**) at position 3, yielding compound **27**, the second ABAO addition commenced in a non-stereoselective way. The reaction mixture with 2.5 eq. of ABAO (**1**) was measured after 2 h and 24 h reaction time and revealed by comparison of integrals that after additional reaction time, compound **26** was further reacted to compound **27.** Table 1 shows the ratio of the compounds and their isomers at the two recorded reaction times. The *cis:trans* ratio of compound **26** remained approximately the same, most probable due to the equilibrium between the two isomers achieved through the opening and closing of the acetal in position 2.

The a:b ratio of compound **27** shifted a small amount, however the difference is not significant enough when integral errors due to overlapping peaks in ^{1}H-NMR are taken into account.

Table 1 Ratio of products after 2 h and 24 h reaction time of 2.5 eq. ABAO (1) with compound 25

	Ratio of components			
Reaction time	**26 cis**	**26 trans**	**27a**	**27b**
2 h	25%	49%	14%	12%
24 h	18%	30%	23%	30%

The key finding here is the fact that ABAO (**1**) adds to both the hemiacetal and the dihydrate in compound **25**, which means that potentially formed acetals in DAS should react in the same way. Additionally, some conclusions about the respective reaction rates of ABAO (**1**) with the hemiacetal and the dihydrate can be drawn. If the rates of these additions were similar, a mixture of products would be obtained with substoichiometrical ABAO (**1**). However, with the substoichiometrical amount of 0.5 eq. ABAO (**1**), the only detected product was the mono-adduct **26**. The complete absence of bis-adduct **27** suggests that the ABAO adduct formation with the dihydrate in position 3 is significantly faster than the addition at the hemiacetal in position 2.

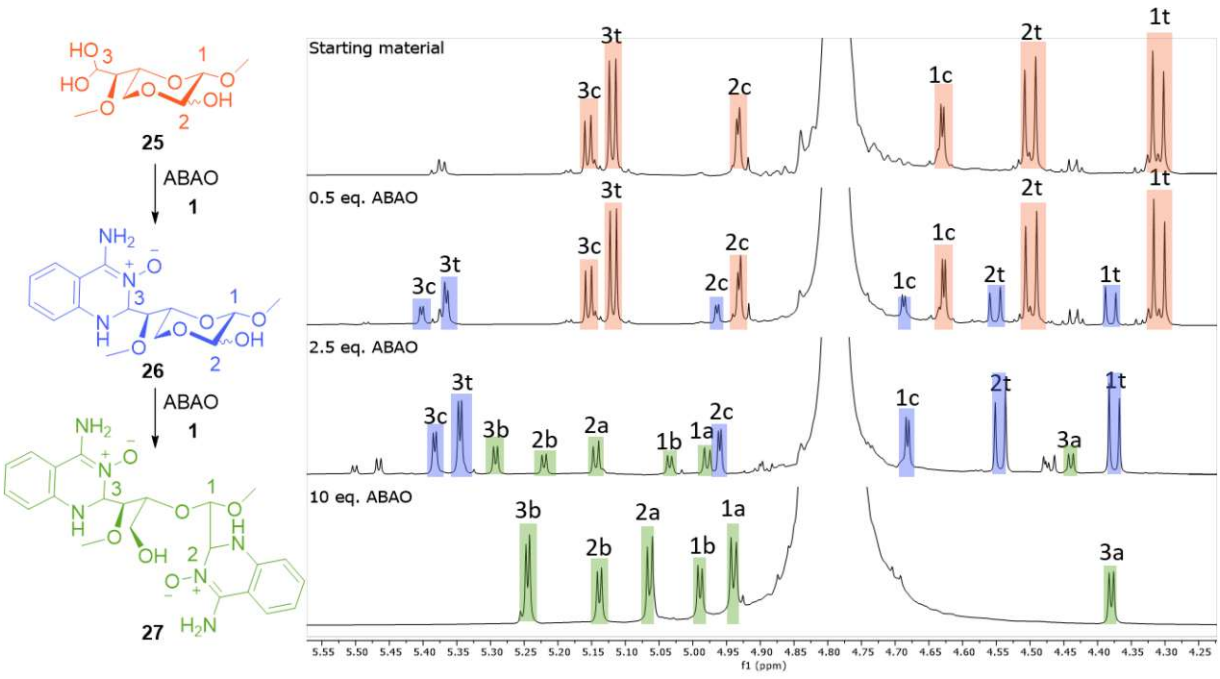

Figure 7 NMR experiment of compound 25 reacted with different equivalents of ABAO (1) after 2-3.5 h of reaction time.

Next, the behavior of the reaction between compound **25** and ABAO (**1**) was studied *via* absorption, with the aim to generate a calibration for the later experiments with DAS. Compound **25** was reacted with ABAO (**1**) under standard quantitative assay conditions and the absorption at 405 nm was measured over time. The absorption over time is shown in Figure

8. Two distinct curves appear to be layered on top of each other, marked with arrows. This is congruent with the observation made in NMR. Supposedly the first, seemingly faster increase of absorption corresponds to the addition of ABAO (**1**) to the faster reacting dihydrate, while the second, slower reaction with the hemiacetal proceeds afterwards.

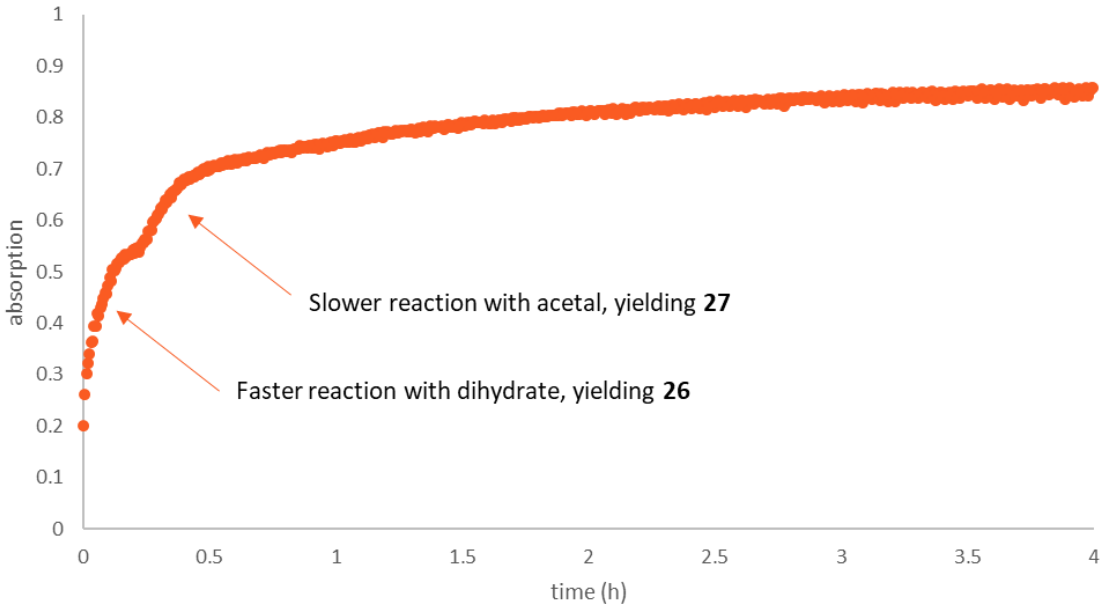

Figure 8 Absorption during reaction of ABAO (1) with compound 25 under standard assay conditions at 405 nm over time

To obtain a calibration suitable for the aldehyde quantification in DAS, compound **25** was mixed with unoxidized **6**, imitating different amounts of conversion (Figure 16), mimicking DAS with varying oxidation degrees. However, as **6** was not reacting with ABAO there was no measurable absorption there in the assay without oxidized **25**.

To obtain a calibration for the application on DAS, the maximum absorptions (reached after about 5 hours) were plotted against the corresponding **25** concentrations, as depicted in Figure 9. It shows a mostly linear relation of **25** concentration and absorption maximum, meaning that the reaction with ABAO (**1**) is suited for dialdehyde quantification.

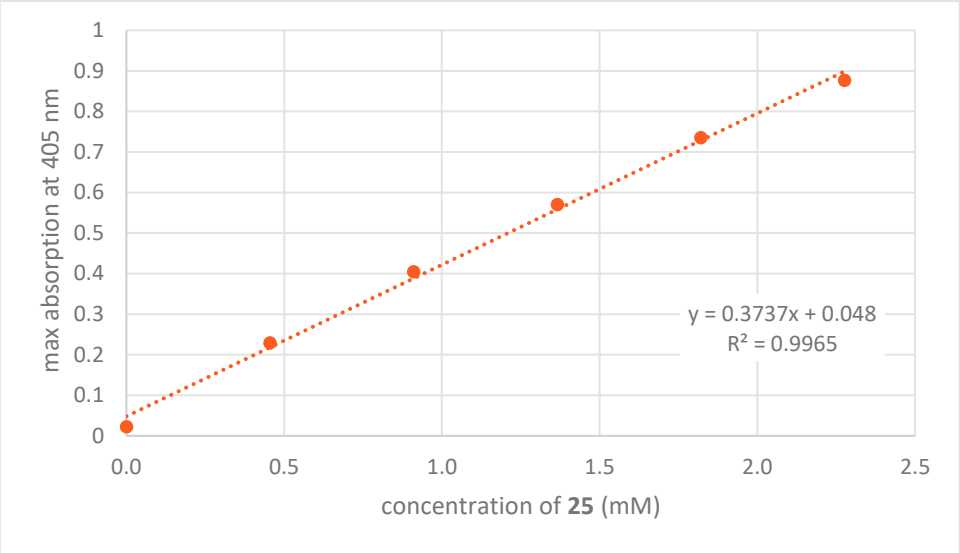

Figure 9 Maximum absorption reached during the reaction of ABAO (1) with compound 25 plotted against different concentrations.

2.2.2 Preparation of DAS

As a first step towards the investigation of DAS with ABAO (**1**), DAS samples with varying oxidation degrees were prepared.

DAS was prepared according to a standard procedure by dissolving $NaIO_4$ in water, adding starch and stirring for 16h at 35°C.[15] Different amounts of $NaIO_4$ were used ranging from 0.25 to 1.5 equivalents per glucose unit. The starch slurries were washed by centrifugation and the remaining oxidized starches were dried under vacuum at 50°C for three days.

The appearance of the starches after the oxidation varied based on the different amounts of $NaIO_4$ used. Some examples are shown in Figure 10. The slight purple and the orange discoloration of the 0.5 eq. $NaIO_4$ and 0.75 eq. $NaIO_4$ starch respectively could be caused by I_3^--starch complexes. The different colors could correspond to differing degrees of degradation. It has been described in the literature that the color of iodine-starch complexes depends on the length of the glucose chains, ranging from blue-green and purple for longer chains to red for shorter chains.[70] DAS prepared with 1 or 1.25 eq. $NaIO_4$ showed no sign of discoloration. It has been reported previously that DAS with higher oxidation degrees (80% or higher) is no longer stainable with iodine.[71]

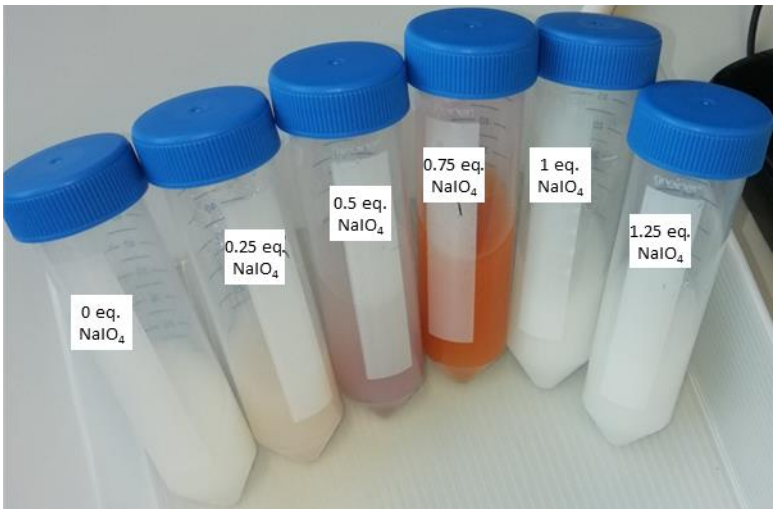

Figure 10 Optical appearance of starch after oxidation with different equivalents of $NaIO_4$

2.2.3 Investigation of DAS *via* the ABAO assay

Then the ABAO assay was applied to the prepared DAS. After dissolving the DAS in buffer by heating to 95°C, the obtained solutions were mixed with ABAO-buffer solutions in 96 well plates in triplicates. The absorption at 405 nm was measured in time resolved fashion, as shown in Figure 11 on an example. The increase of absorption over time (several hours) is in stark contrast to the reaction of ABAO (**1**) with C6 oxidized starch, where the reaction is instantly completed, as observed during experiments within the group done by Hubert Kalaus (manuscript in preparation). The main reason for this slowed reaction lies most probable in the formation of acetals, as seen with model compound **25** in chapter 2.2.1. For this reason, the following experiments involving the ABAO assay with DAS were measured after 21h of reaction time, to reach full saturation of ABAO adducts and maximum absorption.

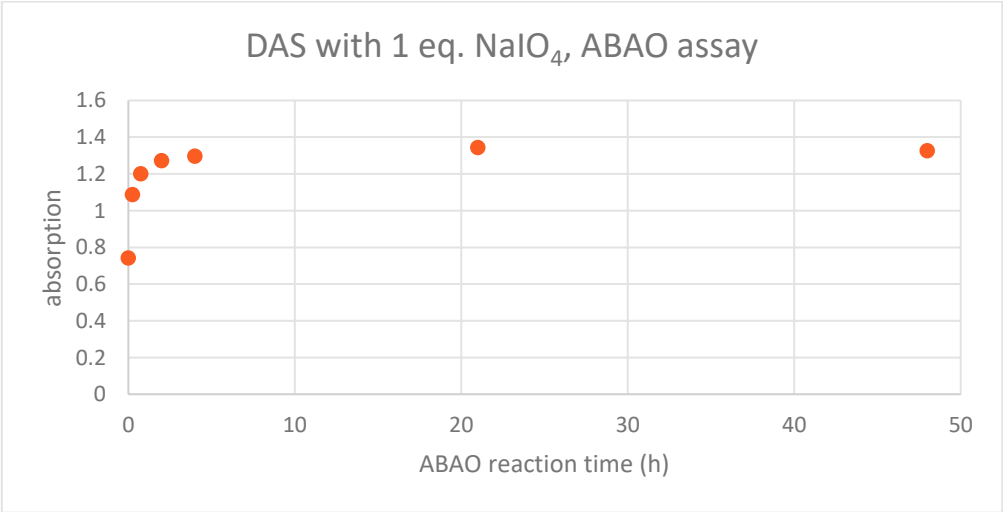

Figure 11 Absorption of reaction between ABAO (1) and DAS oxidized wit 1 eq $NaIO_4$

Figure 12 depicts the results of the aldehyde quantification of DAS with the ABAO assay. The oxidated glucose units were calculated from the measured absorption after 21h of reaction

time with ABAO (**1**) with the calibration curve from Figure 9. Figure 12 shows that the percentage of oxidized glucose units increases with the $NaIO_4$ equivalents (given per glucose unit). However, when more than 1 eq per glucose unit is used, the oxidized percentage decreases again to about 80% for 1.25 and 1.5 eq. The phenomenon of decreased aldehyde content above 1 eq. of $NaIO_4$ has been described in the literature before, where it was explained by overoxidation or loss of highly oxidized starch into the solution due to degradation. Starch fragments small enough to be soluble in water are washed away during the washing/centrifugation steps of the process, causing highly oxidized fragments to be lost.[15]

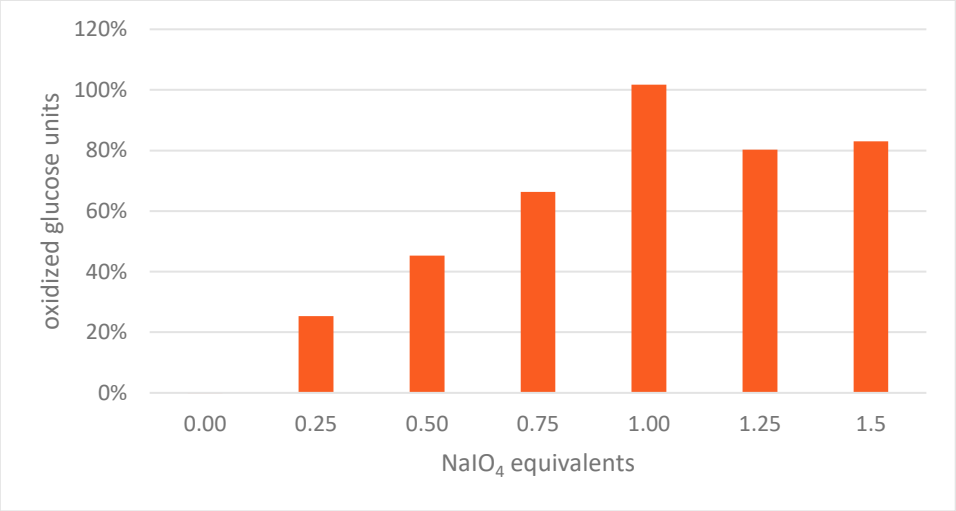

Figure 12 Results of quantification of DAS prepared with different amounts of $NaIO_4$ with ABAO assay

To investigate whether the starch or dialdehyde concentration had an influence on the results of the ABAO assay, the quantification of another batch of 1 eq $NaIO_4$ DAS starch was repeated with varying starch concentrations while the ABAO concentration was kept the same. Figure 13 depicts the results. For 0.5 mg/ml starch concentration – which was the concentration used for the aforementioned measurements in Figure 12 – the dialdehyde content was determined to be 97%, similar to the 105% of the first batch measured the same way. With a starch concentration of 0.25 mg/ml, the same result was measured as with 0.5 mg/ml. However, for higher and lower concentrations, the calculated oxidation varied from these results, indicating that the concentration of starch significantly effects the results of the aldehyde quantification.

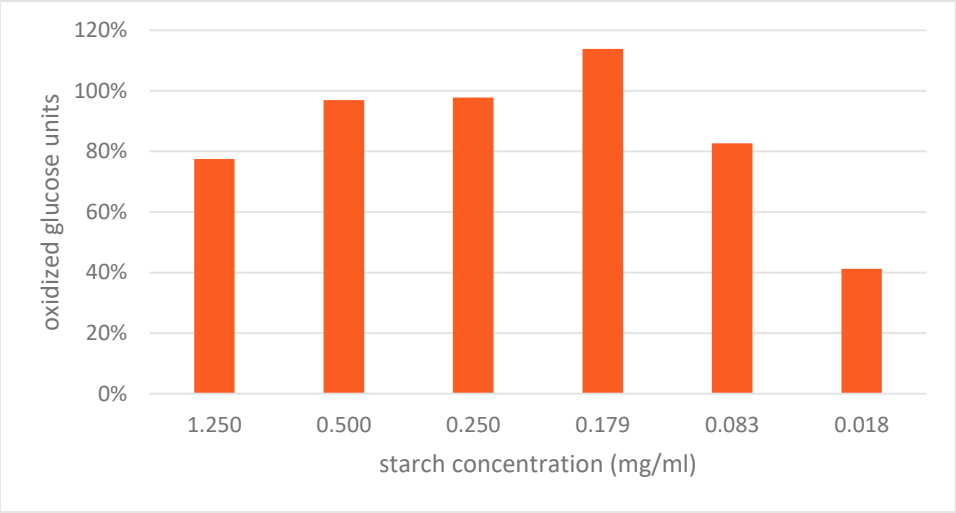

Figure 13 DAS quantification of 1eq $NaIO_4$ DAS with different starch sample concentrations

Overall, further validation is required against conventional, established DAS quantification methods. The quantification as described here is an approximation, assuming that the absorption coefficient of compound **25** would resemble the coefficient of ABAO-DAS adducts. At the least it has been shown here that with the ABAO assay, an increase in absorption in accordance with increasing $NaIO_4$ equivalents during DAS production can be observed and particularly for lower degrees of oxidation also expected aldehyde contents are determined via the ABAO-assay. Thus, our approach seems feasible to measure starches oxidized with new methods to be benchmarked against traditionally prepared starches.

2.3 Selective *O*3-oxidations with catalyst 2

As mentioned in the introduction, one goal of this thesis was the exploration of a new starch oxidation method, yielding DAS in two steps. The first step, which was investigated within this thesis, would consist of a selective oxidation in position 3 of the glucose units with catalyst [(neocuproine)Pd(OAc)]$_2$(OTf)$_2$ (**2**), yielding 3-keto starch. As 3-keto starch has a reactive keto group, it could also be an interesting material for various applications.

Catalyst **2** has been reported to oxidize various carbohydrates selectively in position 3, however, only monosaccharides and rather small oligosaccharides have been tested as substrates.[49-51, 53, 54, 56] The following section is concerned with the investigation of this catalysts **2** ability to oxidize starch, particularly in aqueous medium and with O_2 as final oxidant. As catalyst **2** is not available commercially, this chapter begins with its synthesis. Following that, the model compounds synthesized in 2.1 were reacted with the catalyst **2** to gain an understanding of its reactivity with starch-mimicking compounds. After some optimizations, the catalyst was tested on bigger oligosaccharides: maltodextrins and cyclodextrins. Finally, with knowledge gained from the previous experiments, the catalyst was tested on starch.

2.3.1 Synthesis of catalyst 2

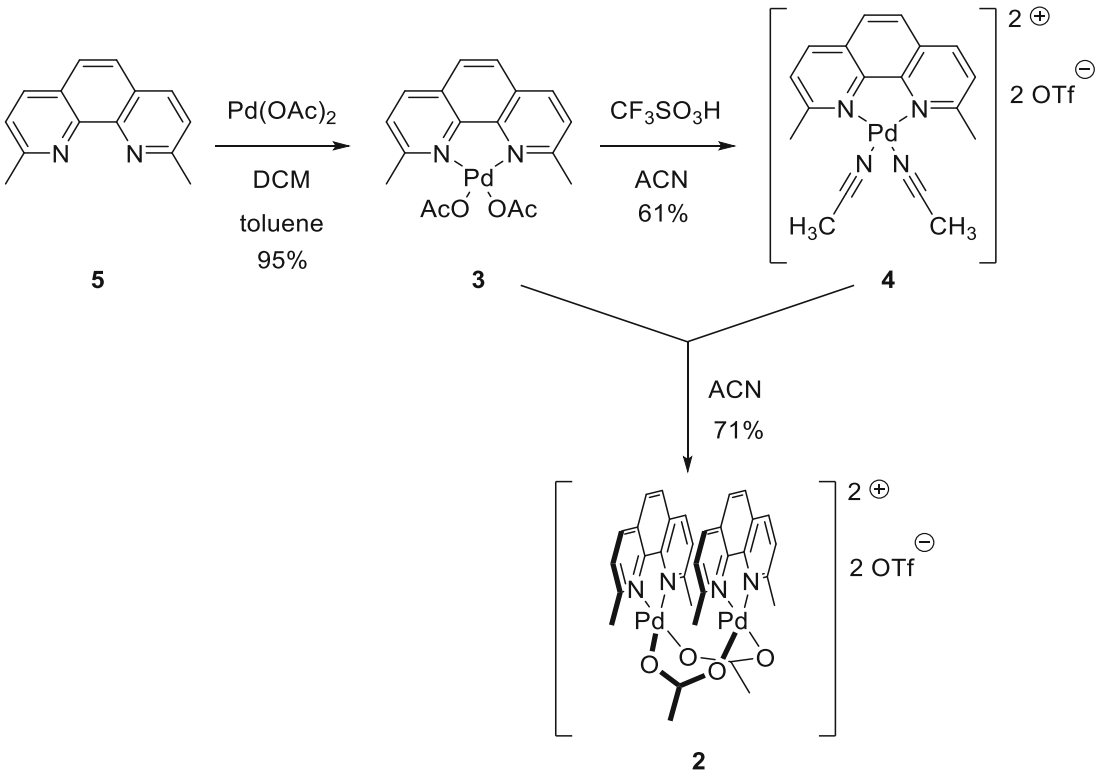

5 **3** **4** **2**

Scheme 16 Synthesis of catalyst 2

As the desired catalyst **2** for the oxidation was not commercially available, it was synthesized in three steps as described in the literature, depicted in Scheme 16.[57, 72]

Complexation of $Pd(OAc)_2$ with neocuproine **5** in DCM and toluene yielded complex **3** with excellent yield. The triflate salt **4** was prepared by adding CF_3SO_3H to **3** in ACN. Workup comprised of precipitation with Et_2O and repeated dissolving in ACN with CF_3SO_3H, yielding the desired product **4** in good yield.

Interestingly, when combining **3** and **4** to give the final catalyst **2**, in one instance only compound **3** was isolated. Most likely this was caused by an incomplete removal of excess CF_3SO_3H. After repeated wash with Et_2O and a repeat of the attempted reaction the target substance was acquired after precipitation with Et_2O.

All three synthesis steps worked as described in the literature with minimal workup, necessitating only filtration or centrifugation after precipitation. Satisfactory yields were achieved in all steps.

2.3.2 Catalytic oxidations of model compounds with catalyst 2 in DMSO

To gain first experience with the catalyst, NMR experiments resembling similar studies by the group of Minnaard[50] were conducted. Substrates were reacted with the catalyst **2** in deuterated solvents, and conversion was determined *via* ^{1}H-NMR measurements of the reaction mixtures and integration of product and substrate peaks.

Methyl α-glucopyranoside (**28**) was chosen as the first test substrate due to its commercial availability. For these first experiments, 3eq. of benzoquinone (BQ) were chosen as the oxidant and DMSO-d6 as the solvent, as these were commonly used conditions within the literature. Repeated NMR measurements after the reaction start were made over the course of 14.5 h to approximate reaction rate. Spectra of selected reaction times are shown in Figure 14. The first measurement after 4 minutes already showed a conversion of approximately 90%. Full conversion was achieved after 8 minutes. This observation is in accordance with the results published by the group of Minnaard, reporting full conversion within 1 h with no sideproducts with the same reaction conditions.[50] However, within our experiments, after full conversion over time at least one sideproduct was forming, consuming the product **29**. After 14.5 h of reaction time, approximately 40% of the keto glucose **29** was converted into this sideproduct.

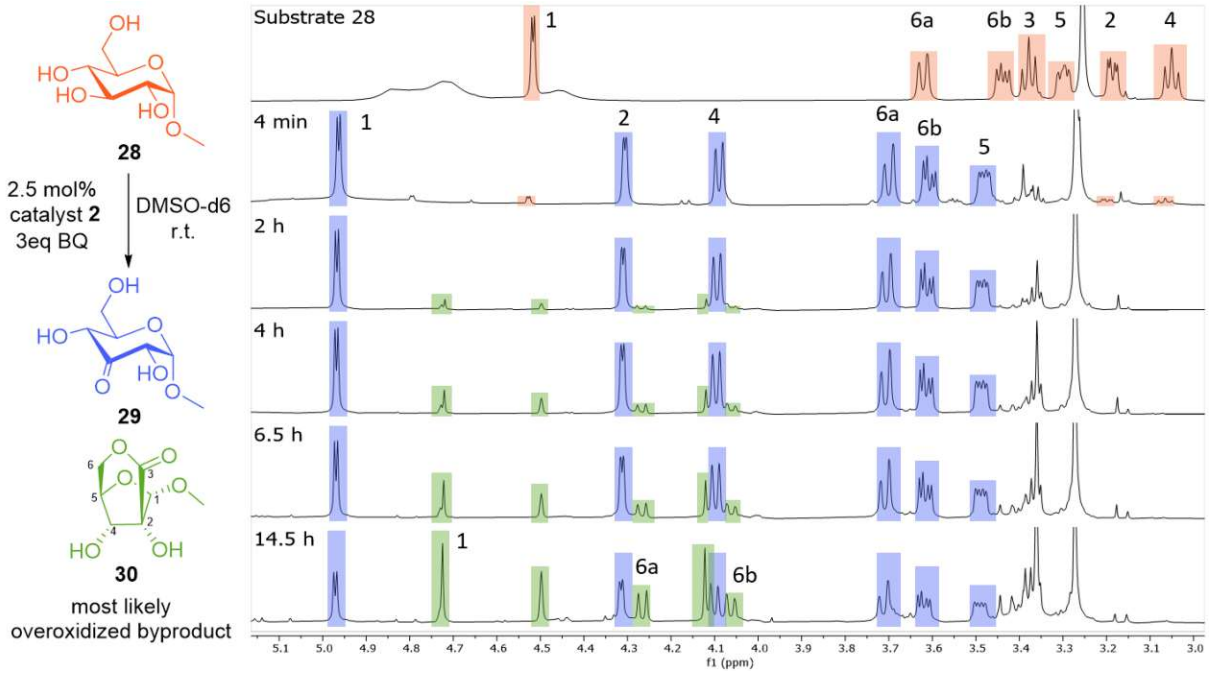

Figure 14 ^{1}H-NMR spectra during reaction of 0.3 M substrate 28 with catalyst 2 at different reaction times.

Looking deeper into the nature of the emerged side product with 2D spectra, a plausible species and its formation mechanism is shown in Scheme 17. The structure of the sideproduct **30** shown in Scheme 17b and Figure 14 formed in the experiments within this thesis cannot be completely confirmed, as it was not isolated, however ^{1}H-NMR and HSQC spectra are in consistence when compared to similar species **31b** reported within the literature.[50] The presence of a cross peak at 171 ppm - the range for esters in ^{13}C-NMR - in the HMBC spectrum further supports this hypothesis. The mechanism for the formation of this species was proposed by Eisink *et al.*[50] Within their paper, the formation of this type of overoxidized side product **31b** was reported with 4-deoxyglucoside (**31a**, shown as the example in Scheme 17a), galactopyranoside and mannopyranoside, but not with glucopyranoside **28**. The mechanism suggests that a ring flip is necessary for this overoxidation to occur, which is how Eisink *et al.* explain the occurrence of this reaction during the reactions with 4-deoxy glucoside **31a** and mannoside and galactoside derivates, where this ring flip is favored.[50]

The occurrence of this side product with model substrate **28,** which is a glucoside derivative where this ring flip is not favored, has not been reported, presumably because the reaction was stopped after full conversion and before a noticeable amount of sideproduct **30** was formed.

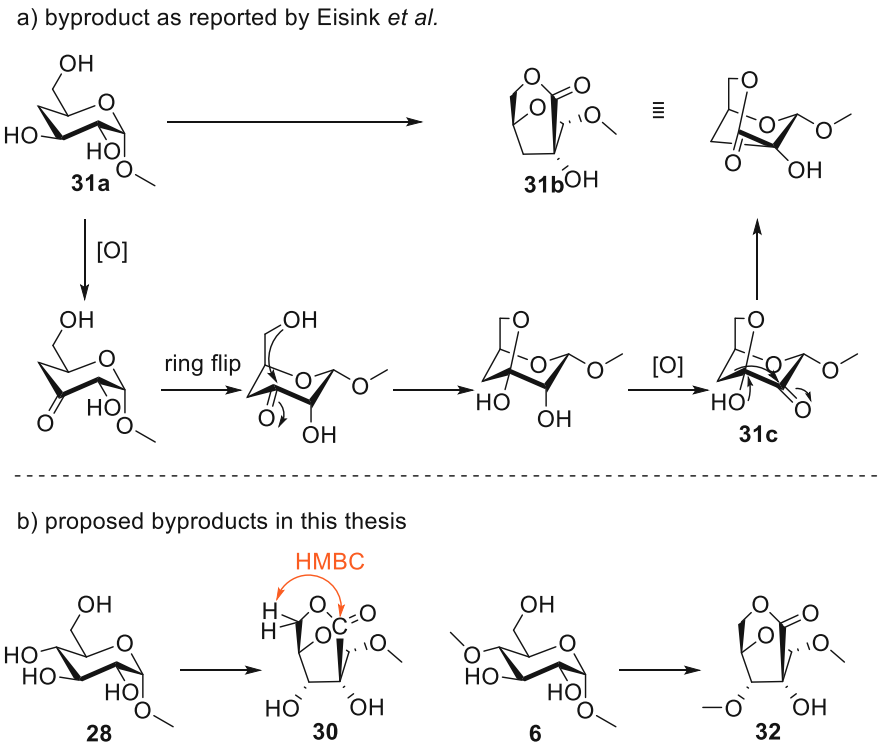

Scheme 17 a) mechanism of substrate overoxidation as proposed by Eisink *et al.*[50] and b) derived plausible sideproducts formed of 28 and 6

When the same reaction was repeated with methyl 4-*O*-methyl-α-glucopyranoside (**6**) and methyl 4,6-di-*O*-methyl-α-glucopyranoside (**7**), the formation of similar side products was observed. For compound **6**, at least two side products were observed, which made interpretation of spectral data difficult, but it is likely that the species are compound **32** and the equivalent of intermediate **31c**, as there are two new CH_2 groups and one signal at 174 ppm and one at 188 ppm in ^{13}C-NMR. The shifts of the peaks in ^{1}H-NMR support this theory as well.

For the compound **7** protected on position *O*6, the mechanism in Scheme 17 is not applicable because there is no free hydroxy group in position 6 capable of forming the internal acetal. However, there was one main sideproduct observed after 2 weeks reaction time, which could possibly be compound **34**, as ^{1}H-NMR, HSQC, HMBC and ^{13}C-NMR suggests. Without the internal acetal, it is possible that an acetal with external nucleophile, most likely OH is formed as suggested in Scheme 18.

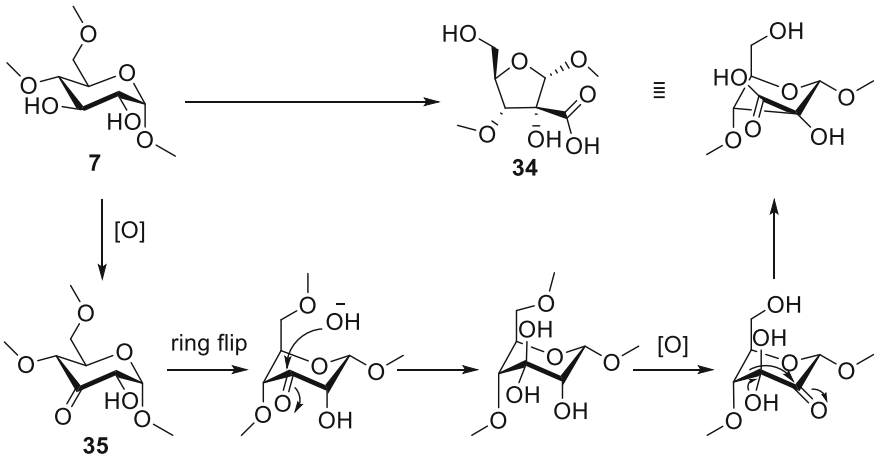

Scheme 18 Possible overoxidation mechanism of compound 7

To investigate the effect of the amount of BQ on the formation of product **29** and sideproduct **30**, experiments with 0.5, 1, 2, and 3 benzoquinone equivalents were conducted, additionally a lower substrate **28** concentration was chosen in order to lower the amount of substrate needed for future experiments. The results are listed in Table 2. They again suggest that the reaction is quite fast, almost all reactions reaching their final conversion after 30 min. With 0.5 eq. BQ, just below 50% conversion were achieved, suggesting that indeed that BQ is needed stoichiometrically.

Interestingly, there was less side product formation with the lower substrate **28** concentration of 0.085 M when compared to the time resolved experiment with 0.3 M concentration, forming approximately 19% sideproduct **30** for both 2 and 3 eq. BQ, while only small traces were visible with lower equivalents oxidant. As the mechanism leading to this sideproduct **30** requires a second oxidation to occur per molecule, the lower oxidant equivalents lead to lower side product **29** formation. This has also been described by Eisink *et al.*[50]

Table 2 Conversion of methyl α-glucopyranoside (28, 0.085 M)) with 2.5 mol% catalyst 2 and varying equivalents of benzoquinone (BQ) in DMSO-d6 at r.t.

	NMR-conversion			
Reaction time	**0.5 eq BQ**	**1 eq BQ**	**2 eq BQ**	**3 eq BQ**
0.5 h	45%	78%	93%	100%
5 h	43%	83%	100%	100%
14 h	45%	86%	100%	100%

Table 3 Conversion during control experiments with methyl α-glucopyranoside (28, 0.085 M), catalyst 2 and benzoquinone (BQ) in DMSO-d6 at r.t. after 24 h reaction time

	NMR-conversion
2.5 mol% catalyst, 0 eq. BQ	9%
2.5 mol% catalyst, 0 eq. BQ, O2 atmosphere	15%
no catalyst, 3 eq. BQ	0%

The results of some control experiments are listed in Table 3They show that catalyst **2** can oxidize substrate **28** without BQ present, reaching 9% conversion. As the observed conversions are higher than the amount that would be converted stoichiometrically with the catalyst, the catalyst must be reoxidized to its active form to some extent. Presumably the reoxidation is performed by O_2 in the solvent, which is supported by the fact that conversion was higher in O_2 atmosphere, reaching 15%. The control experiments also confirmed that there is no direct reaction between substrate **28** and BQ when no catalyst is present.

2.3.3 Optimization of aerobic oxidations of methyl glucoside under aqueous conditions

After the examination of the oxidation of the model compounds and the investigation of their formed byproducts in DMSO, first attempts were made to get closer to the desired reaction conditions for starch oxidation, using water as solvent and O_2 as oxidant.

Figure 15 depicts the ^{1}H-NMR spectra of the reaction between substrate **28** and catalyst **2** in D_2O/CD_3CN solvent with benzoquinone BQ as the oxidant. The CD_3CN content was necessary due to the limited solubility of BQ in water. Based on literature data, a slower reaction in D_2O/CD_3CN compared to DMSO was to be expected.[52] The reaction reached 91% conversion after 18h at room temperature. This is less conversion than the full conversion observed in DMSO, however, on the upside, the side product of the overoxidation was not formed in the aqueous system. Not only did this simplify the interpretation of the results (made obvious when comparing Figure 14 and Figure 15), but the avoidance of overoxidation is also desired for the end goal of oxidizing starch.

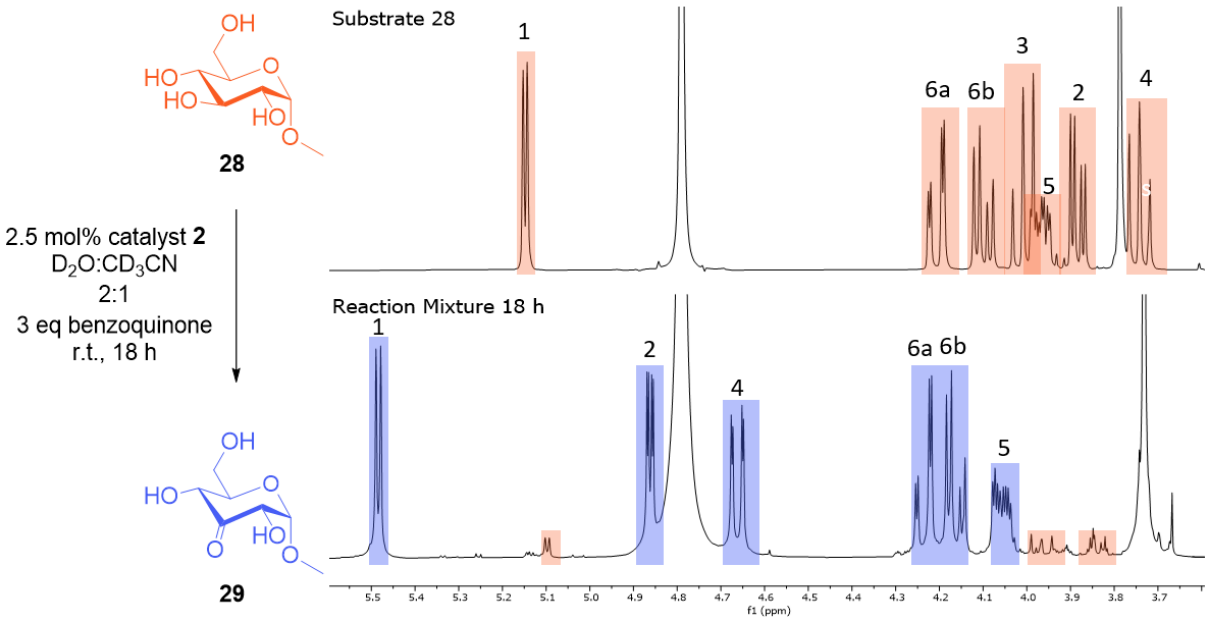

Figure 15 ^{1}H-NMR spectra of reaction between methyl α-glucopyranoside (28) and catalyst 2 in D_2O/CD_3CN with benzoquinone as oxidant

With these promising results, as a next step an exchange of oxidant from BQ to O_2 was attempted. Thus, the solubility of BQ was now irrelevant, enabling a switch of the solvent to pure D_2O. First results at room temperature, both with air and O_2 atmosphere, were rather unsuccessful, reaching quite low yields of 17-19% after 17h reaction time, listed in Table 4. An improvement in conversion was observed with both air (29%) and O_2 (46%) by increasing the reaction temperature to 60°C, consistent with findings by Chung *et al.* for aerobic oxidations of similar substrates with catalyst **2.**[56] Running the reaction longer than 2 h did not further increase conversion. Under inert (Ar) atmosphere, a conversion of 9% was reached, a higher conversion than what would be stoichiometric with 2.5 mol% catalyst used. Before the inert reaction, the used solvent was degassed with argon in an ultrasonic bath, however, there still could be some remainder of O_2 in the solvent causing the higher than expected conversion.

Table 4 Experiments with substrate 28 and 2.5 mol% catalyst 2 in D_2O, using O_2 or air as oxidant

atmosphere	conditions	
	17 h, r.t.	2 h, 60°C
Inert	-	9%
Air	17%	29%
O_2	19%	46%

Literature suggests that the main reason for the low conversion of substrate under aerobic conditions is catalyst degradation due to oxidation and Pd black formation. A way of mitigating the oxidative degradation reported in the literature is the addition of H-radical donors, particularly phenol.[58] Table 5 lists the conversion of the reaction in water with acetic acid, hydroquinone and phenol as additives. Acetic acid was added to test its potential to speed up

the formation of an acetic acid complex that is not as easily oxidized, as is suggested by the catalyst mechanism proposed by Ho *et al.*[58] This approach was not fruitful, as the addition of 2 v% acetic acid decreased the conversion. Various equivalents of phenol were tested to check its potential and to find an optimal amount. It was found that it increased the conversion with air, while the conversion with O_2 was slightly decreased. One reason for this phenomenon is the possibility of the O_2 oxidizing the phenol before it can help to mitigate the oxidation of the catalyst. Perhaps oxidized phenol can then further interact with and destroy the catalyst. A plateau was reached at 64% yield with 0.75 eq. phenol, while 1 eq. phenol increased the yield only slightly to 66 %. Hydroquinone was tested as a less toxic variant of phenol; however, it decreased the conversion with air drastically from 29% to 10%.

Table 5 Conversion of reactions with different additives, substrate 28 (0.085M) with 2.5 mol% catalyst 2 in D_2O, 60°C, 2h

Additive	Conversion with air	Conversion with O_2
None	29%	46%
Acetic acid (2v%)	-	29%
Phenol 0.25 eq	51%	35%
Phenol 0.5 eq	55%	24%
Phenol 0.75 eq	64%	38%
Phenol 1 eq	66%	36%
Phenol 1.25 eq	62%	-
Phenol 1.5 eq	53%	-
Hydroquinone 1 eq	10%	-

To further try and achieve higher conversions, the catalyst loadings were increased to 5 mol% and 10 mol%, each with 1 eq. phenol in relation to the substrate **28**. The results are shown in Table 6. Increasing catalyst amount from 2.5 to 5 mol% catalyst led to no improvement of conversion. With 10 mol%, a conversion of 85% after 2h was achieved. Prolonging the reaction time from 2h to 6h did not further raise conversion, suggesting that the catalyst had fully degraded after this point.

Table 6 Conversion of reactions with different catalyst loadings with substrate 28 with 1 eq phenol in D_2O, 60°C, air

mol% catalyst 28	Conversion after 2 h	Conversion after 6 h
2.5	66%	-
5	68%	67%
10	85%	83%

2.3.4 Aerobic oxidations of model compounds and starch under aqueous conditions

After these optimization experiments in D_2O with methyl α-glucopyranoside (**28**), it was time to move on to model compounds closer to starch. The two simplest model compounds **6** and **7**, methylated at *O*4 and *O*4 and *O*6 respectively, are protected with methyl groups at the positions where glucose units are bonded to the neighboring glucoses in amylose and amylopectin, respectively. They were reacted with the catalyst for 2h at 60 °C in D_2O and yielded the expected keto derivatives **33** and **35** (depicted in Scheme 19) in 23% and 29% yield again with no side product formation according to ^{1}H-NMR. The lower conversions compared to methyl glucoside **28** is likely caused by steric hindrance of the substituents at *O*4 and not a lack of binding to OH at position 4, as found by Eisink *et al.*[50] The higher conversion of methyl 4,6-di-*O*-methyl glucopyranoside (**7**) compared to methyl 4-*O*-glucopyranoside (**6**) is surprising, as the same paper[50] suggested a lower conversion of mannoside after *O6* protection with a TIPS group. Possibly the TIPS group had a bigger steric effect due to its size, while the smaller *O*6 methyl group of compound **7** had less of an effect and the 5% difference are caused by the limits of NMR analysis.

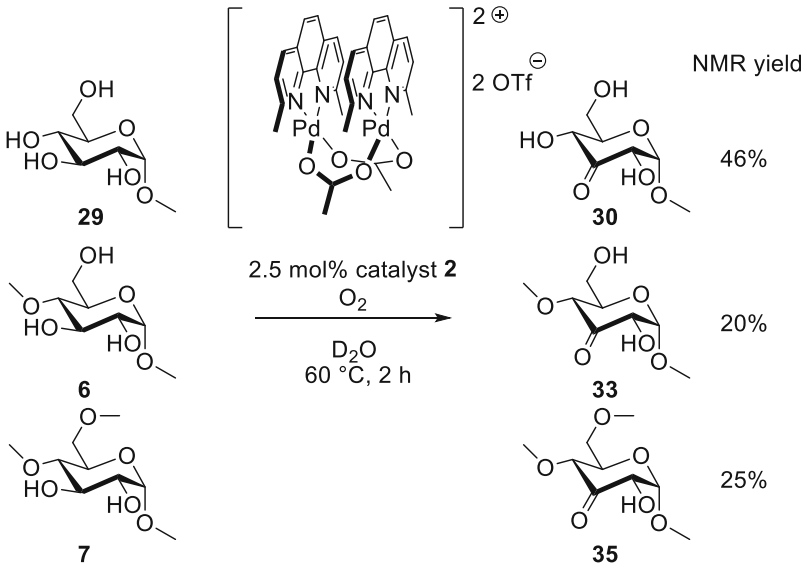

Scheme 19 Reactions with model compounds 29, 6 and 7 and catalyst 2 in D_2O

The next model substrate tested with the catalyst was methyl 4'-*O*-methyl-β-maltoside (**8**). As it consists of two glucose units joined with an α-1,4 glycosidic bond, it should resemble the short-range steric hindrance in starch caused by neighboring glucose units. Scheme 20 depicts the ^{1}H-NMR spectra recorded after 2 h reaction time with 10mol% catalyst and 16 h reaction time with 24 mol% catalyst. The spectra depict a complex mixture of substrate **8** and several products, which makes the identification of these products challenging. The most probable structure of the main product in the reaction with a lower catalyst amount, marked in red in

Scheme 20, is the maltoside oxidized solely in the non-reducing end glucose unit **36**. The H1' is clearly distinguishable in ^{1}H-NMR due to its characteristic coupling constant and its shifts in HSQC. The downfield shift from substrate **8** to oxidized product **36** resembles the shift observed in the simpler model compounds described above. The shifts and coupling constants of the hydrogen atoms 2' and 4' marked red in Scheme 20 are also characteristic. The last characteristic peak of compound **36** is the H1 peak marked in red, which is minimally shifted upfield. This suggests that the other ring of the maltoside is not oxidized. Other side products were much more difficult to analyze. One of the side products seems to be oxidized in the first glucose unit, its characteristic H1-H2-H4 peak set is marked green in Scheme 20. Because this product is present in lower amounts, the corresponding peaks of the second ring of this compound are not distinguishable, and thus no distinction can be made between structure **37a** and **37b** for this product. Catalyst amount and reaction time were increased to 24 mol% and 15 h to attempt to change the ratio of products and enable structure analysis, however an even more complex mixture was obtained, and no further insights were generated.

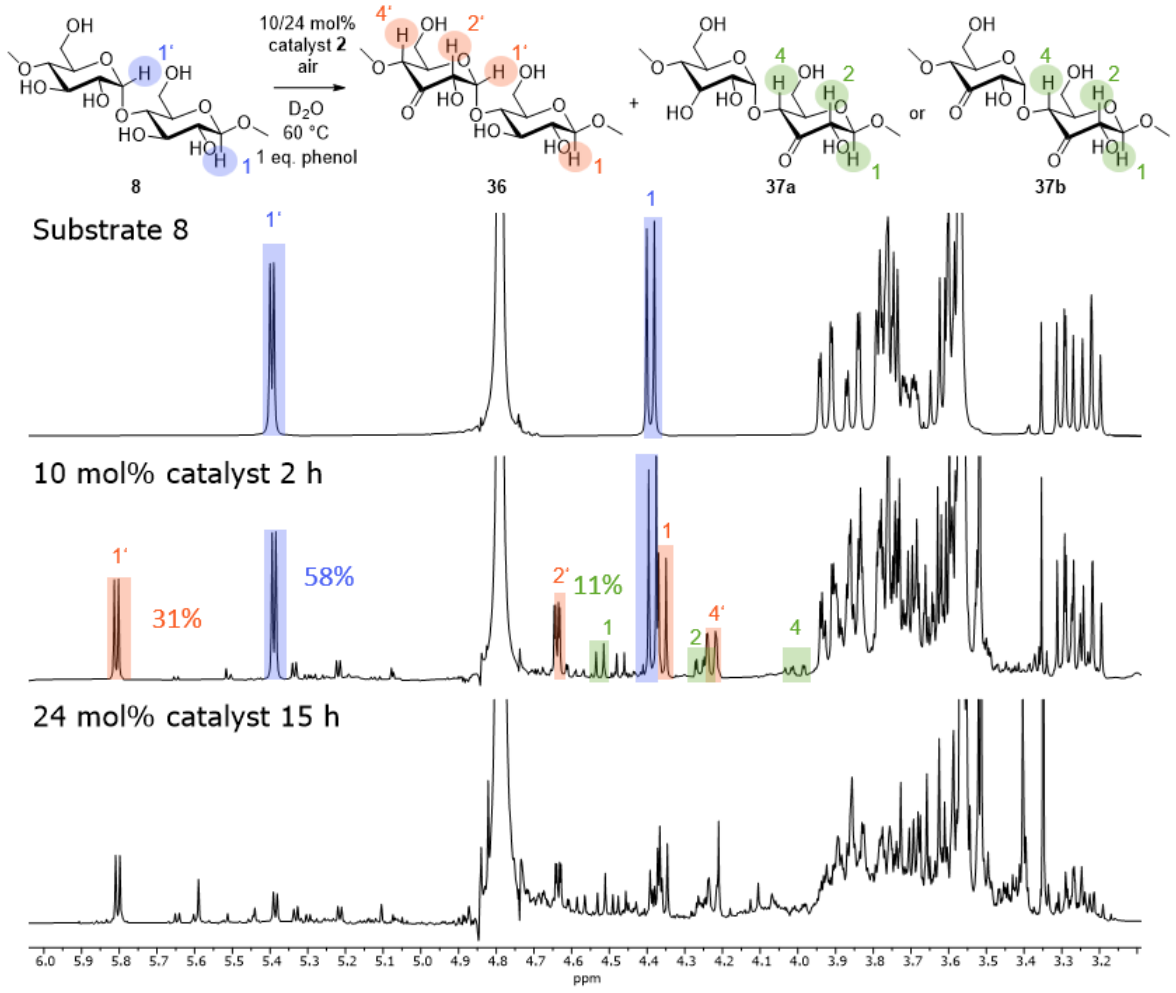

Scheme 20 Reaction of maltoside substrate 8 with catalyst 2 in D_2O. Most likely products are marked in the ^{1}H-NMR spectra.

Even though the structure of the second product was not fully confirmed, the fact that about 11% of the substrate **8** were converted to a product where the more hindered first glucose unit was oxidized is promising. The more sterically available second unit was oxidized more readily (31%), which is congruent to literature data where the terminal end of 1,4-α glucoside oligosaccharides was oxidized selectively.[49]

Moving on to model substrates even closer to starch, cyclodextrins were tested. Cyclodextrins are cyclic oligosaccharides of 1,4-α bonded glucoses, and thus are very good model compounds for starch. The cyclodextrins tested within this thesis were β-cyclodextrin **38**, γ-cyclodextrin **39**, and δ-cyclodextrin **40**[73], with 7, 8 and 9 glucoses per molecule, respectively. Representative of all three compounds, the results of the oxidation of β-cyclodextrin **38** are depicted in Scheme 21. The ^{1}H-NMR signals of the cyclodextrin **38** before oxidation are distinct peaks, as every glucose unit in the molecule is chemically equivalent. The oxidation of glucose units within the ring disturbs this equivalence, resulting in an ^{1}H-NMR spectrum with broad peaks containing multiple similar species. The H1 signals of oxidized glucose units at 5.44 ppm are clearly distinguishable from the unoxidized units due to their characteristic downfield shift, as observed for all previous model compounds. The signals at 4.62 ppm correspond to the H2 and H4 signals of oxidized units. Interestingly, the H1 signals of unoxidized units at 5.03 ppm have an upfield shoulder with the same integral as the oxidized units. Most likely, these upfield shifted protons are H1 signals of unoxidized glucoses neighboring oxidized glucose units, in consistence with the H1 shift of the unoxidized ring of keto-maltoside derivative **36** in Scheme 20. The percentage of oxidized glucoside units determined by integration of the H1 signals was 26%, meaning statistically 1.8 units per cyclodextrin were oxidized.

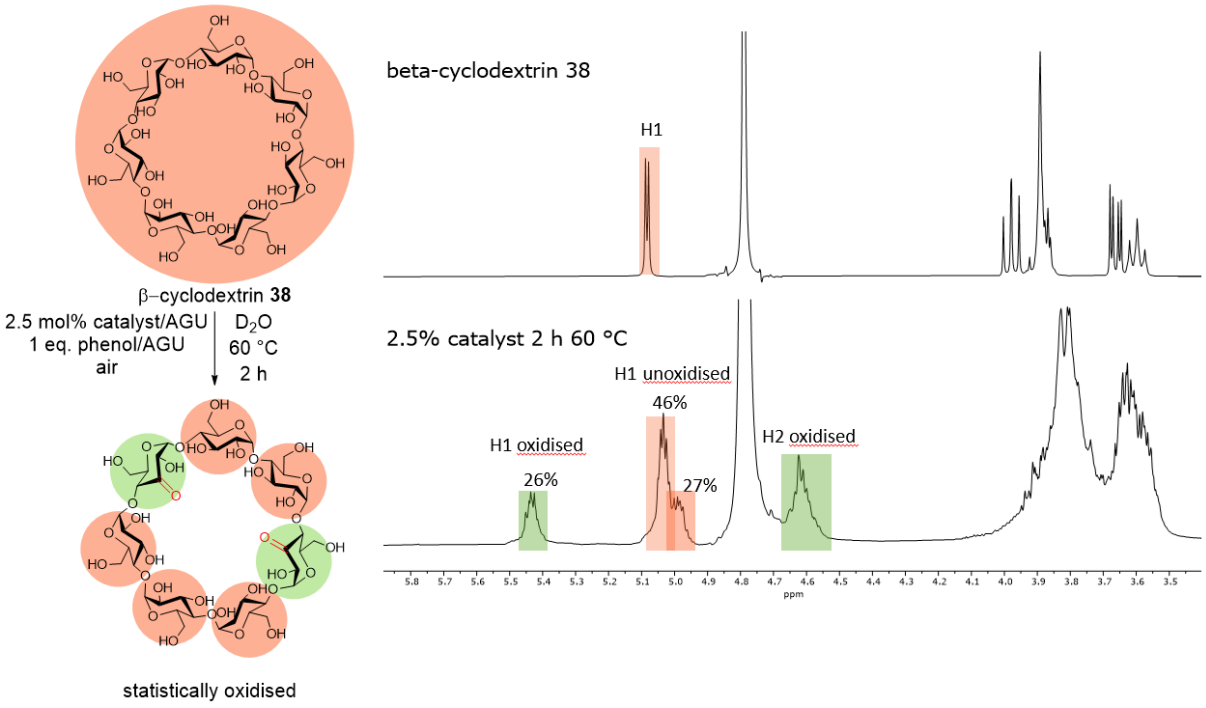

Scheme 21 ^{1}H-NMR spectra of oxidation of β-cyclodextrin 38 with catalyst 2

In analogous experiments, γ- and δ-cyclodextrin **39** and **40** behaved similarly, the results are listed in Table 7. Remarkably, δ-cyclodextrin **40** is not commercially available and was kindly provided by Professor Sophie Beeren.[73] Its reactivity in the oxidation was comparable to its smaller analogues **38** and **39**. There seems to be a small trend of decreasing oxidation degree with increasing molecule size, however.

In cyclodextrins, every single glucose unit is bound to another, meaning every glucose is severely sterically hindered, similarly to the hindrance in starch. The fact that oxidation was achieved nonetheless is promising that also starch could not only be oxidized on nonreducing terminal units, but also within the sterically hindered chain.

Table 7 Oxidized glucose units of reactions of cyclodextrins (0.085 M AGU units) with 2.5 mol% catalyst 2 and 1 eq. phenol per glucose unit in D_2O

Substrate	Glucose units per molecule	Oxidized Glucose Units	Oxidized units per molecule
β-cyclodextrin 38	7	26%	1.8
γ-cyclodextrin 39	8	19%	1.5
δ-cyclodextrin 40	9	15%	1.4

Another readily available oligosaccharide related to starch is maltodextrin. Maltodextrins are obtained by hydrolysis of starch and consist of the same 1,4-α bonded glucoses while also being linear. The results of a reaction between a maltodextrin and the catalyst are depicted in Scheme 22. Maltodextrins can contain very short oligosaccharides and even glucose, which increases the amount of unsubstituted *O*4 positions. These are oxidized more readily, as

described above, and lower the comparability with starch, which contains fewer terminal groups and no monosaccharides. To check the amount of these readily oxidizable groups in the maltodextrin used, ^{1}H-NMR was applied and compared to a spectrum of glucose. A comparison is shown in Scheme 22, revealing a glucose content of approximately 5%. The peak at 3.42 ppm corresponds to terminal H4 peaks of oligosaccharides[74] (excluding glucose, its H4 peak is shifted upfield at 3.28 ppm), their content was determined to be 11%, leading to a total of 16% of readily oxidizable glucose units. After the reaction with the catalyst, the oxidized glucose units were determined as described with the cyclodextrins above, revealing a degree of oxidation of approximately 17%, which fits the amount of easily oxidizable units.

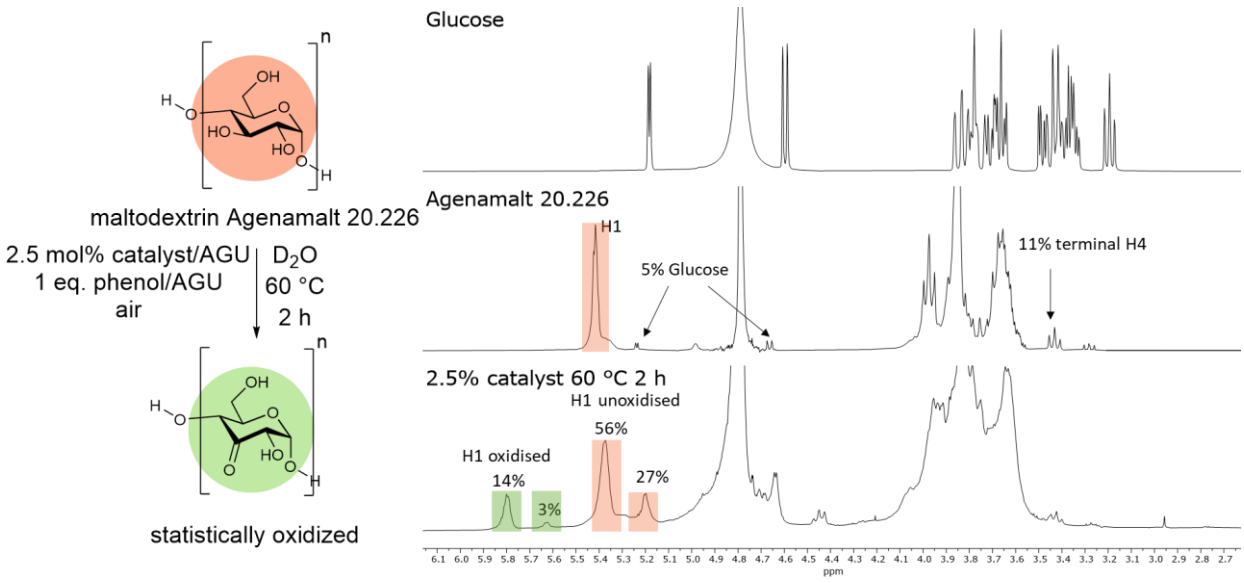

Scheme 22 ^{1}H-NMR spectrum of oxidation of a maltodextrin with catalyst 2

A second maltodextrin sample was treated the same way. Here no glucose was found and the terminal H4 percentage in the unreacted maltoside was 13%. After the reaction, the oxidation degree was determined to be 19%, which is higher than the amount of terminal H4, suggesting that more sterically hindered glucose units within the chain were oxidized as well. The results of the maltodextrin oxidations are listed in Table 8.

Table 8 Oxidized glucose units of maltodextrins (0.085 M glucose units) with 2.5 mol% catalyst 2 and 1 eq. phenol per glucose unit in D_2O

Substrate	Glucose Percentage	Terminal H4 percentage	Oxidized Glucose Units
Maltodextrin Agenamalt 20.226	5%	11%	17%
Maltodextrin ARIC 6499	0%	13%	19%

Ultimately, starch was reacted with catalyst **2**. The results of this experiment are shown in Scheme 23. The integral of the triplet at 3.44 ppm corresponding to the terminal H4 signals

was again used to estimate the amount of terminal glucose units, which are tentatively more easily oxidized, which was approximated to be about 7%. The spectrum resulting from the reaction with catalyst **2** can be interpreted based on the previous findings with the simpler, starch like model compounds. Peaks of H1 of unoxidized and oxidized glucose units are assigned in Scheme 23, analog to the corresponding signals described for all model compounds. The small peak at 5.63 ppm could correspond to oxidized glucose units neighboring another oxidized unit, or terminal units. The peaks at 5.21 ppm most likely correspond to H1 peaks of glucose units next to oxidized ones, as described for cyclodextrin above. The combined oxidized glucose unit percentage sum up to approximately 20%, which is distinctly higher than the easily oxidizable 7% of terminal glucose units. This means the oxidation of starch with catalyst was successful, reaching even more sterically shielded groups inside the glucoside chain. These exciting results conclude the experiments with catalyst **2** within this thesis.

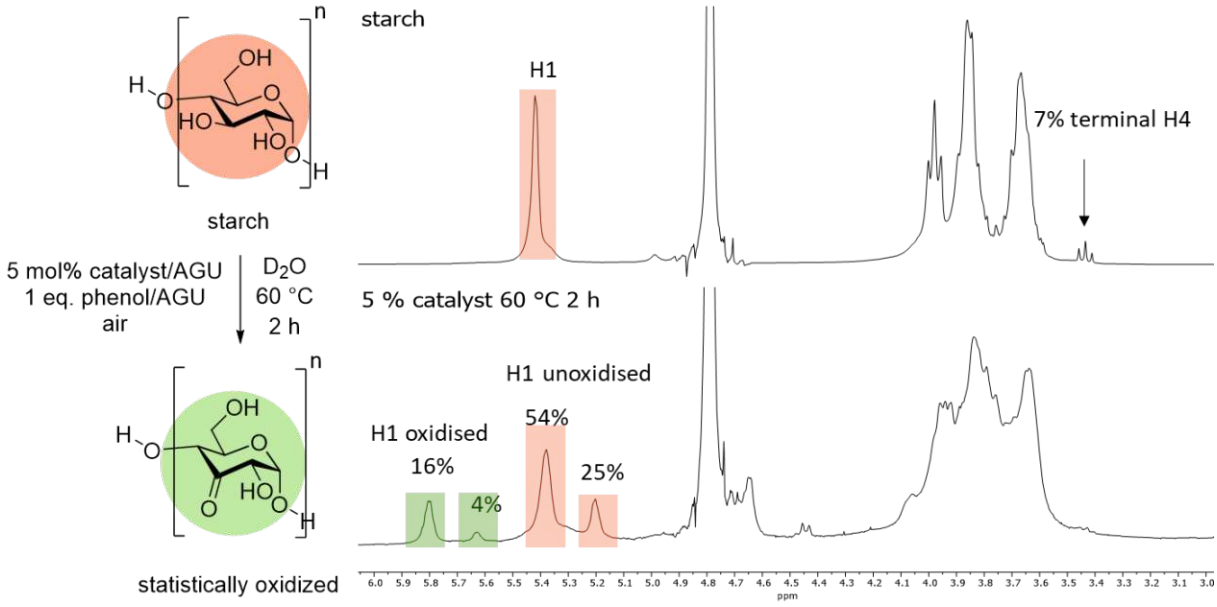

Scheme 23 ^{1}H-NMR spectra of oxidation of starch with catalyst 2

2.4 Summary and Outlook

Within this thesis, progress toward a new, catalytic oxidation method of starch was made.

For a solid analytical basis, model compounds mimicking starch were chosen as test substrates. Three of those model compounds, methyl 4-*O*-methyl-α-D-glucopyranoside (**6**), methyl 4,6-di-*O*-methyl-α-D-glucopyranoside (**7**) and methyl β-maltopyranoside (**8**) are not commercially available and were synthesized in multiple step reactions.

A new approach for the determination of carbonyl content of DAS was demonstrated. For this purpose, model compound methyl-α-glucopyranoside (**28**) was oxidized with $NaIO_4$ and the resulting dialdehyde compound reacted with ABAO (**1**), proving the reactivity of ABAO for this application. DAS samples were prepared by reacting varying amounts of $NaIO_4$ with starch. The absorption of the adducts formed between those DAS samples and ABAO was proportional to the amount of $NaIO_4$ used for the oxidation, showcasing the ability of this assay to determine carbonyl contents of DAS. This approach is much more convenient than current carbonyl content determination methods, and it is suited for high-throughput applications.

Various model compounds mimicking starch were oxidized selectively by catalyst **2**, yielding the respective 3-keto derivatives. The simplest model compound, methyl-α-glucopyranoside (**28**) was used for first optimization experiments. The formation of overoxidized byproducts in DMSO was investigated. In aqueous solvent, the reaction was optimized for aerobic oxidation. It was found that a temperature of 60 °C is necessary for the reaction to occur. With aerobic oxidation, the use of phenol was crucial to mitigate catalyst degradation. Further tests with other model compounds, including the synthesized model compounds **6**, **7** and **8**, cyclodextrins and maltodextrins, were conducted in preparation for the oxidation of starch.

Lastly, starch was oxidized with catalyst **2** and 1 equivalent of phenol with air as terminal oxidant, yielding about 20 % of oxidized glucose units as determined by ^{1}H-NMR.

These are quite promising results, laying the groundwork for future research to push this oxidation method towards industrial applicability.

Firstly, the additive used within this thesis, phenol, is highly toxic and replacements should be investigated for industrial use. Less toxic alternatives should be explored, including catalases.

Another important factor to consider for future research is scale up, as the experiments within this thesis were conducted in NMR-scale only. The catalyst could be further optimized by tuning of the ligand, for example to improve its solubility in water.

Finally, while 3-keto starch could be a potential candidate as a promising, renewably sourced material, DAS is already well researched and could offer many possibilities for a wide range of

applications. Further research is needed to facilitate a second step, cleaving 3-keto starch to produce DAS.

3 Experimental part

3.1 General methods

3.1.1 Reagents and solvents

All chemicals were used directly from commercial sources and used without further purification.

Ion exchange resins were washed with the respective solvent prior to use. Ratios of liquids used as solvents or as eluents are given as volume ratios. Methyl 2,3-di-*O*-benzyl-4,6-*O*-benzylidene-α-D-glucopyranoside (**9**) and ABAO (**1**) was available in the research group. Starch and maltodextrins were provided by AGRANA. δ-cyclodextrin was provided by professor Sophie Beeren from the Technical University of Denmark.

3.1.2 TLC

TLC analysis for reaction monitoring and analyzing fraction from column chromatography was performed on silica gel 60 F254-plates or HPTLC-plates (silica gel 60 F_{254} with concentration zone 20×2.5 cm) with LP/EtOAc or $CHCl_3$/MeOH/H_2O as eluents. The spots were visualized using UV light (254 nm) followed by staining the plates with anisaldehyde solution (180 ml EtOH, 10 ml anisaldehyde, 10 ml H_2SO_4 conc., 2 ml AcOH) or cerium molybdate solution ("Mostain", 21 g $(NH_4)_6Mo_7O_{24}\cdot 4\ H_2O$, 1 g $Ce(SO_4)_2$ 31 ml H_2SO_4 conc., 500 ml H_2O).

3.1.3 Column chromatography

Generally, column chromatography was performed on a Büchi Pure C-850 FlashPrep system or by hand, with silica gel from Merck (40-63 µm; self-packed columns). As eluent gradients of EtOAc in LP were used.

3.1.4 Melting points (m.p.)

Melting points were determined with a Kofler-type Leica Galen III.

3.1.5 NMR

NMR spectra were recorded from D_2O or DMSO-*d6* solutions. For 400 MHz ^{1}H-NMR and 101 MHz ^{13}C-NMR an Avance UltraShield 400 spectrometer and for 600 MHz ^{1}H-NMR and 151 MHz ^{13}C-NMR an Avance III HD 600 spectrometer was. ^{13}C in DMSO-*d6* and ^{1}H spectra were calibrated to the solvent residual peak. In D_2O, ^{13}C spectra were calibrated *via* absolute referencing based on the corresponding ^{1}H spectrum. Chemical shifts (δ) are reported in ppm, coupling constants in Hz. Assignments were based on COSY, HSQC and HMBC experiments.

The labeling of protected carbohydrates is presented here:

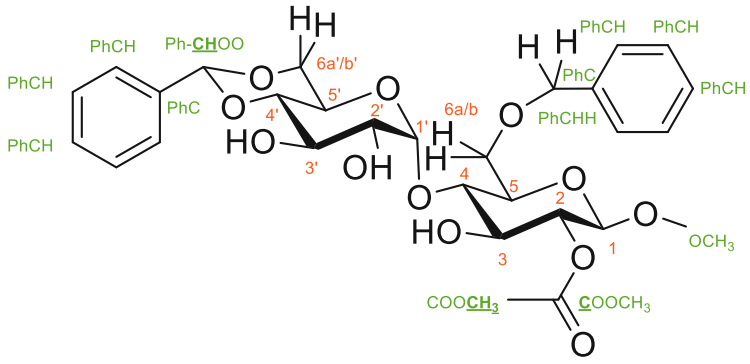

3.1.6 UV-VIS measurements

UV/Vis measurements were performed on a plate reader Zenyth 3100 from Anthos spectrometer equipped with a thermostat at 20 °C.

3.1.7 LCMS

All LCMS samples were dissolved in an acetonitrile/water mixture with a concentration of about 1 mg/ml. Analyses were performed on a Nexera X2® UHPLC system (Shimadzu®) equipped with LC-30AD pumps, a SIL-30AC autosampler, CTO-20AC column oven and a DGU-20$A_{5/3}$ degasser module. Detection was accomplished by concerted efforts of SPD-M20A photo diode array, a RF-20Axs fluorescence detector, an ELS-2041 evaporative light scattering detector (JASCO®) and finally *via* a LCMS-2020 mass spectrometer (ESI/APCI). If not stated otherwise, all separations were performed using a Waters® XSelect® CSH™ C18 2,5 µm (3.0 x 50 mm) Column XP at 40 °C, and a flowrate of 1.7 mL/min and water/acetonitrile + 0.1% formic acid gradient elution.

3.2 Preparation of model compounds

3.2.1 Methyl 2,3,6-tri-*O*-benzyl-α-D-glucopyranoside[63] [10]

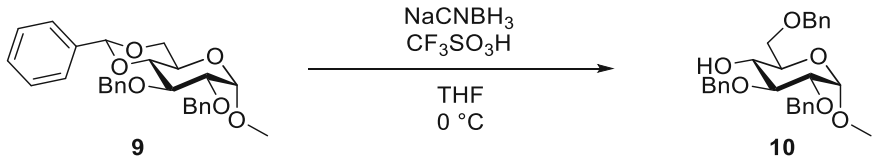

9
$C_{28}H_{30}O_6$
M = 462.54

10
$C_{28}H_{32}O_6$
M = 464.56

Procedure: To a cooled solution (-5 °C) of the benzylidene protected starting material **9** (1.00 g, 2.16 mmol, 1.00 eq.) in anhydrous THF (20 ml) $NaCNBH_3$ (1.00 g, 15.1 mmol, 7.00 eq.) was added, followed by dropwise addition of CF_3SO_3H (1.37 ml, 15.1 mmol, 7.00 eq.) maintaining a maximum temperature of 3 °C. The solution was stirred at 0 °C for 1.5 h, when full conversion was observed *via* TLC (LP:EtOAc = 1:1).

Workup: The mixture was poured into ice water (20 ml). The aqueous phase was extracted with DCM (4 × 20 ml). The combined organic layers were washed with saturated $NaHCO_3$ solution (40 ml), dried over Na_2SO_4 and concentrated. Purification of the crude material was achieved *via* column chromatography with SiO_2 (90 g) and a gradient of EtOAc in LP from 15% to 40% and afforded the product **10** in a yield of 763 mg (76%), pure according to ^{1}H-NMR in and with spectral data in accordance to the literature.[63]

Yield	763 mg (76%)
Appearance	slightly yellow oil
TLC	R_f (LP:EtOAc = 1:1) = 0.44
Optical rotation	$[\alpha]_D^{20}$ = **+13.0** (*c* 1.0, $CHCl_3$), (Lit.: $[\alpha]_D^{25}$ = +12.5 (*c* 1.0, $CHCl_3$))[63]

^{1}H NMR (600 MHz, Chloroform-d) δ 2.35 – 2.41 (s, 1H, OH), 3.39 (s, 3H, OC**H**$_3$), 3.54 (dd, *J* = 9.6, 3.5 Hz, 1H, H2), 3.61 (t, *J* = 9.2 Hz, 1H, H4), 3.68 (d, *J* = 3.8 Hz, 2H, H6a&b), 3.72 (dt, *J* = 9.4, 3.7 Hz, 1H, H5), 3.80 (dd, *J* = 9.6, 8.8 Hz, 1H, H3), 4.55 (d, *J* = 12.2 Hz, 1H, PhC**H**H (*O*6)), 4.60 (d, *J* = 12.2 Hz, 1H, PhCH**H** (*O*6)), 4.64 (d, *J* = 3.6 Hz, 1H, H1), 4.67 (d, *J* = 12.1 Hz, 1H, PhC**H**H (*O*2)), 4.75 (d, *J* = 11.5 Hz, 1H, PhC**H**H (*O*3)), 4.78 (d, *J* = 12.1 Hz, 1H, PhCH**H** (*O*2)), 5.01 (d, *J* = 11.4 Hz, 1H, PhCH**H** (*O*3)), 7.26 – 7.39 (m, 15H, 15 × PhH).

^{13}C NMR (151 MHz, Chloroform-d) δ 55.4 (O**C**H$_3$), 69.6 (C6), 70.0 (C5), 70.8 (C4), 73.3 (Ph-**C**H$_2$ (*O*2)), 73.7 (Ph-**C**H$_2$ (*O*6)), 75.5 (Ph-**C**H$_2$ (*O*3)), 79.7 (C2), 81.6 (C3), 98.3 (C1), 127.7, 127.8, 128.0, 128.07, 128.12, 128.2, 128.5, 128.6, 128.7 (15 × PhCH), 138.1, 138.2 (2 × PhC1), 138.9 (PhC1 (*O*3)).

LC-MS: ($^+$ESI-TOF) m/z $[M + NH_4]^+$: calcd. for $C_{28}H_{36}NO_6$ 482.254, found 482.15

3.2.2 Methyl 2,3,6-tri-*O*-benzyl-4-*O*-methyl-α-D-glucopyranoside[63] [11]

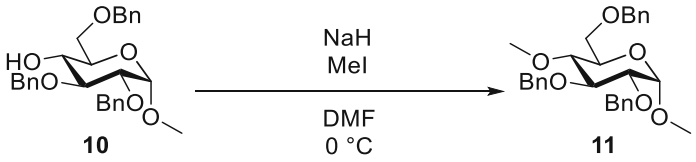

10 $C_{28}H_{32}O_6$ M = 464.56

11 $C_{29}H_{34}O_6$ M = 478.59

Procedure: To a solution of the starting material **10** (6.60 g, 14.2 mmol, 1.00 eq.) in anhydrous DMF (85 ml) sodium hydride (60 w%, 1.25 g, 31.2 mmol, 2.20 eq.) was added at 0 °C. After stirring for 30 min, MeI (1.94 ml, 31.2 mmol, 2.20 eq.) was added. The mixture was warmed to r.t. and stirred for 1 h, when full conversion was observed *via* TLC (LP:EtOAc = 2:1).

Workup: The reaction was quenched by addition of methanol (70 ml), the solvents were removed under reduced pressure and the residue was taken up in H_2O/EtOAc (1:1, 200 ml). The aqueous layer was extracted with EtOAc (2 × 80 ml). The combined organic phases were washed with brine (150 ml), dried over Na_2SO_4 and concentrated. Purification of the crude material was achieved by flash chromatography with SiO_2 (140 g) and a 2:1 LP:EtOAc mixture and afforded the product **11** in a yield of 6.360 g (94%), pure according to ^{1}H-NMR and with spectral data in accordance to the literature.[63]

Yield	6.360 g (94%)
Appearance	slightly yellow syrup
TLC	R_f (LP:EtOAc = 2:1) = 0.57
Optical rotation	$[\alpha]_D^{20}$ = +**37.2** (*c* 1.0, $CHCl_3$), (Lit.: $[\alpha]_D^{25}$ = +39.0 (*c* 1.06, $CHCl_3$))[63]

^{1}H NMR (600 MHz, Chloroform-d) δ 3.26 (dd, *J* = 10.0, 8.9 Hz, 1H, H4), 3.30 (s, 3H, OC**H**$_3$ (*O*1)), 3.39 (s, 3H, OC**H**$_3$ (*O*4)), 3.44 (dd, *J* = 9.7, 3.6 Hz, 1H, H2), 3.57 – 3.55 (m, 1H, H5), 3.57 – 3.59 (m, 1H, H6b), 3.62 (dd, *J* = 10.7, 4.0 Hz, 1H, H6a), 3.79 (t, *J* = 9.3 Hz, 1H, H3), 4.44 (d, *J* = 12.0 Hz, 1H, PhC**H**H), 4.53 (d, *J* = 3.6 Hz, 1H, H1), 4.56 (d, *J* = 12.1 Hz, 1H, PhC**H**H), 4.57 (d, *J* = 12.1 Hz, 1H, PhCH**H**), 4.68 – 4.76 (m, 2H, PhC**H**H (*O*3), PhCH**H**), 4.87 (d, *J* = 10.8 Hz, 1H, PhCH**H** (*O*3)), 7.05 – 7.51 (m, 15H, 15 × PhH).

^{13}C NMR (151 MHz, Chloroform-d) δ 55.3 (O**C**H$_3$ (*O*1)), 60.8 (O**C**H$_3$ (*O*4)), 68.7 (C6), 70.2 (C5), 73.5 (Ph-**C**H$_2$ (*O*2)), 73.6 (Ph-**C**H$_2$ (*O*6)), 75.8 (Ph-**C**H$_2$ (*O*3)), 79.6 (C4), 79.8 (C2), 82.2 (C3), 98.3 (C1), 127.70, 127.74, 127.9, 128.0, 128.1, 128.2, 128.43, 128.47, 128.55 (15 × PhCH), 138.1, 138.3 (2 × PhC1), 139.0 (PhC1 (*O*3)).

LC-MS: ($^+$ESI-TOF) m/z $[M + NH_4]^+$: calcd. for $C_{29}H_{38}NO_6$ 496.270, found 496.20

3.2.3 Methyl 4-*O*-methyl-α-D-glucopyranoside[63] [6]

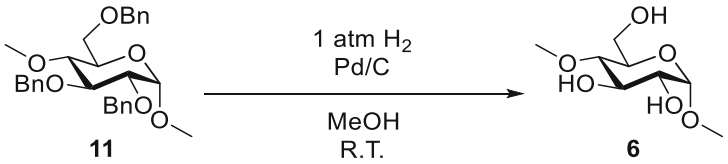

11 $C_{29}H_{34}O_6$ M = 478.59

6 $C_8H_{16}O_6$ M = 208.21

Procedure: To a solution of the starting material **11** (6.00 g, 12.5 mmol, 1.00 eq.) in anhydrous MeOH (300 ml) was added Pd on charcoal (1.25 g, 10% Pd). The mixture was put under H_2 atmosphere (1 atm) and stirred overnight at r.t., when full conversion was observed *via* TLC (LP:EtOAc = 2:1).

Workup: The catalyst was filtered off over Celite. Removal of the solvents under reduced pressure afforded the product **6** in a yield of 2.67 g (100%), pure according to ^{1}H-NMR and with spectral data in accordance to the literature.[63]

Yield	2.67 g (100%)
Appearance	slightly yellow syrup
TLC	R_f ($CHCl_3$:MeOH:H_2O = 7:3:0.5) = 0.53
Optical rotation	$[\alpha]_D^{20}$ = +**154.4** (*c* 0.5, EtOH), (Lit.: $[\alpha]_D^{25}$ = +197.3 (*c* 0.48, EtOH))[63]

^{1}H NMR (600 MHz, Methanol-d_4) δ 3.07 (dd, *J* = 10.0, 8.9 Hz, 1H, H4), 3.38 (m, 4H, H2 & OC**H**$_3$ (*O*1)), 3.48 (ddd, *J* = 10.0, 4.8, 2.2 Hz, 1H, H5), 3.55 (s, 3H, OC**H**$_3$ (*O*4)), 3.64–3.72 (m, 2H, H3 & H6b), 3.76 (dd, *J* = 11.8, 2.2 Hz, 1H, H6a), 4.65 (d, *J* = 3.8 Hz, 1H, H1).

^{13}C NMR (151 MHz, Methanol-d_4) δ 55.5 (O**C**H$_3$ (*O*1)), 60.8 (O**C**H$_3$ (*O*4)), 62.2 (C6), 72.6 (C5), 73.6 (C2), 75.2 (C3), 81.1 (C4),101.2 (C1).

LC-MS: ($^+$ESI-TOF) m/z [M + NH_4]$^+$: calcd. for $C_8H_{20}NO_6$ 226.129, found 226.10

3.2.4 Methyl 2,3-di-*O*-benzyl-α-D-glucopyranoside[62] [12]

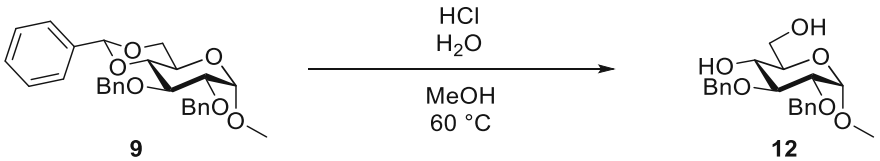

9
$C_{28}H_{30}O_6$
M = 462.54

12
$C_{21}H_{26}O_6$
M = 374.43

Procedure: To a solution of the starting material **9** (5.00 g, 10.8 mmol, 1.00 eq.) in MeOH (125 ml) was added water (13 ml) and HCl (1N, 2.5 ml, 0.23 eq). The mixture was heated (oil bath temperature 60 °C) and stirred for 2 h, when TLC showed full conversion (LP:EtOAc = 3:1).

Workup: The solution was neutralized by addition of $NaHCO_3$-solution. Solvents were removed by azeotroping with toluene. The residue was taken up in EtOAc and water (1:1 200ml), the aqueous phase extracted with EtOAc (2 × 100 ml). The combined organic phases were washed with brine, dried over Na_2SO_4 and the solvents removed. Purification of the crude material was achieved *via* flash chromatography with SiO_2 (150 g) and a LP:EtOAc mixture of first 1:2, then 1:3 and afforded the product **12** in a yield of 3.916 g (88%) in 90% purity according to ^{1}H-NMR and with spectral data in accordance to the literature.[62]

Yield	3.916 g (88%)
Appearance	slightly yellow oil
m.p.	75-79 °C (LP:EtOAc 1:3) (Lit.: 72 – 75 °C)[62]
TLC	R_f (LP:EtOAc = 1:3) = 0.29
Optical rotation	$[\alpha]_D^{20}$ = +**19.0** (*c* 1.0, $CHCl_3$), (Lit.: $[\alpha]_D^{23}$ = +14.9 (*c* 1.0, $CHCl_3$))[62]

^{1}H NMR (600 MHz, Chloroform-d) δ 1.92 (dd, *J* = 7.2, 5.5 Hz, 1H, OH (*O*6)), 2.29 (d, *J* = 2.6 Hz, 1H, OH (*O*4)), 3.38 (s, 3H, OC**H$_3$**), 3.47 – 3.53 (m, 2H, H4, H2), 3.62 (ddd, *J* = 9.8, 4.4, 3.4 Hz, 1H, H5), 3.74 (ddd, *J* = 11.8, 7.1, 4.6 Hz, 1H, H6b), 3.76 – 3.82 (m, 2H, H6a, H3), 4.60 (d, *J* = 3.5 Hz, 1H, H1), 4.66 (d, *J* = 12.0 Hz, 1H, PhC**H**H (*O*2)), 4.70 (d, *J* = 11.5 Hz, 1H, PhC**H**H (*O*3)), 4.77 (d, *J* = 12.1 Hz, 1H, PhCH**H** (*O*2)), 5.03 (d, *J* = 11.5 Hz, 1H, PhCH**H** (*O*3)),7.41 – 7.28 (m, 10H, 10 × PhH).

^{13}C NMR (151 MHz, Chloroform-d) δ 55.4 (O**C**H$_3$), 62.7 (C6), 70.6 (C4), 70.8 (C5), 73.3 (Ph-**C**H$_2$ (*O*2)), 75.5 (Ph-**C**H$_2$ (*O*3)), 79.9 (C2), 81.4 (C3), 98.3 (C1), 128.1, 128.2, 128.3, 128.7, 128.8 (10 × PhCH), 138.1, 138.8 (2 × PhC1).

LC-MS: ($^+$ESI-TOF) m/z [M + NH_4]$^+$: calcd. for $C_{21}H_{30}NO_6$ 392.207, found 392.10

3.2.5 Methyl 2,3-di-*O*-benzyl-4,6-di-*O*-methyl-α-D-glucopyranoside[62] [13]

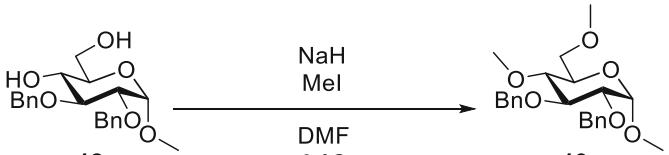

12
$C_{21}H_{26}O_6$
M = 374.43

13
$C_{23}H_{30}O_6$
M = 402.49

Procedure: To a solution of the starting material **12** (3.50 g, 9.35 mmol, 1.00 eq.) in anhydrous DMF (100 ml) was added sodium hydride (60w%, 1.53 g, 38.3 mmol, 4.10 eq.) at 0 °C. After stirring for 1 h, MeI (2.3 ml, 37.4 mmol, 4.0 eq.) was added. The mixture was warmed to r.t. and stirred for 4 h, when full conversion was observed *via* TLC (LP:EtOAc = 1:3).

Workup: The reaction was quenched by addition of methanol (20 ml), the solvents were removed under reduced pressure and the residue was taken up in H_2O/EtOAc (1:1). The aqueous layer was extracted with DCM. The combined organic phases were washed with brine, dried over Na_2SO_4 and concentrated. Purification of the crude material was achieved by flash chromatography with SiO_2 (50 g) and a 2:1 LP:EtOAc mixture and afforded the product **13** in a yield of 3.466 g (89%), pure according to ^{1}H-NMR and with spectral data in accordance to the literature.[62]

Yield	3.466 g (89%)
Appearance	slightly yellow oil
TLC	R_f (LP:EtOAc = 3:1) = 0.36
Optical rotation	$[\alpha]_D^{20}$ = +**45.1** (*c* 0.5, $CHCl_3$), (Lit.: $[\alpha]_D^{23}$ = +30.6 (*c* 0.5, $CHCl_3$))[62]

^{1}H NMR (600 MHz, Chloroform-d) δ 3.27 (dd, *J* = 9.9, 8.9 Hz, 1H, H4), 3.37 (s, 3H, OC**H**$_3$ (*O*1)), 3.39 (s, 3H, OC**H**$_3$ (*O*6)), 3.49 (dd, *J* = 9.7, 3.6 Hz, 1H, H2), 3.53 (s, 3H, OC**H**$_3$ (*O*4)), 3.55 – 3.63 (m, 3H, H5, H6a, H6b), 3.86 (t, *J* = 9.3 Hz, 1H, H3), 4.57 (d, *J* = 3.6 Hz, 1H, H1), 4.64 (d, *J* = 12.1 Hz, 1H, PhC**H**H (*O*2)), 4.78 (d, *J* = 12.1 Hz, 1H, PhCH**H** (*O*2)), 4.81 (d, *J* = 10.9 Hz, 1H, PhC**H**H (*O*3)), 4.94 (d, *J* = 10.9 Hz, 1H, PhCH**H** (*O*3)), 7.26 – 7.41 (m, 10H, 10 × PhH).

^{13}C NMR (151 MHz, Chloroform-d) δ 55.4 (O**C**H$_3$ (*O*1)), 59.3 (O**C**H$_3$ (*O*6)), 60.8 (O**C**H$_3$ (*O*4)), 70.0 (C5), 71.1 (C6), 73.5 (Ph-**C**H$_2$ (*O*2)), 75.7 (Ph-**C**H$_2$ (*O*3)), 79.5 (C4), 79.6 (C2), 82.1 (C3), 98.4 (C1), 127.7, 128.0, 128.1, 128.3, 128.5, 128.6 (10 × PhCH), 138.3, 139.1 (2 × PhC1).

LC-MS: ($^+$ESI-TOF) m/z $[M + NH_4]^+$: calcd. for $C_{23}H_{34}NO_6$ 420.239, found 420.15

3.2.6 Methyl 4,6-di-*O*-methyl-α-D-glucopyranoside[62] [7]

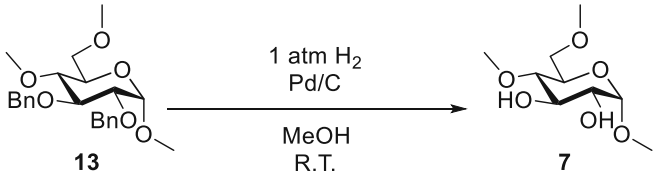

13
$C_{23}H_{30}O_6$
M = 402.49

7
$C_9H_{18}O_6$
M = 222.24

Procedure: To a solution of the starting material **13** (3.21 g, 7.98 mmol, 1.00 eq.) in anhydrous MeOH (300 ml) was added Pd on charcoal (270 mg, 10% Pd). The mixture was put under H_2 atmosphere (1 atm) and stirred for 21 h at r.t. with additional catalyst added in between until full conversion was observed *via* TLC (LP:EA = 2:1).

Workup: The catalyst was filtered off over Celite. Removal of the solvents under reduced pressure afforded a mixture of the fully debenzylated product **7** and the product with one benzylic group remaining. The mixture was purified *via* column chromatography with 50 g SiO_2 and a gradient of MeOH in DCM from 5% to 10%, yielding 395 mg of the desired product **7** and 1.515 g of the mono-benzylated product. The latter was treated again with Pd/C and H_2 and worked up accordingly to afford the product **7**, resulting in an overall yield of 1.499 g (85%), pure according to ^{1}H-NMR and with spectral data in accordance to the literature.[62]

Yield	1.499 g (85%)
Appearance	slightly yellow oil
TLC	R_f ($CHCl_3$:MeOH:H_2O = 7:3:0.5) = 0.70
Optical rotation	$[\alpha]_D^{20}$ = +**152.2** (*c* 1.0, $CHCl_3$), (Lit.: $[\alpha]_D^{23}$ = +152.0 (*c* 1.0, $CHCl_3$))[62]

^{1}H NMR (600 MHz, Chloroform-d) δ 2.30 (s, 1H, OH 3), 2.81 (s, 1H, OH 2), 3.20 (t, *J* = 9.5 Hz, 1H, H4), 3.41 (s, 3H, OC**H**$_3$ (*O*1)), 3.42 (s, 3H, OC**H**$_3$ (*O*6)), 3.55 (s, 3H, OC**H**$_3$ (*O*4)), 3.50 – 3.57 (m, 1H, H2), 3.57 – 3.63 (m, 3H, H5, H6a, H6b), 3.74 (t, *J* = 9.2 Hz, 1H, H3), 4.77 (d, *J* = 3.9 Hz, 1H, H1).

^{13}C NMR (151 MHz, Chloroform-d) δ 55.5 (O**C**H$_3$ (*O*1)), 59.4 (O**C**H$_3$ (*O*6)), 60.7 (O**C**H$_3$ (*O*4)), 70.1 (C5), 71.1 (C6), 72.7 (C2), 75.1 (C3), 79.1 (C4), 99.3 (C1).

LC-MS: ($^+$ESI-TOF) m/z [M + NH_4]$^+$: calcd. for $C_9H_{22}NO_6$ 240.145, found 240.10

3.2.7 2,2',3,3',4',6,6'-hepta-*O*-acetylmaltose[64] [15]

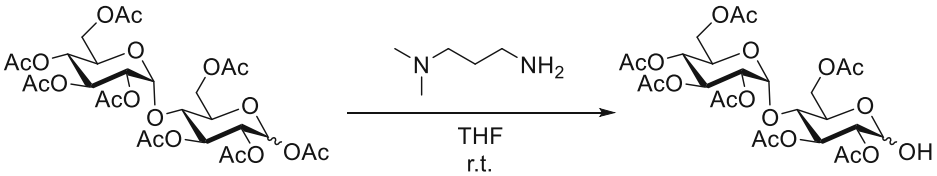

14
$C_{28}H_{38}O_{19}$
M = 678.59

15
$C_{26}H_{36}O_{18}$
M = 636.56

Procedure: To a solution of the maltose peracetate **14** (15.0 g, 22.1 mmol, 1.00 eq.) in anhydrous THF (150 ml) was added 3-dimethylamino-*N*-propylamin (11.3 g, 111 mmol, 5.02 eq.) and the solution was stirred at r.t. for 1 h, when full conversion was observed *via* TLC (LP:EtOAc = 1:4).

Workup: The solution was diluted with DCM (200 ml), washed with HCl (1N, 2 × 100ml) and brine (200 ml), dried over Na_2SO_4 and concentrated to yield 11.23 g (80%) of **15** as a mixture of α and β isomers (α:β approx. 0.7:0.3 according to ^{1}H-NMR), pure according to ^{1}H-NMR and with spectral data in accordance to the literature.[64]

Yield	11.23 g (80%)
Appearance	white solid
m.p.	175 °C (first liquid phase at 125 °C) (DCM) (Lit.: 188 °C)[75]
TLC	R_f (LP:EtOAc = 1:4) = 0.48
Optical rotation	$[\alpha]_D^{20}$ = +**108.0** (*c* 1.0, $CHCl_3$, 24 h), (Lit.: $[\alpha]_D^{22}$ = +114 (*c* 0.9, pyridine, 24 h))[75]

^{1}H NMR (600 MHz, Chloroform-d) δ 2.00 (s, 3H, COOC**H$_3$**), 2.010 (s, 2.1H, COOC**H$_3$**), 2.013 (s, 0.9H, COOC**H$_3$**), 2.02 (s, 3H, COOC**H$_3$**), 2.04 (s, 0.9H, COOC**H$_3$**), 2.050 (s, 3H, COOC**H$_3$**), 2.055 (s, 2.1H, COOC**H$_3$**), 2.10 (s, 3H, COOC**H$_3$**), 2.14 (s, 3H, COOC**H$_3$**), 3.72 – 3.76 (m, 0.3H, β-H5), 3.94 – 4.01 (m, 2H, α-H4, α-H5', β-H4, β-H5'), 4.05 (dd, *J* = 12.5, 2.4 Hz, 1H, α-H6b', β-H6b'), 4.19 – 4.29 (m, 2.7H, α-H6b, α-H6a', α-H5, β-H6b, β-H6a'), 4.46 – 4.51 (m, 1H, α-H6a, β-H6a), 4.73 (dd, *J* = 9.5, 7.9 Hz, 0.3H, β-H2), 4.76 – 4.79 (m, 1H, α-H2, β-H1), 4.86 (dd, *J* = 10.6, 4.1 Hz, 1H, α-H2', β-H2'), 5.06 (t, *J* = 9.7 Hz, 1H, α-H4', β-H4'), 5.29 (t, *J* = 9.2 Hz, 0.3H, β-H3), 5.34 – 5.39 (m, 1.7H, α-H3', α-H1, β-H3'), 5.40 (d, *J* = 4.0 Hz, 0.3H, β-H1'), 5.43 (d, *J* = 4.0 Hz, 0.7H, α-H1'), 5.58 (dd, *J* = 10.1, 8.9 Hz, 0.7H, α-H3).

^{13}C NMR (151 MHz, Chloroform-d) δ 20.73, 20.75, 20.83, 20.99, 21.01, 21.03, 21.10 (7 × COO**C**H$_3$), 61.5 (α-C6'), 61.6 (β-C6'), 62.9 (α-C6), 63.0 (β-C6), 67.9 (α-C5), 68.1 (α-C4', β-C4'), 68.6 (α-C5'), 68.7 (β-C5'), 69.4 (β-C3'), 69.5 (α-C3'), 70.1 (α-C2', β-C2'), 71.7 (α-C2), 72.4 (α-C3), 72.5 (β-C4), 72.67 (α-C4), 72.73 (β-C5), 73.9 (β-C2), 74.9 (β-C3), 90.2 (α-C1), 95.1 (β-C1), 95.6 (α-C1'), 95.7 (β-C1'), 169.61, 169.63, 170.09, 170.12, 170.4, 170.74, 170.78, 170.8, 171.0 (7 × **C**OOCH$_3$).

LC-MS: ($^+$ESI-TOF) m/z $[M + NH_4]^+$: calcd. for $C_{26}H_{40}NO_{18}$ 654.225, found 654.05

3.2.8 Methyl 2,2',3,3',4',6,6'-hepta-*O*-acetyl-β-maltopyranoside[64] [16]

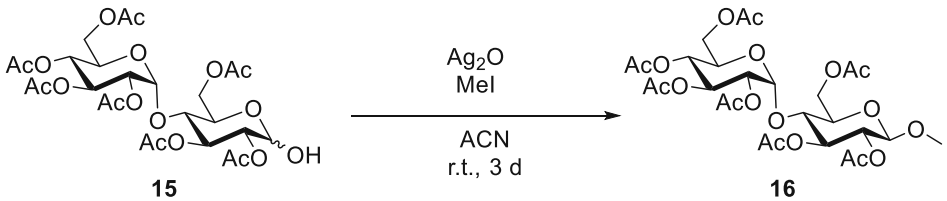

15
$C_{26}H_{36}O_{18}$
M = 636.56

16
$C_{27}H_{38}O_{18}$
M = 650.58

Procedure: To a solution of the anomeric mixture of the starting material **15** (8.87 g, 13.9 mmol, 1.00 eq.) in ACN (60 ml) Ag_2O (6.44 g, 27.8 mmol, 2.00 eq.) was added. After 15 min iodomethane (1.7 ml, 27.8 mmol, 2.00 eq.) was added and the mixture was stirred at r.t. under light protection for 3 days.

Workup: The solution was diluted with DCM (150 ml) and filtered through a plug of celite. After removal of the solvent, the crude was recrystallized from EtOH (20 ml) to yield 3.90 g (43%) of the desired product **16** with only minor impurities according to ^{1}H-NMR.

Yield	3.90 g (43%)
Appearance	brown solid
m.p.	122-125 °C (EtOH) (Lit.: 132 °C (EtOH))[76]
TLC	R_f (LP:EtOAc = 1:3) = 0.43
Optical rotation	$[\alpha]_D^{20}$ = +**56.6** (*c* 2.7, $CHCl_3$), (Lit.: $[\alpha]_D^{23}$ = +53.6 (*c* 2.8, $CHCl_3$))[76]

^{1}H NMR (600 MHz, Chloroform-d) δ 1.991 (s, 3H, COOC**H**$_3$), 1.992 (s, 3H, COOC**H**$_3$), 2.01 (s, 3H, COOC**H**$_3$ (*O*4'), 2.02 (s, 3H, COOC**H**$_3$ (*O*2)), 2.03 (s, 3H, COOC**H**$_3$ (*O*2')), 2.09 (s, 3H, COOC**H**$_3$ (*O*6')), 2.14 (s, 3H, COOC**H**$_3$ (*O*6)), 3.48 (s, 3H, OC**H**$_3$), 3.68 (ddd, *J* = 9.7, 4.3, 2.8 Hz, 1H, H5), 3.95 (ddd, *J* = 10.2, 3.9, 2.3 Hz, 1H, H5'), 4.02 (t, *J* = 9.6 Hz, 1H, H4), 4.03 (dd, *J* = 12.5, 2.4 Hz, 1H, H6b'), 4.23 (dd, *J* = 5.7, 4.1 Hz, 1H, H6b), 4.25 (dd, *J* = 6.0, 4.2 Hz, 1H, H6a'), 4.44 (d, *J* = 7.9 Hz, 1H, H1), 4.48 (dd, *J* = 12.1, 2.8 Hz, 1H, H6a), 4.80 (dd, *J* = 9.4, 7.8 Hz, 1H, H2), 4.85 (dd, *J* = 10.6, 4.1 Hz, 1H, H2'), 5.02 – 5.07 (m, 1H, H4'), 5.24 (t, *J* = 9.1 Hz, 1H, H3), 5.35 (dd, *J* = 10.6, 9.5 Hz, 1H, H3'), 5.40 (d, *J* = 4.0 Hz, 1H, H1').

^{13}C NMR (151 MHz, Chloroform-d) δ 20.71, 20.72, 20.75, 20.83, 20.97, 21.04 (7 × COO**C**H$_3$), 57.2 (O**C**H$_3$), 61.6 (C6'), 62.9 (C6), 68.1 (C4'), 68.6 (C5'), 69.4 (C3'), 70.1 (C2'), 72.20 (C2/C5'), 72.23 (C2/C5'), 72.8 (C4), 75.6 (C3), 95.6 (C1'), 101.2 (C1), 169.6, 169.9, 170.1, 170.4, 170.6, 170.7 (7 × **C**OOCH$_3$).

LC-MS: ($^+$ESI-TOF) m/z $[M + NH_4]^+$: calcd. for $C_{27}H_{42}NO_{18}$ 668.240, found 668.15

3.2.9 Methyl β-maltopyranoside[64] [17]

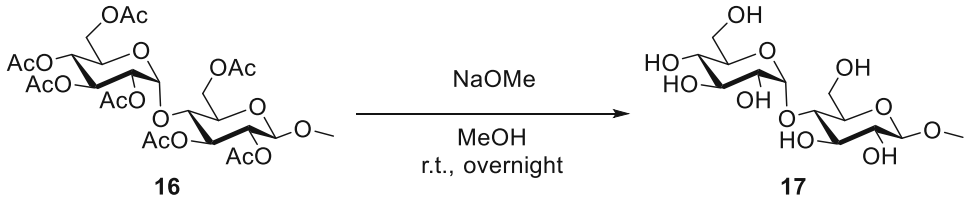

16
$C_{27}H_{38}O_{18}$
M =650.58

17
$C_{13}H_{24}O_{11}$
M =356.32

Procedure: The peracetylated starting material **16** (3.00g, 4.61 mmol, 1.00 eq.) was dissolved in MeOH (70 ml). NaOMe in MeOH (1M, 5 ml, 1.08 eq) was added and the solution was stirred at room temperature overnight. TLC showed full conversion of starting material (LP:EtOAc = 1:3).

Workup: The mixture was neutralized with freshly washed ion exchange resin. Removing the solvent under reduced pressure yielded 1.604 g (98%) of the desired product **17**, pure according to ^{1}H-NMR and with spectral data in accordance to the literature.[66]

Yield	1.604 g (98%)
Appearance	brown foam
TLC	R_f ($CHCl_3$:MeOH:H_2O = 7:3:0.5) = 0.25
Optical rotation	$[\alpha]_D^{20}$ = +**69.0** (*c* 1.0, H_2O), (Lit.: $[\alpha]_D^{20}$ = +71 (*c* 0.4, H_2O))[77]

^{1}H NMR (600 MHz, D_2O) δ 3.27 (dd, *J* = 9.5, 8.0 Hz, 1H, H2), 3.37 – 3.41 (m, 1H, H4'), 3.54-3.59 (m, 5H, H5, H2', OC**H**$_3$), 3.61 (dd, *J* = 9.8, 8.3 Hz, 1H, H4), 3.66 (t, *J* = 9.5 Hz, 1H, H3'), 3.68 – 3.71 (m, 1H, H5'), 3.72-3.77 (m, 3H, H6b, H6b', H3), 3.83 (dd, *J* = 12.3, 2.2 Hz, 1H, H6a'), 3.92 (dd, *J* = 12.2, 2.0 Hz, 1H, H6a), 4.37 (d, *J* = 8.0 Hz, 1H, H1), 5.38 (d, *J* = 3.9 Hz, 1H, H1').

^{13}C NMR (151 MHz, D_2O) δ 57.2 (O**C**H$_3$), 60.5 (C6'), 60.7 (C6), 69.3 (C4'), 71.7 (C2'), 72.7 (C5'/C3'), 72.8 (C5'/C3'), 73.0 (C2), 74.6 (C5), 76.3 (C3), 76.7 (C4), 99.5 (C1'), 103.1 (C1).

LC-MS: ($^+$ESI-TOF) m/z [M + NH_4]$^+$: calcd. for $C_{13}H_{28}NO_{11}$ 374.166, found 374.00

3.2.10 Methyl 4',6'-*O*-benzylidene-β-maltopyranoside[67] [18]

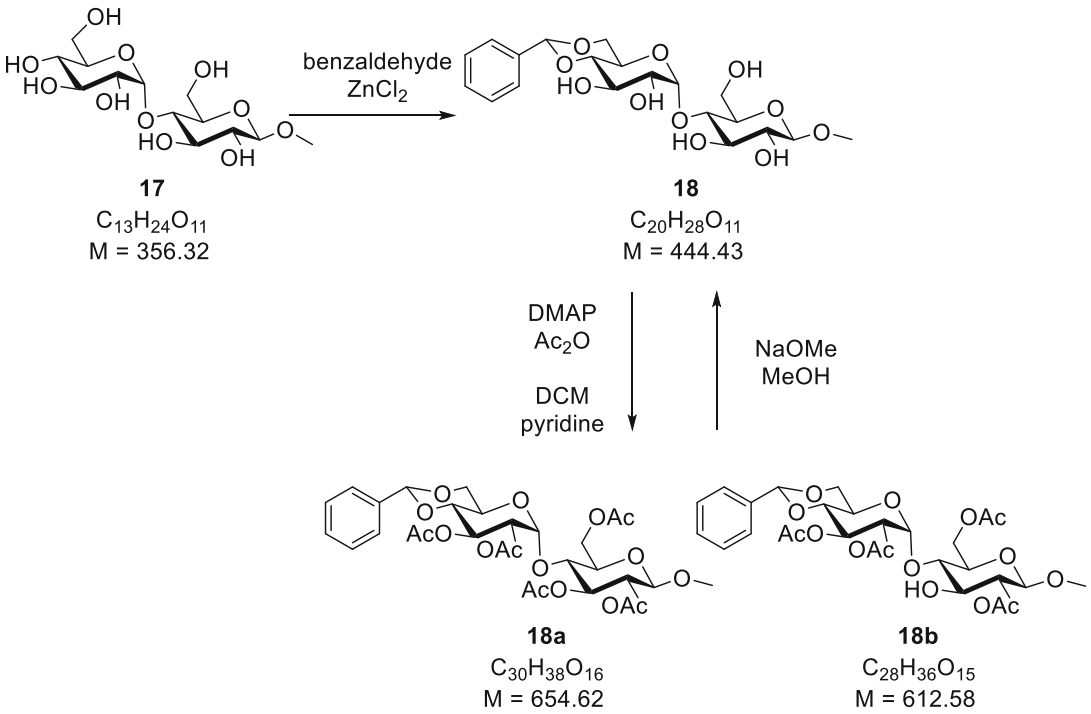

Procedure: $ZnCl_2$ (3.33 g, 24.4 mmol, 7.00 eq.) was weighed into the reaction vessel and put under argon atmosphere. Benzaldehyde (15 ml, 148 mmol, 44 eq.) was added and the mixture stirred at r.t for 20 min before methyl-β-maltoside **17** (1.19 g, 3.35 mmol, 1.00 eq.) was added. Because the mixture had turned into a paste, additional benzaldehyde (5 ml, 49 mmol, 15 eq.) was added. After 22 h of stirring at r.t. diethyl ether was added until no further precipitate was formed, and the mixture was put into an ice bath.

Workup: The precipitate was filtered, taken up in water and extracted with LP three times. The aqueous phase was concentrated and lyophilized, leaving 1.55 g of the product **18** with starting material **17** and smaller amounts of benzaldehyde as impurities.

Purification *via* Acetylation: To a suspension of the crude product **18** (1.29 g, 2.898 mmol, 1 eq.) in DCM (10 ml) and pyridine (3 ml) DMAP (7 mg, 0.05 mmol, 0.02 eq.) was added under argon at 0°C. After 30 min, acetic anhydride (2.8 ml, 29.0 mmol, 10.0 eq.) was added and the mixture was allowed to warm to r.t.. After 16h of stirring the reaction was worked up by adding water and DCM. The aqueous phase was extracted with DCM and the combined organic phases dried over Na_2SO_4 and concentrated. The acetylated compound was purified *via* column chromatography, yielding 156 mg of the fully acetylated compound **18a** and 332 mg of the tetraacetate **18b.**

Deacetylation: The acetylated compounds **18a** and **18b** (150; 144 mg, 0.245; 0.220 mmol, 1 eq.) were deacetylated separately in solutions of MeOH (4; 3.5 ml). NaOMe in MeOH (1M,

0.25 ml, 1.02; 1.14 eq) was added and the solution was stirred at room temperature overnight. TLC showed full conversion of starting material (LP:EtOAc = 1:2).

Workup: The mixtures were neutralized with freshly washed ion exchange resin. The solvent was removed *via* reduced pressure, yielding a total of 350 mg (28%) of target compound **18,** pure according to ^{1}H-NMR.

Yield	350 mg (28%)
Appearance	slightly yellow solid
m.p.	131-134 °C (MeOH) (Lit.: 140-141 °C)[67]
TLC	R_f ($CHCl_3$:MeOH:H_2O = 7:3:0.5) = 0.24
Optical rotation	$[\alpha]_D^{20}$ = +**45.7** (*c* 0.5, EtOH), (Lit.: $[\alpha]_D^{23}$ = +47.6 (*c* 2.0, EtOH))[67]

^{1}H NMR (600 MHz, D_2O) δ 3.28 (dd, *J* = 9.5, 8.0 Hz, 1H, H2), 3.56 (s, 3H, OC**H$_3$**), 3.59 (ddd, *J* = 9.8, 5.0, 2.0 Hz, 1H, H5), 3.64 – 3.72 (m, 3H, H4, H2', H4'), 3.76 (d, *J* = 9.1 Hz, 1H, H3), 3.79 (dd, *J* = 12.0, 5.0 Hz, 1H, H6a), 3.85 – 4.03 (m, 4H, H6a', H5', H3', H6b), 4.30 (dd, *J* = 9.8, 4.3 Hz, 1H, H6b'), 4.38 (d, *J* = 7.9 Hz, 1H, H1), 5.46 (d, *J* = 4.0 Hz, 1H, H1'), 5.74 (s, 1H, Ph-C**H**OO), 7.44 – 7.49 (m, 3H, 3 ×PhCH), 7.50 – 7.55 (m, 2H, 2 × PhCH).

^{13}C NMR (151 MHz, D_2O) δ 57.1 (O**C**H$_3$), 60.5 (C6), 63.2 (C5'), 67.9 (C6'), 69.9 (C3'), 72.1 (C2'), 72.9 (C2), 74.3 (C5), 76.2 (C3), 76.5 (C4), 80.1 (C4'), 100.1 (H1'), 101.7 (Ph-**C**HOO), 103.0 (H1), 126.2, 128.7, 129.9 (5 x PhCH), 136.0 (PhC1).

LC-MS: ($^{+}$ESI-TOF) m/z [M + H]$^{+}$: calcd. for $C_{20}H_{29}O_{11}$ 445.171, found 445.05

3.2.11 Methyl 2,2',3',3,6'-*O*-pentabenzyl-4',6'-*O*-benzylidene-β-maltopyranoside[68] [19]

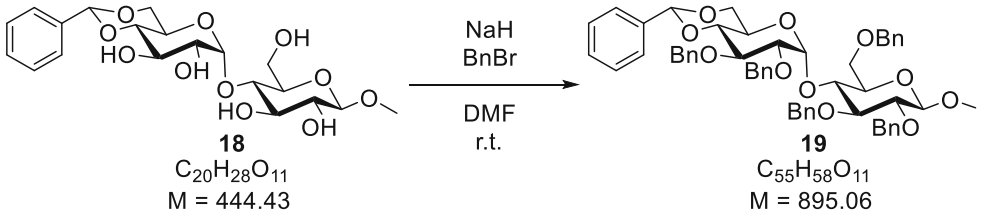

Procedure: Starting material **18** (921 mg, 2.07 mmol, 1.00 eq., approx. 10w% **17** as impurity) was dissolved in DMF (20 ml) and NaH (60 w%, 790 mg, 20 mmol, 9.5 eq.) was added and the mixture was stirred for 45 min. Benzyl bromide (1.4 ml, 11 mmol, 5.5 eq.) was added and the mixture was stirred overnight, after which HPTLC ($CHCl_3$:MeOH:H_2O = 7:3:0.5) indicated full conversion.

Workup: MeOH (25 ml) was added in portions while cooling. The mixture was stirred for 30 min and water (50 ml) was added. The solution was neutralized with 1N HCl and extracted with DCM. The combined organic phases were washed with 1M HCl and saturated $NaHCO_3$, dried over Na_2SO_4 and concentrated. The remaining yellow oil was purified *via* column chromatography, using 160 g of SiO_2 and a gradient of EtOAc in LP from 16 to 25%. This yielded 1.23 g of a colorless syrup, a mixture of 84 w% of the desired product **19**, 6 w% of the perbenzylated maltose (separated after next step) and 9 w% of EtOAc according to ^{1}H-NMR and with spectral data of **19** in accordance to the literature.[68]

Yield	1.23 g (46%)
Appearance	colorless syrup
TLC	R_f (LP:EtOAc = 4:1) = 0.46
Optical rotation	$[\alpha]_D^{20}$ = +**5.4** (*c* 1.0, $CHCl_3$), (Lit.: $[\alpha]_D^{23}$ = +17.7 (*c* 1.9, $CHCl_3$))[68]

^{1}H NMR (400 MHz, Chloroform-d) δ 3.50 (tdd, *J* = 9.5, 9.0, 7.8, 3.9 Hz, 2H, H2, H2'), 3.59 (s, 4H, H5, OC**H$_3$**), 3.60 – 3.67 (m, 2H, H6b + H4), 3.76 – 3.92 (m, 4H, H5' + H6b' + H6a + H3'), 3.99 (t, *J* = 9.3 Hz, 1H, H3), 4.11 (t, *J* = 9.2 Hz, 1H, H4'), 4.17 (dd, *J* = 10.0, 4.6 Hz, 1H, H6a'), 4.35 (d, *J* = 7.8 Hz, 1H, H1), 4.51 – 4.78 (m, 7H, 7 × PhC**H**H), 4.90 (dd, *J* = 11.0, 2.0 Hz, 2H, 2 × PhCH**H**), 4.96 (d, *J* = 11.7 Hz, 1H, PhCH**H**), 5.54 (s, 1H, Ph-C**H**OO), 5.71 (d, *J* = 3.9 Hz, 1H, H1'), 7.15 – 7.42 (m, 28H, 28 × PhCH), 7.49 – 7.53 (m, 2H, 2 × PhCH).

^{13}C NMR (101 MHz, Chloroform-d) δ 57.1 (O**C**H$_3$), 63.4 (C5'), 69.0 (C6/C6'), 69.1 (C6/C6'), 72.1 (C4'), 73.6(Ph-**C**H$_2$), 73.9 (Ph-**C**H$_2$), 74.0 (Ph-**C**H$_2$), 74.4 (C5), 74.7 (Ph-**C**H$_2$), 75.4 (Ph-**C**H$_2$), 78.86 (C3/C2), 78.88 (C3/C2), 82.4 (C4/C2'), 82.5 (C4/C2'), 85.0 (C3'), 97.4 (C1'), 101.3 (Ph-**C**HOO), 104.7 (C1), 126.2, 126.8, 127.3, 127.6, 127.70, 127.75, 127.79, 128.0, 128.1, 128.29, 128.32, 128.4, 128.5, 129.0 (30 × PhCH), 137.7, 138.0, 138.4, 138.5, 138.8, 138.9 (6 × PhC1).

LC-MS: ($^+$ESI-TOF) m/z [M + NH_4]$^+$: calcd. for $C_{55}H_{62}NO_{11}$ 912.432, found 912.20

3.2.12 Methyl 2,2',3,3',6,6'-*O*-hexabenzyl-β-maltopyranoside[68] [20]

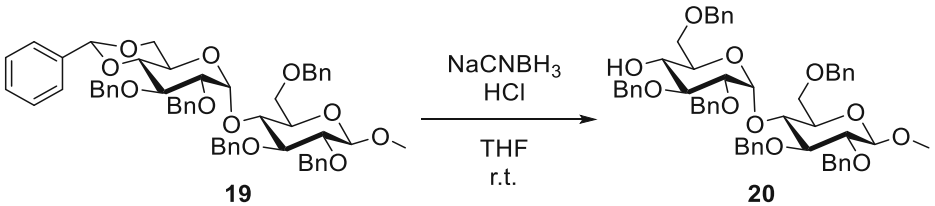

19
$C_{55}H_{58}O_{11}$
M = 895.06

20
$C_{55}H_{60}O_{11}$
M = 897.07

Procedure: To a solution of the acetal **19** (1.10 g, 1.23 mmol, 1.00 eq.) in THF (40 ml) was added $NaCNBH_3$ (976 mg, 14.7 mmol, 12.0 eq.) and HCl in Et_2O (2N, 7.37 ml, 12.0 eq.). After 30 min of stirring at r.t. TLC showed full conversion.

Workup: The mixture was diluted with DCM (50 ml) and washed with water and saturated $NaHCO_3$. The organic phase was dried over Na_2SO_4 and concentrated. The remaining yellow oil was purified *via* column chromatography, using 90 g SiO_2 and EtOAc in LP (20% to 33%), yielding 630 mg (57%) of product **20**, pure according to ^{1}H-NMR.

Yield	630 mg (57%)
Appearance	colorless syrup
TLC	R_f (LP:EtOAc = 4:1) = 0.24
Optical rotation	$[\alpha]_D^{20}$ = +**32.3** (*c* 0.5, $CHCl_3$), (Lit.: $[\alpha]_D^{23}$ = +23.0 (*c* 0.7, $CHCl_3$))[68]

^{1}H NMR (600 MHz, Chloroform-d) δ 3.45 (dd, *J* = 9.7, 3.7 Hz, 1H, H2'), 3.47 – 3.53 (m, 3H, H6b', H2), 3.55 – 3.61 (m, 2H, H5, H6a'), 3.60 (s, 3H, OC**H**$_3$) 3.62 – 3.66 (m, 1H, H4'), 3.72 – 3.77 (m, 2H, H3', H5'), 3.78 – 3.86 (m, 3H, H3, H6a, H6b), 4.07 (t, *J* = 9.4, 8.9 Hz, 1H, H4), 4.35 (d, *J* = 7.7 Hz, 1H, H1), 4.39 (d, *J* = 12.1 Hz, 1H, PhC**H**H (*O*6')), 4.49 (d, *J* = 12.1 Hz, 1H, PhCH**H** (*O*6')), 4.55 (d, *J* = 14.6 Hz, 3H, 3 × PhC**H**H (*O*6, 2 x *O*2')), 4.58 – 4.64 (m, 2H, 2 × PhC**H**H (*O*2, *O*6)), 4.71 (d, *J* = 11.3 Hz, 1H, PhC**H**H (*O*3')), 4.75 (d, *J* = 11.7 Hz, 1H, PhC**H**H (*O*3)), 4.86 – 4.93 (m, 2H, 2 × PhCH**H** (*O*2, *O*3')), 4.98 (d, *J* = 11.7 Hz, 1H, PhC**H**H (*O*3)), 5.69 (d, *J* = 3.7 Hz, 1H, H1'), 7.14 – 7.37 (m, 30H, 30 × PhC**H**).

^{13}C NMR (151 MHz, Chloroform-d) δ 57.1 (O**C**H$_3$), 69.2 (C6), 69.8 (C6'), 70.7 (C5'), 71.5 (C4'), 72.5 (C4), 73.2 (Ph**C**H$_2$ (*O*2')), 73.4 (Ph**C**H$_2$ (*O*6)), 73.7 (Ph**C**H$_2$ (*O*6')), 74.0 (Ph**C**H$_2$ (*O*3)), 74.6 (C5), 74.7 (Ph**C**H$_2$ (*O*2)), 75.4 (Ph**C**H$_2$ (*O*3')), 79.0 (C2'), 81.4 (C3'), 82.4 (C2), 84.9 (C3), 96.7 (C1'), 104.7 (C1), 126.8, 127.3, 127.6, 127.68, 127.76, 127.78, 127.81, 127.86, 127.87, 128.0, 128.3, 128.39, 128.41, 128.43, 128.47, 128.51, 128.6 (30 x Ph**C**H), 138.0, 138.1, 138.45, 138.50, 138.86, 138.88 (6 x Ph**C**).

LC-MS: ($^+$ESI-TOF) m/z $[M + NH_4]^+$: calcd. for $C_{55}H_{64}NO_{11}$ 914.448, found 914.35

3.2.13 Methyl 2,2',3,3',6,6'-*O*-hexabenzyl-4'-*O*-methyl-β-maltopyranoside[78] [21]

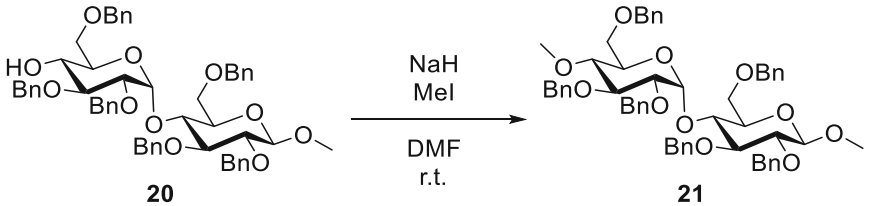

20
$C_{55}H_{60}O_{11}$
M = 897.07

21
$C_{56}H_{62}O_{11}$
M = 911.10

Procedure: To a solution of starting material **20** (628 mg, 0.70 mmol, 1.00 eq.) in anhydrous DMF (20 ml) was added NaH (60 mg, 1.5 mmol, 2.1 eq.). After 30 min of stirring, MeI (100 µl, 1.5 mmol, 2.2 eq.) was added. After 90 min of stirring at r.t., TLC (LP:EtOAc = 5:1) showed full conversion.

Workup: The reaction was quenched by addition of MeOH (30 ml). After removal of solvents under reduced pressure the residue was taken up in H_2O (50 ml) and DCM (50 ml). The aqueous layer was extracted with DCM. The combined organic phases were washed with brine, dried over Na_2SO_4 and concentrated, leaving 645 mg of a colorless oil. Purification *via* column chromatography using 60 g SiO_2 and EtOAc in LP (16% to 20%), yielded 494 mg (72%) of the desired product **21** with 7w% EtOAc according to ^{1}H-NMR and with spectral data in accordance to the literature.[78]

Yield	494 mg (72%)
Appearance	colorless syrup
TLC	R_f (LP:EtOAc = 4:1) = 0.40
Optical rotation	$[\alpha]_D^{20}$ = +**45.6** (*c* 0.5, $CHCl_3$), (Lit.: $[\alpha]_D^{23}$ = +46.6 (*c* 1.3, $CHCl_3$))[78]

^{1}H NMR (600 MHz, Chloroform-d) δ 3.37 (dd, *J* = 10.1, 8.9 Hz, 1H, H4'), 3.42 – 3.47 (m, 5H, OC**H**$_3$ (*O*4') + H2' + H6b'), 3.50 (t, *J* = 9.0, 7.7 Hz, 1H, H2), 3.53 (dd, *J* = 10.7, 3.0 Hz, 1H, H6a'), 3.59 (s, 4H, OC**H**$_3$ (*O*1) + H5), 3.67 (dt, *J* = 10.0, 2.5 Hz, 1H, H5'), 3.77 – 3.85 (m, 4H, H3' + H3 + H6a&b), 4.07 (dd, *J* = 9.6, 8.6 Hz, 1H, H4), 4.35 (d, *J* = 7.7 Hz, 1H, PhC**H**H), 4.37 (d, *J* = 12.1 Hz, 1H, PhC**H**H), 4.52 (d, *J* = 11.9 Hz, 1H, PhCH**H**), 4.56 – 4.60 (m, 4H, 4 × PhC**H**H), 4.61 (d, *J* = 11.0 Hz, 1H, PhCH**H**), 4.74 – 4.79 (m, 2H, 2 × PhCH**H**), 4.85 (d, *J* = 10.8 Hz, 1H, PhCH**H**), 4.89 (d, *J* = 11.0 Hz, 1H, PhCH**H**), 4.96 (d, *J* = 11.6 Hz, 1H, PhCH**H**), 5.68 (d, *J* = 3.7 Hz, 1H, H1'), 7.14 – 7.21 (m, 7H, 7 × PhH), 7.22 – 7.37 (m, 23H, 23 × PhH).

^{13}C NMR (151 MHz, Chloroform-d) δ 57.1 (O**C**H$_3$ (*O*1)), 60.8 (O**C**H$_3$ (*O*4')), 68.4 (C6'), 69.2 (C6), 71.2 (C5'), 72.5 (C4), 73.4, 73.5, 73.6, 74.0 (4 × Ph-**C**H$_2$), 74.67 (C5), 74.70, 75.6 (2 × Ph-**C**H$_2$), 79.2 (C2'), 79.5 (C4'), 82.1 (C3'), 82.5 (C2), 84.9 (C3), 96.8 (C1'), 104.7 (C1), 126.8, 127.2, 127.58, 127.64, 127.67, 127.72, 127.75, 127.76, 127.8, 127.99, 128.04, 128.4, 128.5 (30 × PhCH), 138.1, 138.2, 138.47, 138.52, 138.89, 138.94 (6 × PhC1).

LC-MS: ($^+$ESI-TOF) m/z [M + H]$^+$: calcd. for $C_{56}H_{66}NO_{11}$ 928.464, found 928.20

3.2.14 Methyl 4'-*O*-methyl-β-maltopyranoside[78] [8]

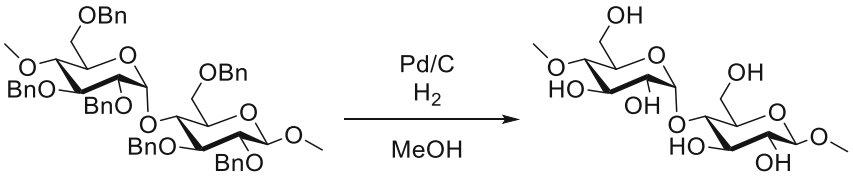

21
$C_{56}H_{62}O_{11}$
M = 911.10

8
$C_{14}H_{26}O_{11}$
M = 370.35

Procedure: To a solution of the starting material **21** (445 mg, 0.49 mmol, 1.00 eq.) in anhydrous MeOH (60 ml) was added Pd on charcoal (90 mg, 10% Pd). The mixture was put under H_2 atmosphere (1 atm) and stirred for 16 h at r.t. with additional catalyst and five drops of acetic acid added in between until full conversion was observed *via* TLC (LP:EA = 4:1).

Workup: The catalyst was filtered off over Celite. Removal of the solvents under reduced pressure afforded 199 mg (quant.) of the product **8** with traces of methanol and 7w% acetic acid according to ^{1}H-NMR and with spectral data in accordance to the literature.[78]

Yield	199 mg (quant.)
Appearance	white solid
m.p.	192-197 °C (MeOH)
TLC	R_f ($CHCl_3$:MeOH:H_2O = 7:3:0.5) = 0.49
Optical rotation	$[\alpha]_D^{20}$ = +**71.9** (*c* 0.5, H_2O)

^{1}H NMR (600 MHz, Deuterium Oxide) δ 5.37 (d, *J* = 3.9 Hz, 1H, H1'), 4.36 (d, *J* = 8.0 Hz, 1H, H1), 3.90 (dd, *J* = 12.3, 2.1 Hz, 1H, H6a), 3.83 (dd, *J* = 12.4, 2.3 Hz, 1H, H6a'), 3.74 (m, 4H, H6b' + H6b + H3 + H3'), 3.67 (ddd, *J* = 10.3, 4.7, 2.3 Hz, 1H, H5'), 3.60 (dd, *J* = 9.7, 8.5 Hz, 1H, H4), 3.58 – 3.55 (m, 2H, H2' + H5), 3.55 (s, 3H, OC**H$_3$** (*O*1)), 3.54 (s, 3H, OC**H$_3$** (*O*4')), 3.26 (t, *J* = 9.5, 8.0 Hz, 1H, H2), 3.20 (t, *J* = 9.6 Hz, 1H, H4').

^{13}C NMR (151 MHz, Deuterium Oxide) δ 57.2 (O**C**H$_3$ (*O*1)), 60.1 (C6'), 60.2 (O**C**H$_3$ (*O*4')), 60.7 (C6), 71.6 (C2'/C5'), 71.7 (C2'/C5'), 72.6 (C3'), 73:0 (C2), 74.5 (C5), 76.2 (C3), 76.6 (C4), 79.0 (C4'), 99.4 (C1'), 103.1 (C1).

LC-MS: ($^+$ESI-TOF) m/z [M + NH_4]$^+$: calcd. for $C_{14}H_{30}NO_{11}$ 388.182, found 388.05

3.3 Oxidation of Methyl 4-*O*-methyl-α-D-glucopyranoside (28) to compound [25]

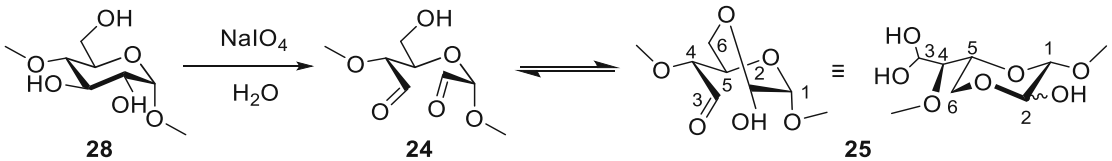

28
$C_8H_{16}O_6$
M = 208,21

24
$C_8H_{14}O_6$
M = 206.19

25
$C_8H_{16}O_7$
M = 224.21

Procedure: To a solution of the starting material **28** (207 mg, 0.994 mmol, 1.00 eq.) in water (5 ml) $NaIO_4$ (270 mg, 1.26 mmol, 1.27 eq.) was added. After 20 min of stirring at r.t., full conversion was observed *via* TLC ($CHCl_3$:MeOH:H_2O = 7:3:0.5).

Workup: The mixture was extracted with DCM and EtOAc, checking for full extraction *via* TLC. The organic phase was dried and solvents were removed under reduced pressure, affording the product **25** in a yield of 92 mg (45%). A cis:trans ratio of the acetal **25** was determined to be 1:0.6 *via* ^{1}H-NMR ($CDCl_3$), with some unknown impurities and with spectral data in accordance to the literature.[69]

Yield	92 mg (45%)
Appearance	yellow oil

^{1}H NMR (400 MHz, $CDCl_3$, cis: trans = 1:0.6) δ 3.468 (s, 3H, OC**H$_3$** cis *O*1), 3.474 (s, 1.8H, OC**H$_3$** trans *O*1), 3.50 (s, 3H, OC**H$_3$** cis *O*4), 3.51 (s, 1.8H, OC**H$_3$** trans O4), 3.62 – 3.71 (m, 1.6H, H6b), 3.72 (dd, *J* = 6.2, 1.7 Hz, 1H, H4 cis), 3.80 (dd, *J* = 7.1, 2.4 Hz, 0.6H, H4 trans), 3.94 – 4.11 (m, 3.2H, H5, H6a), 4.20 (d, *J* = 5.4 Hz, 0.6H, H1 trans), 4.48 (d, *J* = 1.9 Hz, 1H, H1 cis), 4.57 (d, *J* = 5.5 Hz, 0.6H, H2 trans), 4.84 (d, *J* = 1.8 Hz, 1H, H2 cis), 9.71 (dd, *J* = 2.7, 2.2 Hz, 1H, H3).

LC-MS: ($^+$ESI-TOF) m/z [M + NH_4]$^+$: calcd. for $C_8H_{20}NO_7$ 242.124, found 242.10

3.4 Preparation of DAS[15]

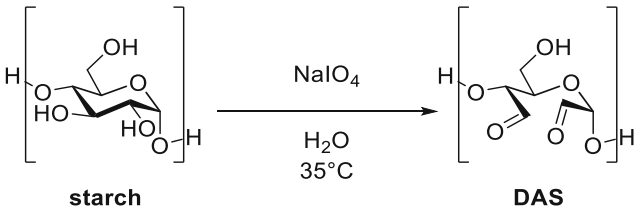

starch DAS

Procedure: Varying amounts of $NaIO_4$ (0 - 2.00 g, 0 - 9.4 mol, 0 – 1.5 eq. based on AGUs) were dissolved in water (7 ml) and starch (1.00 g, 6.17 mol AGU, 1 eq. based on AGUs) was added. The suspension was stirred at r.t. for 16h.

Work up: The suspensions were centrifuged and the precipitated starch was washed by repeated suspension in 35 °C water and centrifugation. The resulting DAS was dried in vacuum at 50 °C for 3 days and crushed in a mortar.

The appearance of the DAS reaction solutions prepared this way and the percentage of oxidized AGUs based on the ABAO assay in chapter 0 are listed in Table 9. The percentage of oxidized AGUs was quantified *via* the ABAO assay described in 3.7 and the calibration with model compound **25** described in 3.6

Table 9 Summary of starch oxidations conditions [a]quantified *via* ABAO assay described in 3.7 [b]reaction diluted 1:1

eq. NaIO4 (based on AGU)	appearance before workup	percentage of oxidized AGUs[a]
0.00	white suspension	0%
0.25	slightly orange suspension	29%
0.50	purple gel	49%
0.50	purple gel	56%
0.75	orange suspension	70%
1.00	white suspension	105%
1.00[b]	white suspension	83%
1.25	white suspension	84%
1.50	white syrup	81%

3.5 NMR experiment of ABAO (1) with oxidized model compound (25)

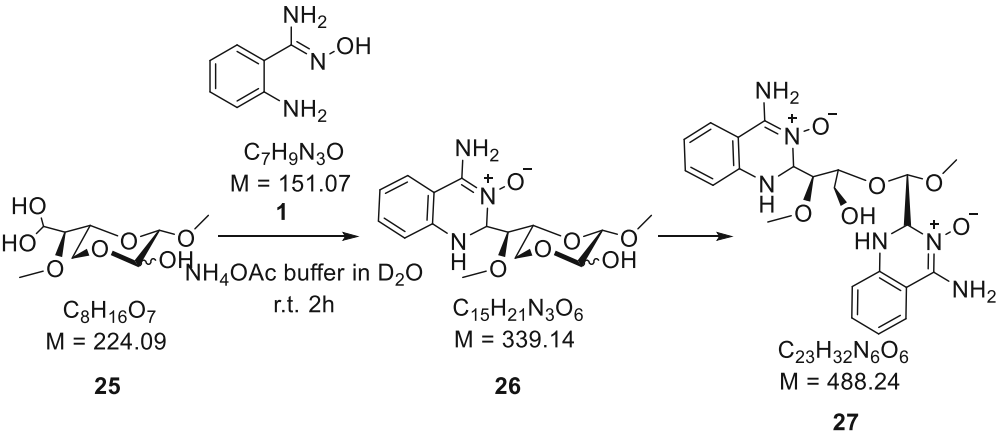

Procedure: To a solution of starting material **25** (4.7 mg, 0.021 mmol, 1.0 eq.) in deuterated buffer (0.7 ml, 100mM NH_4OAc in D_2O, pH = 4.5) varying amounts of ABAO (**1**) (1.6; 8.9; 31.7 mg, 0.011; 0.053; 0.21 mmol, 0.5; 2.5; 10 eq.) were added. After 2-3.5 h of stirring at r.t., ^{1}H-NMR, HSQC and COSY spectra were measured.

Exemplary peaks of both compounds were identifiable and are listed:

Compound 26, after 2 h and 2.5 eq. ABAO (mixture with 25, ratio of 26c:26t 0.55:1)
^{1}H NMR (400 MHz, D_2O) δ 4.38 (d, *J* = 6.1 Hz, 1H, trans H1), 4.54 (d, *J* = 6.1 Hz, 1H, trans H2), 4.68 (d, *J* = 1.7 Hz, 0.55H, cis H1), 4.96 (d, *J* = 1.7 Hz, 0.55H, cis H2), 5.35 (d, *J* = 1.9 Hz, 1H, trans H3), 5.38 (d, *J* = 1.8 Hz, 0.55H, cis H3).

Compound 27, after 3.5 h and 10 eq. ABAO (ratio of 27a:27b 0.6:1):
^{1}H NMR (400 MHz, D_2O) δ 3.10 (s, 1.8H, OC$\underline{H}_3$ (*O*4a)), 3.24 (s, 3H, OC$\underline{H}_3$ (*O*4b)), 3.43 (s, 1.8H, OC$\underline{H}_3$ (*O*1b)), 3.45 – 3.50 (m, 0.6H, 6a), 3.54 (s, 2H, OC$\underline{H}_3$ (*O*1a)), 3.55 – 3.63 (m, 1.8H, 6b, 4a), 3.69 – 3.76 (m, 2.2H, H6a, H5a, H5b), 3.81 (dd, *J* = 12.7, 2.3 Hz, 1H, H6b), 3.86 (dd, *J* = 8.1, 2.2 Hz, 1H, H4b), 4.38 (d, *J* = 2.6 Hz, 0.6H, H3a), 4.94 (d, *J* = 3.0 Hz, 1H, H1b), 4.99 (d, *J* = 2.5 Hz, 0.6H, H1a), 5.06 (d, *J* = 3.0 Hz, 0.6H, H2b), 5.14 (d, *J* = 2.5 Hz, 0.6H, H2a), 5.24 (d, *J* = 2.1 Hz, 1H, H3b), 6.57 (dd, *J* = 8.3, 1.0 Hz, 1H, PhC$\underline{H}$), 6.69 (dd, *J* = 8.3, 1.0 Hz, 1H, PhC$\underline{H}$), 6.77 – 6.90 (m, 44H, PhC$\underline{H}$), 7.24 – 7.33 (m, 41H, PhC$\underline{H}$), 7.40 – 7.50 (m, 5H, PhC$\underline{H}$).

3.6 ABAO assay with model compound (25)

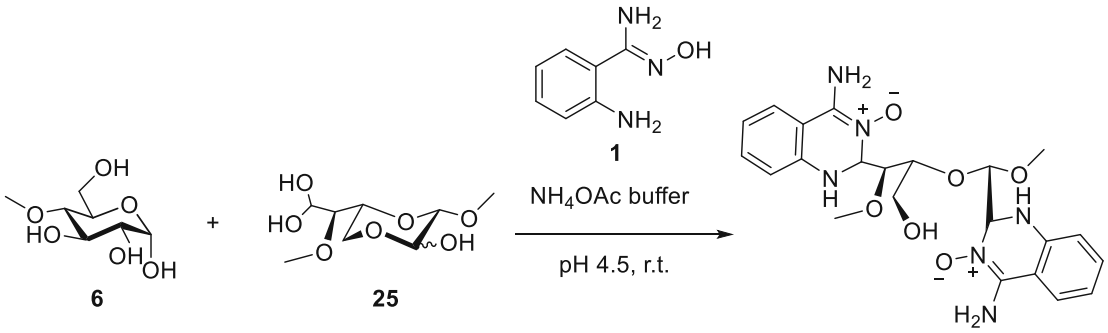

The formation of **27** was followed *via* absorption measurements based on an assay previously used for kinetic applications.[37]

Procedure: A 42.1 mM stock solution of ABAO (**1**) in NH_4OAc buffer (100 mM NH_4OAc, pH = 4.5) was prepared. 190 µl of the ABAO stock solution were put into the wells of a 96 well microplate and solutions of **6** (52.6 mM) and **25** (40 mM) were added in varying amounts, always adding up to 10 µl. Blanks were measured by adding 10 µl of water instead. All reactions were prepared in triplicates. A lid was placed on the plate and the absorption at 405 nm was measured for 20h. The results are shown in Figure 16. Figure 17 shows the calibration obtained by plotting the maximum absorption reached during the reaction between **25** and ABAO **1** against the used **25** concentrations.

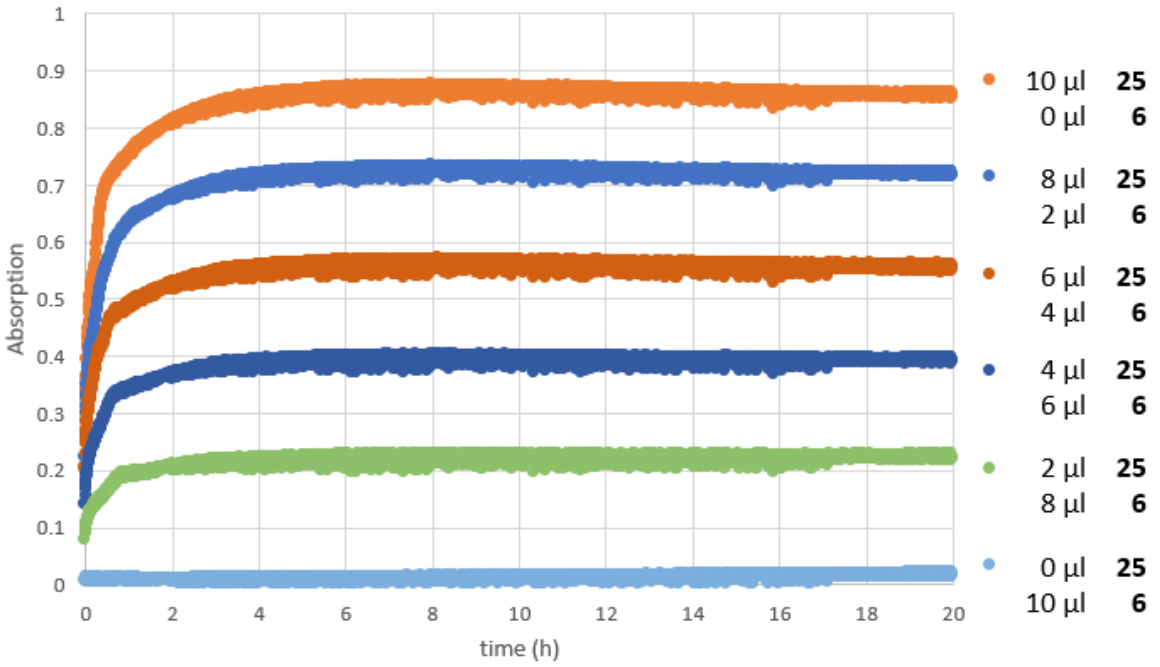

Figure 16 Absorption of the reaction between 25 and 6 and ABAO (1) at 405 nm over time

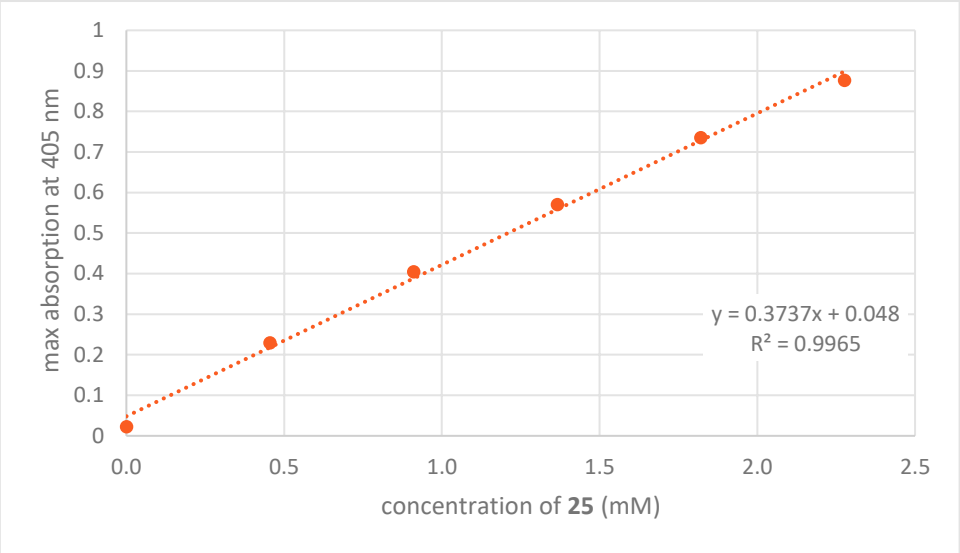

Figure 17 Maximum absorption reached during the reaction of ABAO (1) with compound 25 plotted against different concentrations.

3.7 ABAO assay with DAS

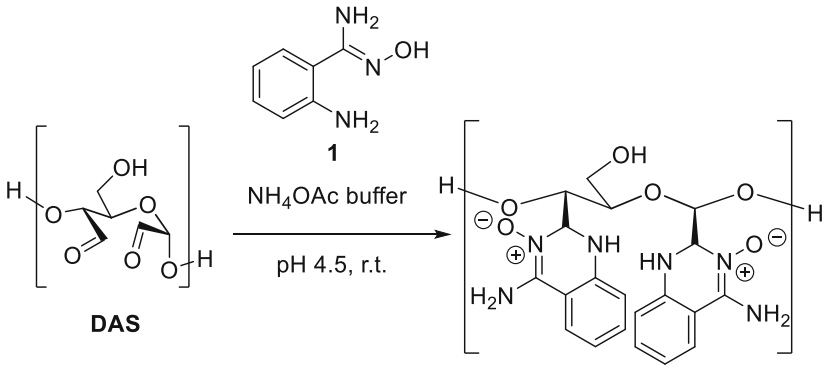

The formation of DAS-ABAO adducts was followed *via* absorption measurements based on an assay previously used for kinetic applications.[37]

Procedure: A 80 mM stock solution of ABAO (**1**) in NH_4OAc buffer (100 mM NH_4OAc, pH = 4.5) was prepared. 52 mg of DAS (synthesized as described in 3.4) were dissolved in NH_4OAc buffer (2 ml) by heating for 10 min at 95 °C. The DAS solutions were diluted 1:25 with NH_4OAc buffer. 100 µl of the DAS solutions were mixed with 100 µl of the ABAO stock solution or 100 µl of NH_4OAc buffer in a 96 well plate. All mixtures were prepared in triplicates. A lid was placed on the plate and the absorption at 405 nm was measured at different time points up to 48h, the results are shown in Figure 18. The experiment was repeated with 1 eq. $NaIO_4$-DAS with varying starch concentrations during the ABAO assay. The results are shown in Figure 19.

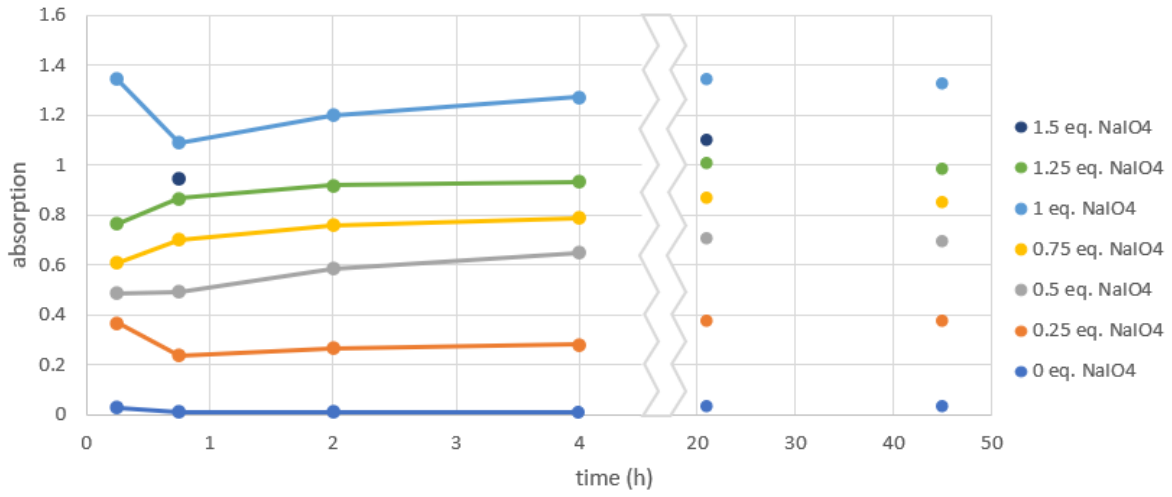

Figure 18 Absorption of the reaction between DAS prepared with various eq. $NaIO_4$ and ABAO (1) at 405 nm over time

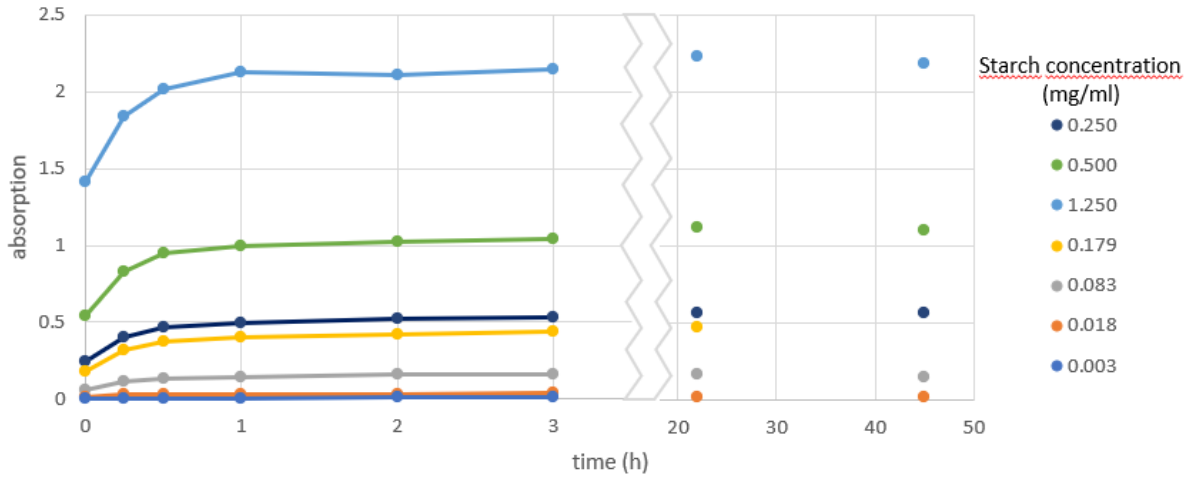

Figure 19 Absorption of the reaction between DAS prepared with 1 eq. $NaIO_4$ and ABAO (1) at 405 nm over time with varying starch concentrations during ABAO assay.

Calculation of oxidized glucose units: For the evaluation of oxidized glucose units, blank values of the ABAO buffer and blank values of the respective starch sample with buffer without ABAO were subtracted from the absorption values of the starch samples with ABAO buffer solution. Dialdehyde concentration was then determined using the calibration in Figure 17 and divided by the concentration of AGU in the sample, calculated from the sample weight of DAS. For representative values, the absorption measurements after 21 h were used to ensure a full reaction with the acetal species in the DAS.

3.8 (Neocuproine)Pd(OAc)$_2$[72] [3]

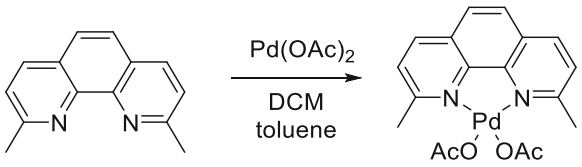

$C_{14}H_{12}N_2$
M = 208.26
5

$C_{18}H_{18}N_2O_4Pd$
M = 432.77
3

Procedure: To a solution of neocuproine **5** (1.25 g, 6.00 mmol, 1.2 eq.) in anhydrous DCM (20 ml) was added a solution of $Pd(OAc)_2$ (1.12 g, 5.00 mmol, 1.0 eq.) in anhydrous toluene (100 ml). The mixture was stirred overnight at room temperature under argon atmosphere.

Workup: To the yellow suspension was added LP (200 ml) to fully precipitate the product. The yellow precipitate was filtered and washed with LP, yielding 2.06 g (95%) of the desired product **3** as a yellow solid, pure according to ^{1}H-NMR and with spectral data in accordance with the literature.[72]

Yield	2.06 g (95%)
Appearance	yellow solid

^{1}H NMR (400 MHz, $CDCl_3$) δ 2.05 (s, 6H, COOC**H$_3$**), 2.91 (s, 6H, ArC**H$_3$**), 7.42 (d, *J* = 8.3 Hz, 2H, Ar**H**), 7.86 (s, 2H, Ar**H**), 8.36 (d, *J* = 8.4 Hz, 2H, Ar**H**).

^{13}C NMR (101 MHz, $CDCl_3$) δ 23.1 (COO**C**H$_3$), 24.7 (Ar**C**H$_3$), 126.4 (Ar**C**H), 126.9 (Ar**C**H), 128.0 (Ar**C**), 138.4 (Ar**C**H), 147.5 (Ar**C**), 165.5 (Ar**C**), 178.6 (**C**OOCH$_3$).

3.9 (Neocuproine)Pd(ACN)$_2$(OTf)$_2$[57] [4]

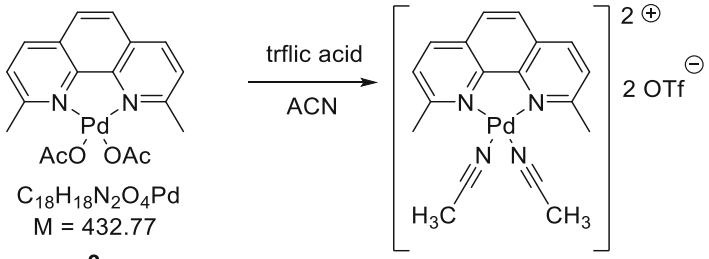

$C_{18}H_{18}N_2O_4Pd$
M = 432.77
3

$C_{20}H_{18}N_4O_6S_2F_6Pd$
M = 694.92
4

Procedure: The synthesis was carried out in centrifuge tubes. To the precursor **3** (600 mg, 1.39 mmol, 1.00 eq.) was added ACN (3 ml). Then a solution of triflic acid (319 µl, 3.47 mmol, 2.50 eq.) in CAN (11.4) ml was added. Immediately a yellow precipitate started to form. The suspension was stirred briefly at room temperature.

Workup: The product was fully precipitated with diethyl ether. The precipitate was isolated *via* centrifugation, suspended in acetonitrile and a solution of triflic acid in acetonitrile (0.33 M) was added. The precipitation, centrifugation and washing were repeated two more times. Drying under vacuum left the 878 mg (61%) desired product **4** as a slightly yellow solid, pure according to ^{1}H-NMR and with spectral data in accordance with the literature.[57]

Yield	878 mg (61%)
Appearance	slightly yellow solid

^{1}H NMR (400 MHz, CD_3CN) δ 3.00 (s, 6H, PhC**H**$_3$), 7.78 (d, *J* = 8.4 Hz, 2H, Ph**H**), 8.08 (s, 2H, Ph**H**), 8.69 (d, *J* = 8.4 Hz, 2H, Ph**H**).

3.10 [(Neocuproine)Pd(μ-OAc)]$_2$(OTf)$_2$ [2][57]

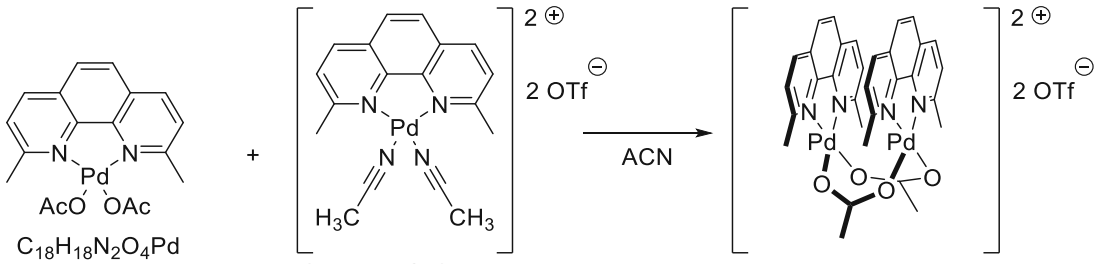

$C_{18}H_{18}N_2O_4Pd$
M = 432.77
3

$C_{20}H_{18}N_4O_6S_2F_6Pd$
M = 694.92
4

$C_{34}H_{30}N_4O_{10}S_2F_6Pd_2$
M = 1045.59
2

Procedure: Starting materials **3** (65 mg, 0.15 mg, 1.00 eq.) and **4** (117 mg, 0.15 mmol, 1.00 eq.) were suspended in acetonitrile and stirred for 15 min at r.t. until all solids had dissolved. The product was precipitated with diethyl ether. The solid was isolated by centrifugation, washed with diethyl ether and dried under vacuum, yielding 111 mg (71%) of the desired product **2** as an orange solid with some minor unknown impurities of similar species according to ^{1}H-NMR and with spectral data in accordance with the literature.[57]

Yield 111 mg (71%)

Appearance orange solid

^{1}H NMR (400 MHz, CD_3CN) dimer peaks δ 2.24 (s, 6H, COOC**H$_3$**), 2.63 (s, 12H, PhC**H$_3$**), 7.38 (d, *J* = 8.4 Hz, 4H, Ph**H**), 7.70 (s, 4H, Ph**H**), 8.26 (d, *J* = 8.4 Hz, 4H, Ph**H**).

3.11 NMR experiments with catalyst 2

3.11.1 General procedure for NMR experiments with catalyst 2[50]

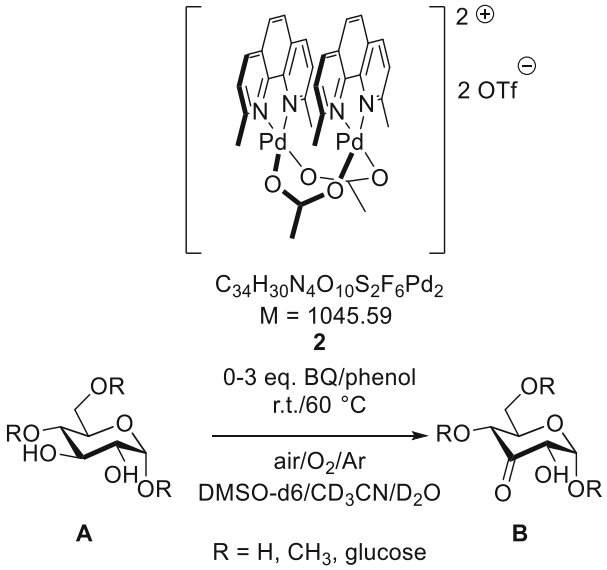

Procedure: The catalyst **2** (2.5-10 eq.) was weighed into 8 ml flasks and suspended in 0.6 ml of solutions of substrate **A** (typical concentration: 0.085 M of glucose units) in deuterated solvent (DMSO-d6, CD_3CN, D_2O) and for some experiments additives were added (0-3 eq. BQ/phenol). For reactions under O_2/inert atmosphere, oxygen/argon balloons were bubbled through the solutions. The mixtures were then stirred for the given time at the given temperature (r.t. or 60°C). Without further workup, ^{1}H-NMR measurements of the reaction mixtures were obtained and the yields of the products **B** were calculated by comparing the integrals of selected peaks of **A** and **B** in ^{1}H-NMR.

The exact compositions of individual experiments and determined yields are listed in the chapters below.

3.11.2 Oxidation of methyl α-glucopyranoside (28) to keto-glucoside [29]

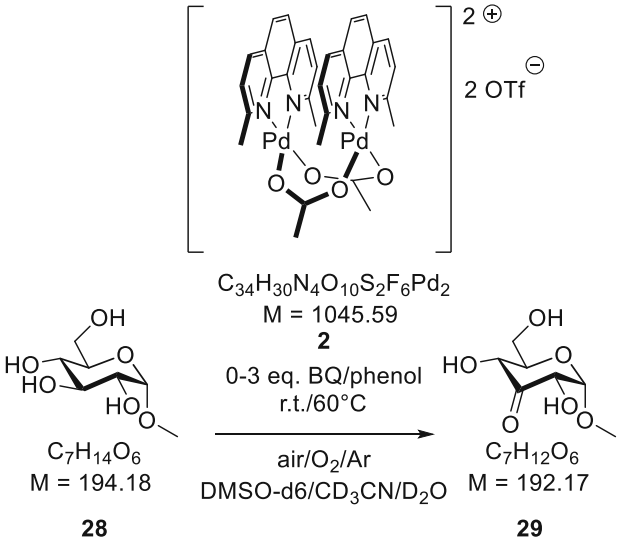

NMR experiments with catalyst **2** and substrate **28** were conducted as described in general procedure in 3.11.1. Exact equivalents of the reagents used, reaction conditions and NMR yields are given in Table 10, Table 11, Table 12, Table 13, and Table 14.

Reactions in D_2O

Table 10 Conditions and yields of reactions of 28 with catalyst 2 in DMSO-d6 [a]blank experiment with no catalyst.

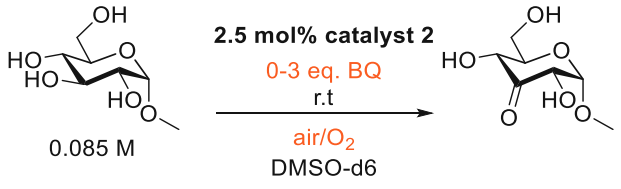

Oxidant	Oxidant eq.	Reaction time	NMR yield
BQ	3	0.5 h	100%
BQ	2	0.5 h	100%
BQ	1	0.5 h 5 h 14 h	78% 83% 87%
BQ	0.5	0.5 – 14 h	45%
none	-	24 h	9%
O2	-	24 h	15%
BQ	3	24 h	0%a

Reaction in D_2O:CD_3CN 2:1

Table 11 Conditions and yields of reaction of 28 (0.15 M) with catalyst 2 in D_2O:CD_3CN 2:1

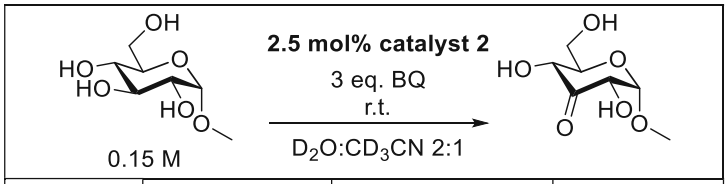

Oxidant	Oxidant eq.	Reaction time	NMR yield
BQ	3	12 h	91%

Reaction in D_2O with varying temperatures and oxidants

Table 12 Conditions and yields of reactions with varying temperatures and oxidants

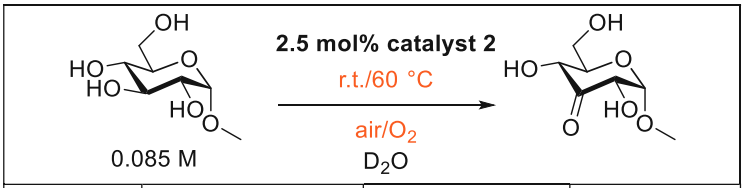

Oxidant	Reaction time	Temperature	NMR yield
O_2	2 h	r.t.	17%
Air	2 h	r.t.	17%
O_2	2 h	60 °C	46%
Air	2 h	60 °C	28%
Inert	24 h	60 °C	8%

Reaction in D_2O with varying additives

Table 13 Conditions and yields of reactions with varying additives

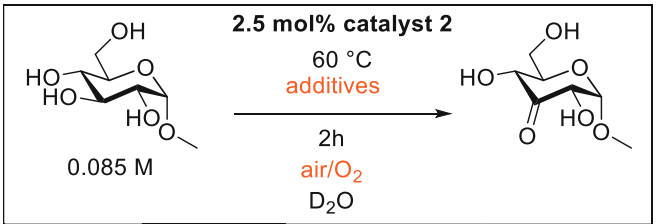

Oxidant	Additive	Additive eq.	NMR yield
O_2	AcOH	0.005	28%
Air	HQ	1	10%
O_2	Phenol	0.25	35%
O_2	Phenol	0.75	38%
O_2	Phenol	1	36%
Air	Phenol	0.25	51%
Air	Phenol	0.75	64%
Air	Phenol	1	66%
Air	Phenol	1.25	62%
Air	Phenol	1.5	53%

Reaction in D_2O with varying catalyst amounts

Table 14 Conditions and yields of reactions with varying catalyst amounts

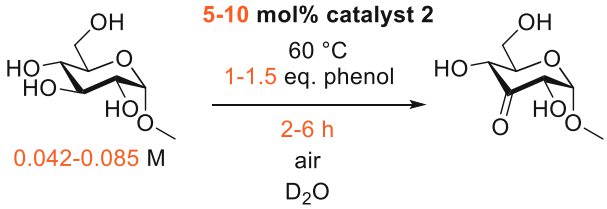

Catalyst 2 amount	Substrate 28 concentration	Phenol eq.	Reaction time	NMR yield
5 mol%	0.085 M	1	2 h 6 h	68% 67%
10 mol%	0.042 M	1.5	2 h 6 h	85% 83%

^{1}H NMR (600 MHz, DMSO) δ 3.27 (s, 3H, OC**H**$_3$), 3.48 (ddd, *J* = 9.9, 4.9, 1.9 Hz, 1H, H5), 3.61 (dd, *J* = 12.0, 5.0 Hz, 1H, H6a), 3.70 (dd, *J* = 12.1, 1.9 Hz, 1H, H6b), 4.09 (dd, *J* = 9.7, 1.5 Hz, 1H, H4), 4.31 (dd, *J* = 4.3, 1.6 Hz, 1H, H2), 4.96 (d, *J* = 4.2 Hz, 1H, H1).

Spectral data taken from time resolved reaction (0.085 M substrate **28**, 3 eq. BQ) and in accordance with the literature.[51]

^{1}H NMR (400 MHz, D_2O) δ 3.42 (s, 3H, OC**H**$_3$), 3.79 (dddd, *J* = 9.9, 4.6, 2.2, 0.6 Hz, 1H, H5), 3.87 (dd, *J* = 12.5, 4.5 Hz, 1H, H6a), 3.95 (dd, *J* = 12.5, 2.2 Hz, 1H, H6b), 4.39 (dd, *J* = 9.9, 1.6 Hz, 1H, H4), 4.61 (dd, *J* = 4.3, 1.6 Hz, 1H, H2), 5.20 (dd, *J* = 4.3, 0.6 Hz, 1H, H1).

Spectral data taken from reaction with 10 mol% catalyst.

3.11.3 Oxidation of methyl 4-*O*-methyl-α-glucopyranoside (6) to keto glucoside [33]

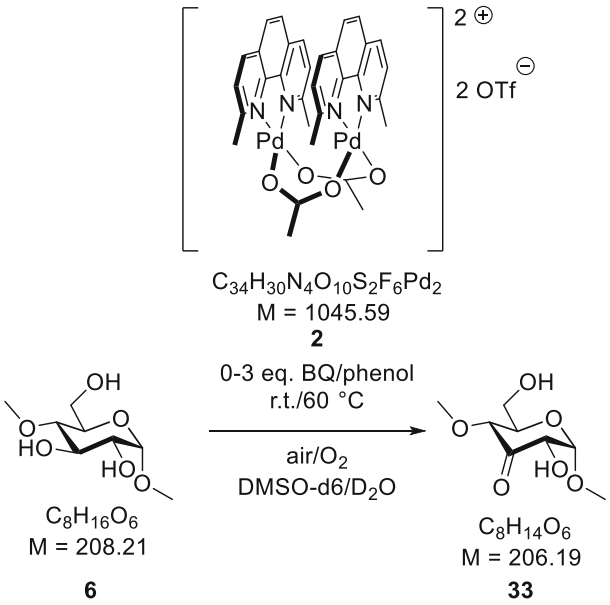

NMR experiments with catalyst **2** and substrate **6** were conducted as described in general procedure in 3.11.1. Exact equivalents of the reagents used, reaction conditions and NMR yields are given in Table 15 and Table 16.

Table 15 Conditions and yields of reactions of 6 (0.085 M) with catalyst 2 in DMSO-d6

Catalyst 2 amount	Oxidant	Oxidant eq.	Reaction time	Temperature	NMR yield
2.5 mol%	BQ	3	1 h	r.t.	62%
2.5 mol%	BQ	2	1 h	r.t.	57%
2.5 mol%	BQ	1	1 h	r.t.	48%
2.5 mol%	BQ	0.5	1 h	r.t.	40%

Table 16 Conditions and yields of reactions of 6 (0.085 M) with catalyst 2 in D_2O

Catalyst 2 amount	Oxidant	Reaction time	Temperature	NMR yield
2.5 mol%	O_2	2 h	60°C.	20%

^{1}H NMR (600 MHz, DMSO) δ 3.26 (s, 3H, OC**H$_3$**), 3.36 (s, 3H, OC**H$_3$**), 3.51 (ddd, *J* = 9.8, 4.4, 1.8 Hz, 1H, H5), 3.57 (dd, *J* = 12.0, 4.4 Hz, 1H, H6a), 3.64 (dd, *J* = 12.0, 1.9 Hz, 1H, H6b), 3.95 (dd, *J* = 9.7, 1.5 Hz, 1H, H4), 4.27 (dd, *J* = 4.2, 1.5 Hz, 1H, H2), 4.94 (d, *J* = 4.2 Hz, 1H, H1).

Spectral data taken from reaction with 3 eq. BQ after 3 h reaction time.

^{1}H NMR (400 MHz, D_2O) δ 3.93 (dd, *J* = 12.4, 2.1 Hz, 1H, H6b), 4.19 (dd, *J* = 9.7, 1.4 Hz, 1H, H3), 4.60 (dd, *J* = 4.4, 1.4 Hz, 1H, H2), 5.18 (d, *J* = 4.3 Hz, 1H, H1).

Other peaks were unidentifiable due to overlap with substrate **6**.

3.11.4 Oxidation of methyl 4,6-di-*O*-methyl-α-glucopyranoside (7) to keto glucoside [35]

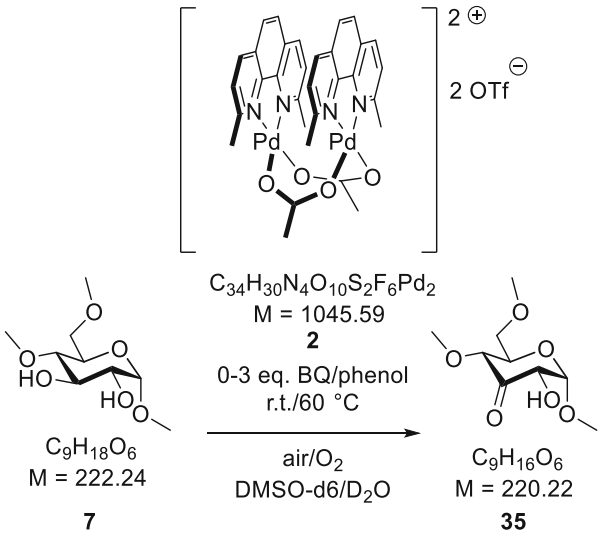

NMR experiments with catalyst **2** and substrate **7** were conducted as described in general procedure in 3.11.1. Exact equivalents of the reagents used, reaction conditions and NMR yields are given in Table 17 and Table 18.

Table 17 Conditions and yields of reactions of 7 (0.085 M) with catalyst 2 in DMSO-d6

Catalyst 2 amount	Oxidant	Oxidant eq.	Reaction time	Temperature	NMR yield
2.5 mol%	BQ	3	1 h	r.t.	93%
2.5 mol%	BQ	2	1 h	r.t.	93%
2.5 mol%	BQ	1	1 h	r.t.	90%
2.5 mol%	BQ	0.5	1 h	r.t.	41%

Table 18 Conditions and yields of reactions of 7 (0.085 M) with catalyst 2 in D_2O

Catalyst 2 amount	Oxidant	Reaction time	Temperature	NMR yield
2.5 mol%	O_2	2 h	60°C.	25%

^{1}H NMR (600 MHz, DMSO) δ 3.26 (s, 3H, OC**H**$_3$), 3.32 (s, 3H, OC**H**$_3$), 3.37 (s, 3H, OC**H**$_3$), 3.52 – 3.59 (m, 2H, H6a, H6b), 3.64 (ddd, *J* = 10.0, 4.6, 2.1 Hz, 1H, H5), 3.94 (dd, *J* = 9.9, 1.4 Hz, 1H, H4), 4.30 (dd, *J* = 4.1, 1.5 Hz, 1H, H2), 4.94 (d, *J* = 4.2 Hz, 1H, H1).

Spectral data taken from reaction with 2 eq. BQ after 1 h reaction time.

^{1}H NMR (400 MHz, D2O) δ 3.90 (ddd, *J* = 10.0, 4.2, 2.6 Hz, 1H, H5), 4.17 (dd, *J* = 9.9, 1.4 Hz, 1H, H4), 4.60 (dd, *J* = 4.3, 1.4 Hz, 1H, H2), 5.17 (d, *J* = 4.3 Hz, 1H, H1).

Other peaks were unidentifiable due to overlap with substrate **7**.

3.11.5 Oxidation of methyl 4'-*O*-methyl-β-maltopyranoside (8) to keto maltoside [36]

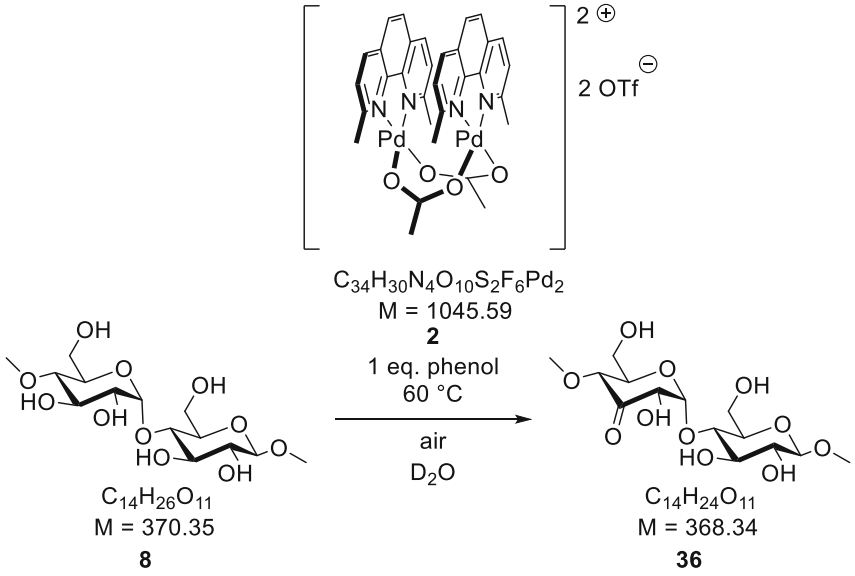

NMR experiments with catalyst **2** and substrate **8** were conducted as described in general procedure in 3.11.1. Exact equivalents of the reagents used, reaction conditions and NMR yields are given in Table 19.

Table 19 Conditions and yields of reactions of 8 (0.023 M) with catalyst 2 in D_2O

Catalyst 2 amount	Oxidant	Additive	Additive eq.	Reaction time	Temperature	NMR yield
2.5 mol%	air	Phenol	1.2	2 h	60°C.	35%
24 mol%	air	Phenol	1.2	15 h	60°C.	Not identifiable

^{1}H NMR (400 MHz, D_2O) δ 4.36 (d, *J* = 8.0 Hz, 1H, H1), 4.64 (dd, *J* = 4.5, 1.4 Hz, 1H, H2'), 5.81 (d, *J* = 4.5 Hz, 1H, H1').

Spectral data taken from reaction with 2.5 mol% catalyst. Other peaks were unidentifiable due to overlap with substrate **8** and not fully determinable byproducts, see discussion for details.

3.11.6 Oxidation of cyclodextrins 38, 39 and 40 to keto derivatives

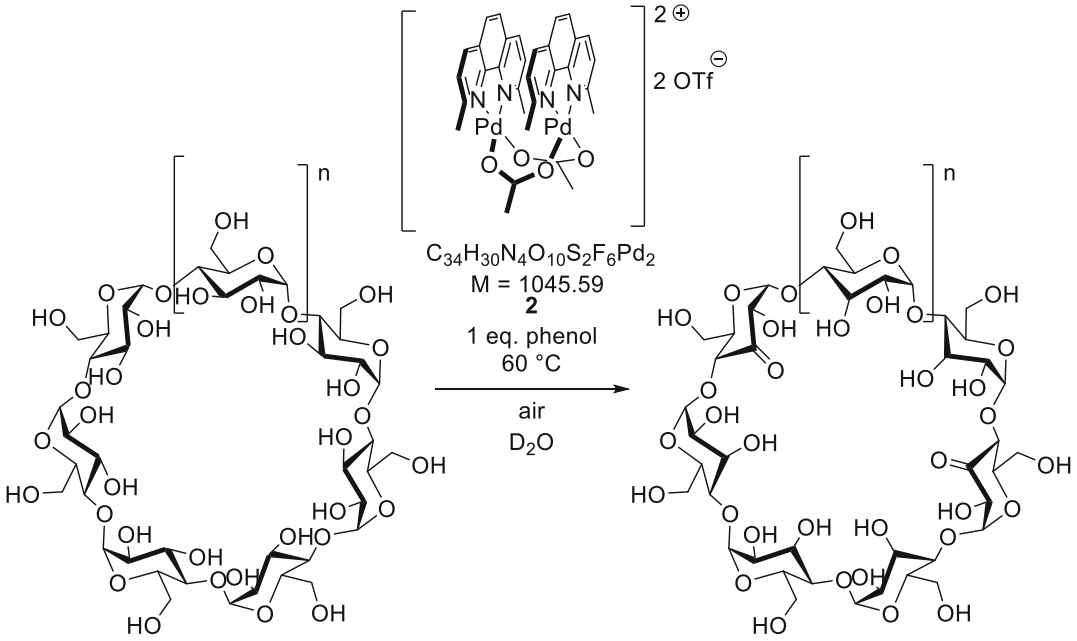

n = 1 β-cyclodextrin **38**
n = 2 γ-cyclodextrin **39**
n = 3 δ-cyclodextrin **40**

n = 1 oxidized β-cyclodextrin
n = 2 oxidized γ-cyclodextrin
n = 3 oxidized δ-cyclodextrin

NMR experiments with catalyst **2** and cyclodextrins **38**, **39**, and **40** were conducted as described in general procedure in 3.11.1. Exact equivalents of the reagents used based on AGU units, reaction conditions and NMR yields are given in Table 20.

Table 20 Conditions and yields of reactions of 38, 39 and 40 (0.085 M glucose units) with 2.5 mol% catalyst 2 in D_2O

Substrate	Oxidant	Additive	Additive eq.	Reaction time	Temperature	NMR yield
β-cyclodextrin 38	air	Phenol	1	2 h	60°C.	26%
γ-cyclodextrin 39	air	Phenol	1	2 h	60°C.	19%
δ-cyclodextrin 40	air	Phenol	1	2 h	60°C.	15%

3.11.7 Oxidation of maltodextrins and starch

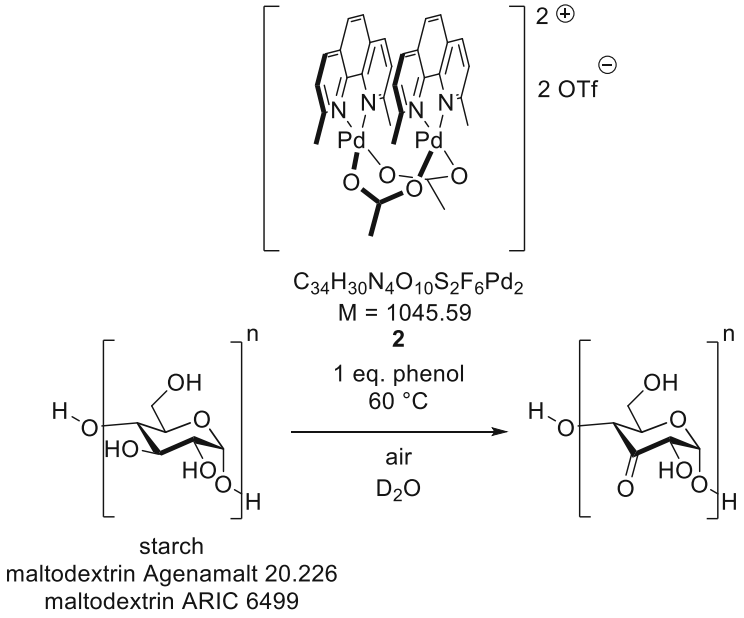

starch
maltodextrin Agenamalt 20.226
maltodextrin ARIC 6499

NMR experiments with catalyst **2** and starch and two different maltodextrins were conducted as described in general procedure in 3.11.1. Exact equivalents of the reagents used based on glucose units, reaction conditions and NMR yields are given in Table 20.

Table 21 Conditions and yields of reactions of starch and maltodextrins (0.085 M glucose units) with catalyst 2 and 1 eq. phenol per glucose unit in D_2O

Substrate	Catalyst **2** mol% per glucose unit.	Reaction time	Temperature	NMR yield
Starch	5 %	2 h	60°C.	16%
Maltodextrin Agenamalt 20.226	2.5 %	2 h	60°C.	17%
Maltodextrin ARIC 6499	2.5 %	2 h	60°C.	20%

4 References

1. Waterschoot, J.; Gomand, S. V.; Fierens, E.; Delcour, J. A., Production, structure, physicochemical and functional properties of maize, cassava, wheat, potato and rice starches. *Starch - Stärke* **2015,** *67* (1-2), 14-29.

2. Jane, J.-l., Chapter 6 - Structural features of starch granules II. In *Starch (Third Edition)*, BeMiller, J.; Whistler, R., Eds. Academic Press: San Diego, 2009; pp 193-236.

3. Copeland, L.; Blazek, J.; Salman, H.; Tang, M. C., Form and functionality of starch. *Food Hydrocolloids* **2009,** *23* (6), 1527-1534.

4. Ellis, R. P.; Cochrane, M. P.; Dale, M. F. B.; Duffus, C. M.; Lynn, A.; Morrison, I. M.; Prentice, R. D. M.; Swanston, J. S.; Tiller, S. A., Starch production and industrial use. *J. Sci. Food Agric.* **1998,** *77* (3), 289-311.

5. Wurzburg, O. B., Modified starch. *Food Sci. Technol. (Boca Raton, FL, U. S.)* **2006,** *160*, 87-118.

6. Neelam, K.; Vijay, S.; Lalit, S., Various techniques for the modification of starch and the applications of its derivatives. *Int. Res. J. Pharm.* **2012,** *3*, 25-31.

7. Garrido, L. H.; Schnitzler, E.; Zortéa, M. E.; de Souza Rocha, T.; Demiate, I. M., Physicochemical properties of cassava starch oxidized by sodium hypochlorite. *J Food Sci Technol* **2014,** *51* (10), 2640-7.

8. Sangseethong, K.; Termvejsayanon, N.; Sriroth, K., Characterization of physicochemical properties of hypochlorite- and peroxide-oxidized cassava starches. *Carbohydr. Polym.* **2010,** *82* (2), 446-453.

9. Whistler, R. L.; Schweiger, R., Oxidation of Amylopectin with Hypochlorite at Different Hydrogen Ion Concentrations. *J. Am. Chem. Soc.* **1957,** *79* (24), 6460-6464.

10. Floor, M.; Kieboom, A. P. G.; van Bekkum, H., Preparation and Calcium Complexation of Oxidized Polysaccharides. Part I: Oxidation of Maltodextrins and Starch with Alkaline Sodium Hypochlorite. *Starch - Stärke* **1989,** *41* (9), 348-354.

11. Boruch, M., Transformations of Potato Starch During Oxidation with Hypochlorite. *Starch - Stärke* **1985,** *37* (3), 91-98.

12. Vanier, N. L.; El Halal, S. L. M.; Dias, A. R. G.; da Rosa Zavareze, E., Molecular structure, functionality and applications of oxidized starches: A review. *Food Chem.* **2017,** *221*, 1546-1559.

13. Yi, X.; Zhang, S.; Ju, B., Preparation of water-soluble oxidized starch with high carbonyl content by sodium hypochlorite. *Starch - Stärke* **2014,** *66* (1-2), 115-123.

14. Wang, S.; Li, C.; Copeland, L.; Niu, Q.; Wang, S., Starch Retrogradation: A Comprehensive Review. *Compr. Rev. Food Sci. Food Saf.* **2015,** *14* (5), 568-585.

15. Zhang, S.-D. o. S.; Wang, X.-L.; Zhang, Y.-R.; Yang, K.-K.; Wang, Y.-Z., Preparation of a new dialdehyde starch derivative and investigation of its thermoplastic properties. *J. Polym. Res.* **2010,** *17*, 439-446.

16. Fiedorowicz, M.; Para, A., Structural and molecular properties of dialdehyde starch. *Carbohydr. Polym.* **2006,** *63* (3), 360-366.

17. Yu, J.; Chang, P. R.; Ma, X., The preparation and properties of dialdehyde starch and thermoplastic dialdehyde starch. *Carbohydr. Polym.* **2010,** *79* (2), 296-300.

18. Liu, X.; Wang, Y.; Yu, L.; Tong, Z.; Chen, L.; Liu, H.; Li, X., Thermal degradation and stability of starch under different processing conditions. *Starch - Stärke* **2013,** *65* (1-2), 48-60.

19. Mathew, A. P.; Dufresne, A., Plasticized Waxy Maize Starch: Effect of Polyols and Relative Humidity on Material Properties. *Biomacromolecules* **2002,** *3* (5), 1101-1108.

20. Jelkmann, M.; Leichner, C.; Menzel, C.; Kreb, V.; Bernkop-Schnürch, A., Cationic starch derivatives as mucoadhesive and soluble excipients in drug delivery. *Int. J. Pharm.* **2019,** *570*, 118664.

21. Para, A.; Karolczyk-Kostuch, S.; Fiedorowicz, M., Dihydrazone of dialdehyde starch and its metal complexes. *Carbohydr. Polym.* **2004,** *56* (2), 187-193.

22. Yin, Q.-F.; Ju, B.-Z.; Zhang, S.-F.; Wang, X.-B.; Yang, J.-Z., Preparation and characteristics of novel dialdehyde aminothiazole starch and its adsorption properties for Cu (II) ions from aqueous solution. *Carbohydr. Polym.* **2008,** *72* (2), 326-333.

23. Para, A.; Karolczyk-Kostuch, S., Semicarbazone of starch dialdehyde and its complexes with metal ions. *Carbohydr. Polym.* **2002,** *48* (1), 55-60.

24. Para, A., Complexation of metal ions with dioxime of dialdehyde starch. *Carbohydr. Polym.* **2004,** *57* (3), 277-283.

25. Martucci, J. F.; Ruseckaite, R. A., Tensile properties, barrier properties, and biodegradation in soil of compression—Molded gelatin-dialdehyde starch films. *J. Appl. Polym. Sci.* **2009,** *112* (4), 2166-2178.

26. Tang, R.; Du, Y.; Fan, L., Dialdehyde starch-crosslinked chitosan films and their antimicrobial effects. *J. Polym. Sci., Part B: Polym. Phys.* **2003,** *41* (9), 993-997.

27. Chen, X.; Pizzi, A.; Zhang, B.; Zhou, X.; Fredon, E.; Gerardin, C.; Du, G., Particleboard bio-adhesive by glyoxalated lignin and oxidized dialdehyde starch crosslinked by urea. *Wood Sci. Technol.* **2022,** *56* (1), 63-85.

28. Luo, J.; Zhang, J.; Gao, Q.; Mao, A.; Li, J., Toughening and Enhancing Melamine–Urea–Formaldehyde Resin Properties via in situ Polymerization of Dialdehyde Starch and Microphase Separation. *Polymers* **2019,** *11* (7), 1167.

29. Li, P.; Wu, Y.; Zhou, Y.; Zuo, Y., Preparation and characterization of resorcinol-dialdehyde starch-formaldehyde copolycondensation resin adhesive. *Int. J. Biol. Macromol.* **2019,** *127*, 12-17.

30. Pfeifer, V. F.; Sohns, V. E.; Conway, H. F.; Lancaster, E. B.; Dabic, S.; Griffin, E. L., Two Stage Process for Dialdehyde Starch Using Electrolytic Regeneration of Periodic Acid. *Ind. Eng. Chem.* **1960,** *52* (3), 201-206.

31. Smith, R. J., Characterization and Analysis of Starches. In *Starch: chemistry and Technology (Vol. II)*, Whistler, R. L.; Paschall, E. F., Eds. Academic Press: New York, NY

1967; pp 620-625.

32. Veelaert, S.; de Wit, D.; Tournois, H., An improved kinetic model for the periodate oxidation of starch. *Polymer* **1994,** *35* (23), 5091-5097.

33. Veelaert, S.; de Wit, D.; Gotlieb, K. F.; Verhé, R., Chemical and physical transitions of periodate oxidized potato starch in water. *Carbohydr. Polym.* **1997,** *33* (2), 153-162.

34. Rankin, J.; Mehltretter, C., Determination of Dialdehyde Units in Periodate-Oxidized Cornstraches. *Anal. Chem.* **1956,** *28* (6), 1012-1014.

35. Schwendenwein, D.; Ressmann, A. K.; Doerr, M.; Höhne, M.; Bornscheuer, U. T.; Mihovilovic, M. D.; Rudroff, F.; Winkler, M., Random Mutagenesis-Driven Improvement of Carboxylate Reductase Activity using an Amino Benzamidoxime-Mediated High-Throughput Assay. *Adv. Synth. Catal.* **2019,** *361* (11), 2544-2549.

36. Ressmann, A. K.; Schwendenwein, D.; Leonhartsberger, S.; Mihovilovic, M. D.; Bornscheuer, U. T.; Winkler, M.; Rudroff, F., Substrate-Independent High-Throughput Assay for the Quantification of Aldehydes. *Adv. Synth. Catal.* **2019,** *361* (11), 2538-2543.

37. Kalaus, H.; Reichetseder, A.; Scheibelreiter, V.; Rudroff, F.; Stanetty, C.; Mihovilovic, M. D., A Kinetic Photometric Assay for the Quantification of the Open-Chain Content of Aldoses. *Eur. J. Org. Chem.* **2021,** *2021* (18), 2589-2593.

38. Kitov, P. I.; Vinals, D. F.; Ng, S.; Tjhung, K. F.; Derda, R., Rapid, Hydrolytically Stable Modification of Aldehyde-Terminated Proteins and Phage Libraries. *J. Am. Chem. Soc.* **2014,** *136* (23), 8149-8152.

39. Mei, Z.; Zhang, K.; Qu, G.; Li, J.-K.; Liu, B.; Ma, J.-A.; Tu, R.; Sun, Z., High-Throughput Fluorescence Assay for Ketone Detection and Its Applications in Enzyme Mining and Protein Engineering. *ACS Omega* **2020,** *5* (23), 13588-13594.

40. Amadio, E.; González-Fabra, J.; Carraro, D.; Denis, W.; Gjoka, B.; Zonta, C.; Bartik, K.; Cavani, F.; Solmi, S.; Bo, C.; Licini, G., Efficient Vanadium-Catalyzed Aerobic C−C Bond Oxidative Cleavage of Vicinal Diols. *Adv. Synth. Catal.* **2018,** *360* (17), 3286-3296.

41. Domingo, J. L., Vanadium: A review of the reproductive and developmental toxicity. *Reprod. Toxicol.* **1996,** *10* (3), 175-182.

42. García, N.; Rubio-Presa, R.; García-García, P.; Fernández-Rodríguez, M. A.; Pedrosa, M. R.; Arnáiz, F. J.; Sanz, R., A selective, efficient and environmentally friendly method for the oxidative cleavage of glycols. *Green Chem.* **2016,** *18* (8), 2335-2340.

43. Takezawa, E.; Sakaguchi, S.; Ishii, Y., Oxidative Cleavage of vic-Diols to Aldehydes with Dioxygen Catalyzed by Ru(PPh3)3Cl2 on Active Carbon. *Org. Lett.* **1999,** *1* (5), 713-715.

44. Meng, S.-S.; Lin, L.-R.; Luo, X.; Lv, H.-J.; Zhao, J.-L.; Chan, A. S. C., Aerobic oxidation of alcohols with air catalyzed by decacarbonyldimanganese. *Green Chem.* **2019,** *21* (22), 6187-6193.

45. Deruer, E.; Duguet, N.; Lemaire, M., Thiazolylidene-Catalyzed Cleavage of Methyl Oleate-Derived α-Hydroxy Ketone to the Corresponding Free Aldehydes. *ChemSusChem* **2015,** *8* (15), 2481-2486.

46. Draskovits, M.; Kalaus, H.; Stanetty, C.; Mihovilovic, M. D., Intercepted dehomologation of aldoses by N-heterocyclic carbene catalysis – a novel transformation in carbohydrate chemistry. *Chem. Commun.* **2019,** *55* (81), 12144-12147.

47. Buck, J. S.; Ide, W. S., Mixed Benzoins. V. Reversibility of the Benzoin Condensation and the Preparation of Mixed from Simple Benzoins. *J. Am. Chem. Soc.* **1931,** *53* (6), 2350-2353.

48. Armenise, N.; Tahiri, N.; Eisink, N. N. H. M.; Denis, M.; Jäger, M.; De Vries, J. G.; Witte, M. D.; Minnaard, A. J., Deuteration enhances catalyst lifetime in palladium-catalysed alcohol oxidation. *Chem. Commun.* **2016,** *52* (10), 2189-2191.

49. Eisink, N. N.; Lohse, J.; Witte, M. D.; Minnaard, A. J., Regioselective oxidation of unprotected 1, 4 linked glucans. *Org. Biomol. Chem.* **2016,** *14* (21), 4859-4864.

50. Eisink, N. N. H. M.; Witte, M. D.; Minnaard, A. J., Regioselective Carbohydrate Oxidations: A Nuclear Magnetic Resonance (NMR) Study on Selectivity, Rate, and Side-Product Formation. *ACS Catal.* **2017,** *7* (2), 1438-1445.

51. Jäger, M.; Hartmann, M.; de Vries, J. G.; Minnaard, A. J., Catalytic regioselective oxidation of glycosides. *Angew. Chem.* **2013,** *125* (30), 7963-7966.

52. Jäger, M.; Hartmann, M.; de Vries, J. G.; Minnaard, A. J., Catalytic Regioselective Oxidation of Glycosides. *Angew. Chem. Int. Ed.* **2013,** *52* (30), 7809-7812.

53. Jumde, V. R.; Eisink, N. N. H. M.; Witte, M. D.; Minnaard, A. J., C3 Epimerization of Glucose, via Regioselective Oxidation and Reduction. *J. Org. Chem.* **2016,** *81* (22), 11439-11443.

54. Wan, I. C.; Hamlin, T. A.; Eisink, N. N. H. M.; Marinus, N.; de Boer, C.; Vis, C. A.; Codée, J. D. C.; Witte, M. D.; Minnaard, A. J.; Bickelhaupt, F. M., On the Origin of

Regioselectivity in Palladium-Catalyzed Oxidation of Glucosides. *Eur. J. Org. Chem.* **2021,** *2021* (4), 632-636.

55. Chung, K.; Banik, S. M.; De Crisci, A. G.; Pearson, D. M.; Blake, T. R.; Olsson, J. V.; Ingram, A. J.; Zare, R. N.; Waymouth, R. M., Chemoselective Pd-Catalyzed Oxidation of Polyols: Synthetic Scope and Mechanistic Studies. *J. Am. Chem. Soc.* **2013,** *135* (20), 7593-7602.

56. Chung, K.; Waymouth, R. M., Selective Catalytic Oxidation of Unprotected Carbohydrates. *ACS Catal.* **2016,** *6* (7), 4653-4659.

57. Conley, N. R.; Labios, L. A.; Pearson, D. M.; McCrory, C. C. L.; Waymouth, R. M., Aerobic Alcohol Oxidation with Cationic Palladium Complexes: Insights into Catalyst Design and Decomposition. *Organometallics* **2007,** *26* (23), 5447-5453.

58. Ho, W. C.; Chung, K.; Ingram, A. J.; Waymouth, R. M., Pd-Catalyzed Aerobic Oxidation Reactions: Strategies To Increase Catalyst Lifetimes. *J. Am. Chem. Soc.* **2018,** *140* (2), 748-757.

59. Ingram, A. J.; Solis-Ibarra, D.; Zare, R. N.; Waymouth, R. M., Trinuclear Pd3O2 Intermediate in Aerobic Oxidation Catalysis. *Angew. Chem. Int. Ed.* **2014,** *53* (22), 5648-5652.

60. Pearson, D. M.; Conley, N. R.; Waymouth, R. M., Oxidatively Resistant Ligands for Palladium-Catalyzed Aerobic Alcohol Oxidation. *Organometallics* **2011,** *30* (6), 1445-1453.

61. Pearson, D. M.; Waymouth, R. M., Mechanistic Studies of the Oxidative Dehydrogenation of Methanol Using a Cationic Palladium Complex. *Organometallics* **2009,** *28* (13), 3896-3900.

62. Matwiejuk, M.; Thiem, J., Defining oxyanion reactivities in base-promoted glycosylations. *Chem. Commun.* **2011,** *47* (29), 8379-8381.

63. Matwiejuk, M.; Thiem, J., New Method for Regioselective Glycosylation Employing Saccharide Oxyanions. *Eur. J. Org. Chem.* **2011,** *2011* (29), 5860-5878.

64. Gebbie, S. J.; Gosney, I.; Harrison, P. R.; Lacan, I. M. F.; Sanderson, W. R.; Sankey, J. P., A convenient large-scale synthesis of methyl α-maltoside: a simple model for amylose. *Carbohydr. Res.* **1998,** *308* (3), 345-348.

65. Andersen, S. M.; Heuckendorff, M.; Jensen, H. H., 3-(Dimethylamino)-1-propylamine: A Cheap and Versatile Reagent for Removal of Byproducts in Carbohydrate Chemistry. *Org. Lett.* **2015,** *17* (4), 944-947.

66. Koto, S.; Hirooka, M.; Tashiro, T.; Sakashita, M.; Hatachi, M.; Kono, T.; Shimizu, M.; Yoshida, N.; Kurasawa, S.; Sakuma, N.; Sawazaki, S.; Takeuchi, A.; Shoya, N.; Nakamura, E., Simple preparations of alkyl and cycloalkyl α-glycosides of maltose, cellobiose, and lactose. *Carbohydr. Res.* **2004,** *339* (14), 2415-2424.

67. Aspinall, G. O.; Krishnamurthy, T. N.; Mitura, W.; Funabashi, M., Base-catalyzed Degradations of Carbohydrates. IX. β-Eliminations of 4-O-Substituted Hexopyranosiduronates. *Can. J. Chem.* **1975,** *53* (14), 2182-2188.

68. Bock, K.; Pedersen, H., The substrate specificity of the enzyme amyloglucosidase (AMG). Part I. Deoxy derivatives. *Acta Chem. Scand., Ser. B* **1987,** *41* (8), 617-28.

69. Heidelberg, T.; Thiem, J., Structure and Reactions of Glycopyranoside Derived Dialdehydes. *J. Prakt. Chem.* **1998,** *340* (3), 223-232.

70. Bailey, J. M.; Whelan, W. J., Physical properties of starch. I. Relationship between iodine stain and chain length. *J. Biol. Chem.* **1961,** *236*, 969-73.

71. Sloan, J. W.; Hofreiter, B. T.; Mellies, R. L.; Wolff, I. A., Properties of Periodate Oxidized Starch. *Ind. Eng. Chem.* **1956,** *48*, 1165-1172.

72. Brink, G.-J. t.; Arends, I. W. C. E.; Hoogenraad, M.; Verspui, G.; Sheldon, R. A., Catalytic Conversions in Water. Part 23: Steric Effects and Increased Substrate Scope in the Palladium-Neocuproine Catalyzed Aerobic Oxidation of Alcohols in Aqueous Solvents. *Adv. Synth. Catal.* **2003,** *345* (12), 1341-1352.

73. Erichsen, A.; Peters, G. H. J.; Beeren, S. R., Templated Enzymatic Synthesis of δ-Cyclodextrin. *J. Am. Chem. Soc.* **2023,** *145* (8), 4882-4891.

74. Nilsson, G. S.; Gorton, L.; Bergquist, K.-E.; Nilsson, U., Determination of the Degree of Branching in Normal and Amylopectin Type Potato Starch with 1H-NMR Spectroscopy Improved resolution and two-dimensional spectroscopy. *Starch - Stärke* **1996,** *48* (10), 352-357.

75. Rowell, R. M.; Feather, M. S., Synthesis and properties of anomerically unsubstituted hepta-O-acetyl disaccharides. *Carbohydr. Res.* **1967,** *4* (6), 486-491.

76. Takeo, K. i., A reinvestigation of the reaction of β-maltose octaacetate with phosphorus pentachloride. *Carbohydr. Res.* **1976,** *48* (2), 290-293.

77. Cheetham, N. W. H.; Sirimanne, P., Synthesis of methyl α- and β-maltosides. *Carbohydr. Res.* **1981,** *96* (1), 126-128.

78. Adelhorst, K.; Bock, K.; Pedersen, H.; Refn, S.; Karjalainen, A.; Berg, J.-E.; Bartók, M.; Pelczer, I.; Dombi, G., The Substrate Specificity of the Enzyme Amyloglucosidase (AMG). Part III. Synthesis of Epimers and Mono-O-methyl Ethers of Methyl beta-Maltoside. *Acta Chem. Scand., Ser. B* **1988,** *42*, 196-201.